Boundary integral equation methods for elastic and plastic problems

Marc Bonnet

Boundary Integral Equation Methods for Elastic and Plastic Problems

Marc Bonnet
École Polytechnique, Palaiseau, France

1 INTRODUCTION

The solutions of many fundamental linear field equations of physics can be expressed explicitly in terms of boundary integrals involving unknown primary and derivative field values (e.g., potential and flux, displacement, and traction) on the boundary. To exploit such relationships, one therefore needs to first formulate and solve a boundary integral equation (BIE) over the boundary field variables (see **Boundary Element Methods: Foundation and Error Analysis**). The application of BIE techniques in quasi-static problems of solid mechanics, to which the present chapter is devoted, is based on integral equations for linear elasticity, where, in addition, nonlinear effects can be incorporated by means of volume potentials associated with body forces or initial strains. BIE formulations are however known for other physical problems as well, including wave propagation (see **Time-Dependent Problems with the Boundary Integral Equation Method**, **Boundary Element Methods for the Dynamic Analysis of Elastic, Viscoelastic, and Piezoelectric Solids**), heat transfer, electromagnetics (see **Finite Element Methods for Maxwell's Equations**), and fluid flow. The boundary element method (BEM) then consists of applying discretization and interpolation techniques adapted from those initially introduced for finite element methods (FEMs), (see **Finite Element Methods**, **Finite Element Methods for Elasticity with Error-Controlled Discretization and Model Adaptivity**).

BIE formulations are rooted in the potential theory; see, for example, Kellogg (1967) for scalar problems and Parton and Perlin (1982) and Kupradze (1979) for elasticity. The theory of Fredholm integral equations allows in many cases to state general results (e.g., existence and uniqueness of solution). Numerical techniques for solving BIEs appeared in the 1960s, and early works in solid mechanics include Rizzo, 1967 and Cruse, 1969. The initial motivation for using BEMs was the dimensionality gain in the discretization (e.g., surface elements instead of finite elements). BEMs have been thoroughly investigated since, and monographs on BEMs in solid mechanics have been written by Aliabadi (2001), Antes and Panagiotopoulos (1992), Balas *et al.* (1989), Banerjee (1994), Beskos (1991), Bonnet (1999a), Chandra and Mukherjee (1997), Cruse (1988), Kane (1994),

and Pozrikidis (2002) among others. Moreover, the mathematical theory underpinning BIE formulations and their discretization is presented in Sauter and Schwab (2011) and Steinbach (2008), while the classical approach to BEM programming is expounded in Beer *et al.* (2008). As a result, BEMs are much better understood now. In particular, the apparent dimensionality advantage is far from clear-cut because BEMs involve fully populated matrices instead of the sparse symmetric matrices associated with FEMs. This feature indeed constitutes a major bottleneck, preventing the application of BEMs in their traditioonal version (where system matrices are fully computed) to large-scale models. The latter have fortunately been made tractable thanks to the advent of accelerated versions of the BEM, based on, for example, fast multipole or hierarchical matrix concepts, see, for example, the books by Gumerov and Duraiswami (2005) and Rjasanow and Steinbach (2007) or theses by Yoshida (2001) or Chaillat (2008). BEMs are useful, either alone or in combination with FEMs, for problems involving intricate or evolving domain discretizations (fracture mechanics analyses, crack propagation, shape optimization, defect identification), unbounded media, specific shapes for which fundamental solutions satisfying suitable boundary conditions are known, and superficial nonlinear phenomena (e.g., in contact and wear mechanics). Generally speaking, they provide specialized tools rather than general-purpose analysis environments, for which the flexibility of FEMs regarding nonlinear or heterogeneous constitutive properties cannot be matched by the BEMs.

This chapter is organized as follows. After a brief review of the basic integral identities of solid mechanics (Section 2), the BEM discretization techniques based on collocation and symmetric Galerkin BIE formulations are presented in Sections 3 and 4, respectively, followed by an overview of fast solution techniques (Section 5). Then, BEMs are described for fracture mechanics (Section 6) and small-strain elastoplasticity (Section 7). Next, Section 8 is devoted to shape sensitivity concepts. The chapter closes with a symmetric formulation for BEM–FEM coupling (Section 9).

2 BASIC INTEGRAL IDENTITIES

This chapter is concerned with equilibrium problems for three-dimensional solid bodies whose constitutive properties involve linear elasticity. In particular, unless stated otherwise (i.e., except for Section 7.4), infinitesimal deformations and strains are assumed, so that the strain tensor $\boldsymbol{\varepsilon}$ is related to the displacement field $\boldsymbol{u}$ via the linearized compatibility equation

$$\boldsymbol{\varepsilon} = \frac{\boldsymbol{\nabla u} + \boldsymbol{\nabla}^{\mathrm{T}}\boldsymbol{u}}{2} \tag{1}$$

The relationship between the strain tensor $\boldsymbol{\varepsilon}$ and the stress tensor $\boldsymbol{\sigma}$ is then assumed to be of the form

$$\boldsymbol{\sigma} = \boldsymbol{C} : (\boldsymbol{\varepsilon} - \boldsymbol{\varepsilon}^{\mathrm{I}}) \tag{2}$$

where $\boldsymbol{C}$ denotes the fourth-order tensor of elastic moduli and $\boldsymbol{\varepsilon}^{\mathrm{I}}$ denotes an initial strain distribution. The latter may account for several possibilities, including (i) residual (e.g., plastic) strain resulting from previous mechanical events, (ii) thermal strain, and (iii) inelastic strain in the context of inelastic constitutive properties and a quasi-static evolution problem. For isotropic elasticity, one has

$$C_{ijk\ell} = \mu \left[\frac{2\nu}{1-2\nu} \delta_{ij}\delta_{k\ell} + (\delta_{ik}\delta_{j\ell} + \delta_{i\ell}\delta_{jk}) \right] \tag{3}$$

where μ and ν denote the shear modulus and the Poisson ratio, respectively. Finally, letting $\boldsymbol{f}$ denote a prescribed body force distribution, the local equilibrium is governed by the field equation

$$\operatorname{div} \boldsymbol{\sigma} + \boldsymbol{f} = \boldsymbol{0} \tag{4}$$

2.1 Integral representation of displacement

The usual basis for integral formulations is a reciprocity identity between the unknown state $(\boldsymbol{u}, \boldsymbol{\varepsilon}, \boldsymbol{\sigma})$ and a known *fundamental solution*, here chosen to be an elastic field generated by a unit point force applied at a fixed source point $\tilde{\boldsymbol{x}}$ and along a fixed direction k in a fictitious body endowed with the same elastic moduli $\boldsymbol{C}$. Combining the fundamental field equations (1), (2), and (4), the components u_i of the unknown displacement field are governed by

$$C_{ijab}(u_{a,bj} - \varepsilon^{\mathrm{I}}_{ab,j}) + f_i = 0 \tag{5}$$

(commas denoting partial differentiations w.r.t. coordinates of the field point $\boldsymbol{x}$), while the components $U^k_i(\tilde{\boldsymbol{x}}, \boldsymbol{x})$ of the fundamental displacement are governed by the equation

$$C_{ijab}U^k_{a,bj} + \delta(\boldsymbol{x} - \tilde{\boldsymbol{x}})\delta_{ik} = 0 \tag{6}$$

where $\delta(\boldsymbol{x} - \tilde{\boldsymbol{x}})$ is the Dirac distribution at point $\tilde{\boldsymbol{x}}$. Multiplying (5) by $U^k_i(\tilde{\boldsymbol{x}}, \boldsymbol{x})$ and (6) by $u_i(\boldsymbol{x})$, integrating both equations over the domain Ω of interest, invoking the defining property of $\delta(\boldsymbol{x} - \tilde{\boldsymbol{x}})$, integrating by parts the remaining integrals, and subtracting the resulting identities, one obtains the representation formula for the displacement at $\tilde{\boldsymbol{x}}$:

$$\kappa(\tilde{\boldsymbol{x}})u_k(\tilde{\boldsymbol{x}}) = \int_{\partial\Omega} \{ U^k_i(\tilde{\boldsymbol{x}}, \boldsymbol{x})t_i(\boldsymbol{x}) - T^k_i(\tilde{\boldsymbol{x}}, \boldsymbol{x})u_i(\boldsymbol{x}) \} \, \mathrm{d}S_x + \int_{\Omega} \{ U^k_i(\tilde{\boldsymbol{x}}, \boldsymbol{x})f_i(\boldsymbol{x}) + \Sigma^k_{ab}(\tilde{\boldsymbol{x}}, \boldsymbol{x})\varepsilon^{\mathrm{I}}_{ab}(\boldsymbol{x}) \} \, \mathrm{d}V_x \tag{7}$$

where $\kappa(\tilde{\boldsymbol{x}}) = 1$ or 0 according to whether the source point $\tilde{\boldsymbol{x}}$ is interior or exterior to the domain Ω (in the latter case, the identity thus obtained is sometimes termed the *exterior representation formula*) and t_i, T_i^k, and Σ_{ij}^k denote the components of unknown tractions, fundamental tractions, and fundamental stresses, respectively, with

$$t_i(\boldsymbol{x}) = \sigma_{ij}(\boldsymbol{x}) n_j(\boldsymbol{x}), \qquad T_i^k(\tilde{\boldsymbol{x}}, \boldsymbol{x}) = \Sigma_{ij}^k(\tilde{\boldsymbol{x}}, \boldsymbol{x}) n_j(\boldsymbol{x}),$$
$$\Sigma_{ij}^k(\tilde{\boldsymbol{x}}, \boldsymbol{x}) = C_{ijab} U_{a,b}^k(\tilde{\boldsymbol{x}}, \boldsymbol{x})$$

Equation (7) thus expresses the displacement at a given interior point $\tilde{\boldsymbol{x}}$, often called the *observation point*, as a function of the distributions of body forces and initial strains and the displacement and traction over the boundary.

Obviously, the representation formula (7) requires that the fundamental solution is defined in Ω. Since the field equation (6) does not define U_i^k uniquely, one may in addition prescribe conditions for U_i^k or T_i^k on a boundary $\partial\hat{\Omega}$ chosen in such a way that $\Omega \subseteq \hat{\Omega}$, where $\hat{\Omega}$ denotes the domain enclosed by $\partial\hat{\Omega}$. The simplest, and most commonly used, choice is $\hat{\Omega} = \mathbb{R}^3$ with decay conditions at infinity, which define the well-known Kelvin fundamental solution, given by

$$U_i^k(\tilde{\boldsymbol{x}}, \boldsymbol{x}) = \frac{1}{16\pi\mu(1-\nu)r}[r_{,i} r_{,k} + (3-4\nu)\delta_{ik}] \tag{8}$$

$$T_i^k(\tilde{\boldsymbol{x}}, \boldsymbol{x}) = -\frac{1}{8\pi(1-\nu)r^2}[3r_{,i} r_{,k} r_{,j} n_j(\boldsymbol{x}) + (1-2\nu)(\delta_{ik} r_{,j} n_j(\boldsymbol{x}) + r_{,i} n_k(\boldsymbol{x}) - r_{,k} n_i(\boldsymbol{x}))] \tag{9}$$

with $r = |\boldsymbol{x} - \tilde{\boldsymbol{x}}|$ and $r_{,a} = \partial r / \partial x_a = (x_a - \tilde{x}_a)/r$. Other fundamental solutions are defined in terms of (usually) homogeneous boundary conditions on $\partial\hat{\Omega}$. They can sometimes be used to advantage in equation (7), in order to selectively eliminate contributions in the surface integrals. However, such fundamental solutions are known explicitly only in a few cases, and their mathematical complexity increases quite rapidly with the complexity of the underlying configuration $\hat{\Omega}$. Fundamental solutions are in particular known for a homogeneous traction-free half-space (see Mindlin, 1936 for the three-dimensional case) a layered, traction-free half-space (Chan *et al.*, 1974), a bimaterial full space with perfect bonding at a plane interface (Rongved, 1955; Guzina and Pak, 1999), and an elastic layer bounded by two parallel traction-free planes (Benitez and Rosakis, 1987), assuming isotropic elasticity in all cases. In addition, fundamental solutions are known for anisotropic elasticity, in the form of a Fourier angular integral for general anisotropy (Mura, 1982) and in explicit form for some special cases of anisotropy (see, e.g., Willis, 1965 or Pan and Chou, 1976).

It is essential to note that the fundamental solutions $U_i^k(\tilde{\boldsymbol{x}}, \boldsymbol{x})$ and $T_i^k(\tilde{\boldsymbol{x}}, \boldsymbol{x})$, respectively, behave like $O(1/r)$ and $O(1/r^2)$ for $\boldsymbol{x}$ close to $\tilde{\boldsymbol{x}}$, a feature that is apparent in (8), (9) for the Kelvin solution. In the context of BEMs $O(1/r)$ and $O(1/r^2)$, fundamental solutions are often referred to as being *weakly singular* and *strongly singular*, respectively.

2.2 Displacement boundary integral equation

Since the boundary conditions of a well-posed problem are such that either $\boldsymbol{u}$ or $\boldsymbol{t}$ (or some combination thereof) is known, equation (7) is not fully explicit in that it requires solving for the missing information on the boundary. It is therefore necessary, for that purpose, to set up equations that do not involve interior field values. However, merely selecting $\tilde{\boldsymbol{x}} \in \partial\Omega$ in (7), apparently an obvious solution to this issue, is not a valid procedure because the $(1/r^2)$ singularity of T_i^k makes the corresponding surface integral potentially divergent for $\tilde{\boldsymbol{x}} \in \partial\Omega$. Another possibility, namely to select $\tilde{\boldsymbol{x}} \in \bar{\Omega} = \mathbb{R}^3 \backslash \text{closure}(\Omega)$ (i.e., $\tilde{\boldsymbol{x}}$ exterior to Ω), is known to lead to ill-conditioned equations.

The standard procedure consists in finding a mathematically valid formulation for (7) with the observation point on $\partial\Omega$. Among the possible approaches for doing so, the ones most often used are as follows, denoting by $\boldsymbol{y}$ a generic observation point on $\partial\Omega$. The limit-to-the-boundary approach (Figure 1a), where the limiting form of the representation (7) for $\tilde{\boldsymbol{x}} = \boldsymbol{y} + \chi \boldsymbol{n}(\boldsymbol{y})$ as $\chi \to 0$ is sought, is used in classical monographs on potential theory (e.g., Kellogg, 1967 for scalar problems or Kupradze, 1979 in elasticity), and has been investigated in connection with BEMs by, for example, Gray *et al.* (1990). The limiting form of (7) thus obtained involves a free term and a singular surface integral, which is convergent according to a specific definition. Usually, Cauchy principal value (CPV) integrals are used for that purpose, in which case (7) leads to

$$\frac{1}{2} u_k(\boldsymbol{y}) + \fint_{\partial\Omega} T_i^k(\boldsymbol{y}, \boldsymbol{x}) u_i(\boldsymbol{x}) \, \mathrm{d}S_x - \int_{\partial\Omega} U_i^k(\boldsymbol{y}, \boldsymbol{x}) t_i(\boldsymbol{x}) \, \mathrm{d}S_x = \int_\Omega \{ U_i^k(\boldsymbol{y}, \boldsymbol{x}) f_i(\boldsymbol{x}) + \Sigma_{ab}^k(\boldsymbol{y}, \boldsymbol{x}) \varepsilon_{ab}^{\mathrm{I}}(\boldsymbol{x}) \} \, \mathrm{d}V_x \tag{10}$$

where the symbol $\fint$ indicates a CPV integral. The direct approach (Guiggiani and Gigante, 1990; Guiggiani, 1998) consists in removing a small *exclusion neighborhood* of characteristic size ε and specified shape around the singular point $\boldsymbol{y}$ and seek the limiting form of the exterior representation (7) for the punctured domain Ω_ε thus defined and its boundary $\partial\Omega_\varepsilon$ and with $\tilde{\boldsymbol{x}} = \boldsymbol{y}$ (Figure 1b). If the exclusion neighborhood chosen is spherical, the same limiting form (10) is found for the continuous integral equation.

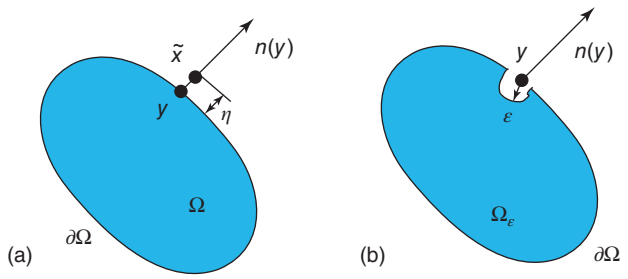

Figure 1. Notation for the limit-to-the-boundary approach (a) and the direct approach (b).

Finally, the indirect regularization approach (Rizzo and Shippy, 1977; Bui *et al.*, 1985) consists of using additional identities obtained by substituting simple solutions into (7). Here, applying (7) to the rigid-body displacement $\boldsymbol{v}(\boldsymbol{x})$ defined by $\boldsymbol{v}(\boldsymbol{x}) = \boldsymbol{u}(\boldsymbol{y})$ and subtracting the resulting identity from (7), both written for the punctured domain Ω_ε to ensure the mathematical validity of the process, one easily obtains the displacement integral equation in the regularized form as

$$\bar{\kappa} u_k(\boldsymbol{y}) + \int_{\partial\Omega} \left\{ T_i^k(\boldsymbol{y},\boldsymbol{x})[u_i(\boldsymbol{x}) - u_i(\boldsymbol{y})] - U_i^k(\boldsymbol{y},\boldsymbol{x}) t_i(\boldsymbol{x}) \right\} \mathrm{d}S_x = \int_\Omega \left\{ U_i^k(\boldsymbol{y},\boldsymbol{x}) f_i(\boldsymbol{x}) + \Sigma_{ab}^k(\boldsymbol{y},\boldsymbol{x}) \varepsilon_{ab}^{\mathrm{I}}(\boldsymbol{x}) \right\} \mathrm{d}V_x \tag{11}$$

with $\bar{\kappa} = 0$ (Ω bounded) or $\bar{\kappa} = 1$ ($\mathbb{R}^3 \backslash \Omega$ bounded). This integral equation is regularized, that is, all singular integrals over $\partial\Omega$ are convergent in the ordinary sense, provided $\boldsymbol{u}$ has $C^{0,\alpha}$ Hölder regularity at $\boldsymbol{x} = \boldsymbol{y}$. In particular, all domain integrals in (11) are convergent in the ordinary sense, that is, no regularization is needed for them.

2.3 Representation formulas for strains and stresses on the boundary

The displacement BIE (10) or (11) is sufficient for solving ordinary elasticity boundary value problems. However, neither the integral equations nor the representation formulas obtained up to now allow the direct computation of derivative quantities (i.e., displacement gradients, strains, stresses, etc.) when the observation point $\boldsymbol{y}$ is located on the domain boundary. Nevertheless, there are situations in which the availability of either an integral equation or a representation formula expressing such derivative quantities at boundary points is desirable, including (i) accurate evaluation of tangential stresses on the boundary, (ii) problems involving cracks (Section 6), (iii) symmetric Galerkin integral equation formulations (Section 4), (iv) the computation of local error indicators on the boundary, and (v) elastic–plastic problems where the plastic region reaches the boundary (Section 7).

Assuming for the moment that initial strains are absent, a straightforward application of compatibility equation (1) or constitutive equation (2) to (7) yields a representation formula for the linearized strain or the stress. For example, the stress tensor components at $\tilde{\boldsymbol{x}}$ are given by

$$\kappa(\tilde{\boldsymbol{x}})\sigma_{ij}(\tilde{\boldsymbol{x}}) = \int_{\partial\Omega} \left\{ \Sigma_{ij}^a(\boldsymbol{x},\tilde{\boldsymbol{x}}) t_a(\boldsymbol{x}) - D_{ijab}(\tilde{\boldsymbol{x}},\boldsymbol{x}) u_a(\boldsymbol{x}) \times n_b(\boldsymbol{x}) \right\} \mathrm{d}S_x + \int_\Omega \Sigma_{ij}^a(\boldsymbol{x},\tilde{\boldsymbol{x}}) f_a(\boldsymbol{x}) \, \mathrm{d}V_x \tag{12}$$

having utilized the identity $C_{ijk\ell} U^k_{a,\tilde{\ell}}(\tilde{\boldsymbol{x}},\boldsymbol{x}) = \Sigma_{ij}^a(\boldsymbol{x},\tilde{\boldsymbol{x}})$, which stems from symmetry properties of the fundamental solution (the tilde in $(\,)_{,\tilde{\ell}}$ denoting a partial derivative w.r.t. the ℓ-coordinate of $\tilde{\boldsymbol{x}}$), and with the new kernel $D_{ijab}(\tilde{\boldsymbol{x}},\boldsymbol{x})$ defined by

$$D_{ijab}(\tilde{\boldsymbol{x}},\boldsymbol{x}) = C_{ijk\ell} \Sigma^k_{ab,\tilde{\ell}}(\tilde{\boldsymbol{x}},\boldsymbol{x})$$

Since the interior integral representation formulas for derivative quantities, such as (12), have a nonintegrable singularity for $\tilde{\boldsymbol{x}} \in \partial\Omega$, they cannot directly be used in that case. Instead, one has to resort to a more involved procedure, based on either a careful limiting process or a regularization, in order to formulate mathematically valid integral representation formulas for observation points on the boundary. Obtaining such identities is the subject of an abundant literature, as witnessed in the survey paper by Tanaka *et al.* (1994). For example, combining an integration by parts procedure (Sladek and Sladek, 1983) and a regularization approach (Bonnet, 1989; Bonnet and Bui, 1993; Krishnasamy *et al.*, 1992), one obtains the following representation formula for stresses at boundary points:

$$\frac{1}{2}\sigma_{ij}(\boldsymbol{x}) = C_{ijk\ell} \int_{\partial\Omega} [D_{\ell b} u_a(\boldsymbol{x}) - D_{\ell b} u_a(\boldsymbol{y})] \Sigma^k_{ab}(\boldsymbol{y},\boldsymbol{x}) \, \mathrm{d}S_x - \int_{\partial\Omega} [t_a(\boldsymbol{x}) - t_a(\boldsymbol{y})] \Sigma^a_{ij}(\boldsymbol{x},\boldsymbol{y}) \, \mathrm{d}S_x + \int_\Omega \Sigma^a_{ij}(\boldsymbol{x},\tilde{\boldsymbol{x}}) f_a(\boldsymbol{x}) \, \mathrm{d}V_x + D_{\ell b} u_a(\boldsymbol{y}) C_{ijk\ell} A^k_{ab}(\boldsymbol{y},\partial\Omega) - t_a(\boldsymbol{y}) A^a_{ij}(\boldsymbol{y},\partial\Omega) \tag{13}$$

where it is assumed that the Kelvin fundamental solution (8), (9) is used and with

$$A^k_{ij}(\boldsymbol{x},S) = \frac{-1}{8\pi(1-\nu)} [(1-2\nu)(\delta_{ik} I_j + \delta_{sk} I_i - \delta_{ij} I_k) + 3 J_{ijk}] \tag{14}$$

$$I_a(\boldsymbol{x},S)=\int_S\left(\frac{1}{r}r_{,n}-K\right)n_a\frac{\mathrm{d}S_x}{r}-\int_{\partial S}\nu_a\frac{\mathrm{d}s_x}{r} \tag{15}$$

$$\begin{aligned}3J_{abc}(\boldsymbol{x},S)&=\delta_{ac}I_b(\boldsymbol{x},S)+\delta_{bc}I_a(\boldsymbol{x},S)\\&+\int_S(r_{,b}r_{,p}D_{pa}n_c\\&-D_a(n_bn_c)-D_b(n_an_c))\frac{\mathrm{d}S_x}{r}\\&+\int_S(2n_an_b-r_{,a}r_{,b})n_{,c}K\frac{\mathrm{d}S_x}{r}\\&+\delta_{ab}\int_S n_cr_{,n}\frac{\mathrm{d}S_x}{r^2}-2\int_S n_an_cn_br_{,n}\frac{\mathrm{d}S_x}{r^2}\\&+\int_{\partial S}(\nu_an_cn_b+\nu_bn_cn_a-r_{,a}r_{,b}\nu_c)\frac{\mathrm{d}s_x}{r}\\&+\int_{\partial S}(\nu_pn_a-\nu_an_p)r_{,p}r_{,b}n_c\frac{\mathrm{d}s_x}{r}\end{aligned} \tag{16}$$

In equations (13)–(16), the notation D_if stands for the tangential part of the Cartesian derivative $f_{,i}$ (i.e., $D_if:=f_{,i}-n_in_jf_{,j}$), $D_{ij}f:=n_if_{,j}-n_jf_{,i}=n_iD_jf-n_jD_if$ is another combination of tangential derivatives, $K:=D_in_i$ is (minus twice) the mean curvature of the surface, $r_{,n}:=(x_i-y_i)n_i(\boldsymbol{x})/r$ is the normal derivative of the distance function, and $\boldsymbol{\nu}$ denotes the unit normal to the edge ∂S of S lying in the plane tangent to S and pointing outside of S.

The stress representation formula (13) is regularized in that the differences $[D_{\ell b}u_a(\boldsymbol{x})-D_{\ell b}u_a(\boldsymbol{y})]$ and $[t_a(\boldsymbol{x})-t_a(\boldsymbol{y})]$ partially cancel the corresponding singular factor, so that overall the surface integrals are convergent in the ordinary sense. The regularization is effective only provided $\boldsymbol{\nabla u}$ (and hence $\boldsymbol{\sigma}$) is continuous at $\boldsymbol{y}$ (technically, one needs to assume that $\boldsymbol{\nabla u}$ has $C^{0,\alpha}$ Hölder regularity at $\boldsymbol{x}=\boldsymbol{y}$). This smoothness requirement is clearly sufficient, and numerical implementations are generally designed so as not to violate it, despite the severe constraints entailed (Section 6). Still, its necessary character has been the subject of some controversy (Cruse and Richardson, 1996; Martin and Rizzo, 1996; Martin *et al.*, 1998). Representation formulas of strain or stress on the boundary have been obtained using many strategies, including the direct approach, so that many equivalent forms have been proposed. A selection of references includes studies on fundamental issues (Frangi and Guiggiani, 2001; Schwab and Wendland, 1992), the development of direct approaches for defining BIEs with hypersingular kernels (Guiggiani *et al.*, 1992; Guiggiani, 1994, 1998; Frangi and Guiggiani, 1999, 2000), and other works of interest (Hildenbrand and Kuhn, 1992; Toh and Mukherjee, 1994).

3 THE BOUNDARY ELEMENT METHOD IN ELASTICITY: COLLOCATION

3.1 BEM discretization

To introduce the BEM discretization in its simplest form, let us consider the regularized integral equation (11) without body forces and initial strains, that is

$$\begin{aligned}\bar{\kappa}u_k(\boldsymbol{y})+\int_{\partial\Omega}\{&T_i^k(\boldsymbol{y},\boldsymbol{x})[u_i(\boldsymbol{x})-u_i(\boldsymbol{y})]\\&-U_i^k(\boldsymbol{y},\boldsymbol{x})t_i(\boldsymbol{x})\}\,\mathrm{d}S_x=0\qquad(\boldsymbol{y}\in\partial\Omega)\end{aligned} \tag{17}$$

where $\boldsymbol{y}\in\partial\Omega$ is generally referred to as a *collocation point* (generally speaking, a collocation is a discretization procedure involving exact enforcement of a continuous equation at a finite number of points). The basic BEM discretization process consists in dividing the surface $\partial\Omega$ into N_E *boundary elements* E_e ($1\le e\le N_\mathrm{E}$) of simple shape (usually curvilinear triangles or quadrangles), each of which being mapped on a reference element Δ_e (usually each Δ_e is either the square $\boldsymbol{\xi}=(\xi_1,\xi_2)\in[-1,1]^2$ or the triangle $0\le\xi_1+\xi_2\le1,\xi_1\ge0,\xi_2\ge0$). Each physical element E_e of the approximate boundary is mapped onto its parent element Δ_e (Figure 2) through

$$\boldsymbol{\xi}\in\Delta_e\to\boldsymbol{x}(\boldsymbol{\xi})=\sum_{q=1}^{N_e}N^q(\boldsymbol{\xi})\boldsymbol{x}^q\quad\boldsymbol{\xi}\in\Delta_e \tag{18}$$

in terms of N_e geometrical nodes $\boldsymbol{x}^q$ of $\partial\Omega$ and N_e *shape functions* $N^q(\boldsymbol{\xi})$, which are usually taken as interpolation polynomials originally introduced for the FEM in two dimensions. Then, the natural basis $(\boldsymbol{a}_1,\boldsymbol{a}_2)$, metric tensor $\boldsymbol{g}$, and unit normal $\boldsymbol{n}$ on E_e are given by

$$\boldsymbol{a}_\alpha(\boldsymbol{\xi})=\sum_{q=1}^{N}N^q_{,\alpha}(\boldsymbol{\xi})\boldsymbol{x}^q\qquad g_{\alpha\beta}(\boldsymbol{\xi})=\boldsymbol{a}_\alpha(\boldsymbol{\xi})\cdot\boldsymbol{a}_\beta(\boldsymbol{\xi})$$

$$J(\boldsymbol{\xi})\boldsymbol{n}(\boldsymbol{\xi})=\boldsymbol{a}_1\wedge\boldsymbol{a}_2\qquad J^2(\boldsymbol{\xi})=(g_{11}g_{22}-g_{12}^2)(\boldsymbol{\xi})$$

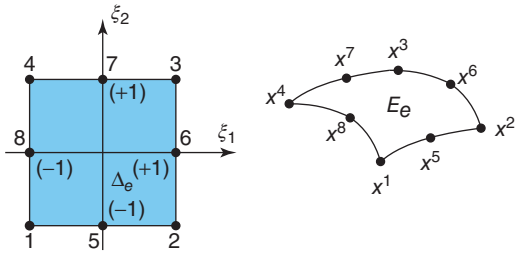

Figure 2. The eight-noded quadrilateral element: notation for the boundary element discretization.

$$(\boldsymbol{\xi} \in \Delta_e \,; \alpha, \beta = 1, 2) \tag{19}$$

The unknown boundary fields $(\boldsymbol{u}, \boldsymbol{t})$ are also interpolated in terms of nodal values $\boldsymbol{u}^k = \boldsymbol{u}(\boldsymbol{z}^k)$ and $\boldsymbol{t}^k = \boldsymbol{t}(\boldsymbol{z}^k)$ at interpolation nodes $\boldsymbol{z}^k$. In general, the set of interpolation nodes may differ from the set of the geometrical nodes, and the set of interpolation functions does not necessarily coincide with the set of shape functions. The presentation is here limited to the simplest case, referred to as *isoparametric interpolation*, where all these sets coincide, in which case, the unknowns are interpolated using

$$\boldsymbol{u}(\boldsymbol{y}) = \sum_{q=1}^{N_e} N_q(\boldsymbol{\xi}) \boldsymbol{u}^q \quad \boldsymbol{t}(\boldsymbol{y}) = \sum_{q=1}^{N_e} N_q(\boldsymbol{\xi}) \boldsymbol{t}^q \quad (\boldsymbol{\xi} \in \Delta_e) \tag{20}$$

Usually, the integral equation (17) is collocated at all nodes of the mesh (i.e., for $\boldsymbol{y} = \boldsymbol{y}^Q$, $1 \le Q \le N_\mathrm{N}$), and thus takes after the discretization process the following form:

$$\begin{aligned} 0 = \sum_{e \in \bar{I}(\boldsymbol{y}^Q)} \Bigg\{ & -u_i^Q \hat{A}_{ki}(\boldsymbol{y}^Q, e) + \sum_{p=1}^{N_e} \Big\{ A_{ki}(\boldsymbol{y}^Q, e, p) u_i^{m(e,p)} \\ & - B_{ki}(\boldsymbol{y}^Q, e, p) t_i^{m(e,p)} \Big\} \Bigg\} + \sum_{e \in I(\boldsymbol{y}^Q)} \sum_{p=1}^{N_e} \big\{ \tilde{A}_{ki}(\boldsymbol{y}^Q, e, p) \\ & \times u_i^{m(e,p)} - B_{ki}(\boldsymbol{y}^Q, e, p) t_i^{m(e,p)} \Big\} \\ & (1 \le Q \le N_\mathrm{N}, 1 \le k \le 3) \end{aligned} \tag{21}$$

where $m(e, p)$ denotes the global number of the pth node of element E_e and with the element matrices

$$\begin{aligned} B_{ki}(\boldsymbol{y}^Q, e, p) &= \int_{E_e} M_p(\boldsymbol{\xi}) U_i^k(\boldsymbol{y}^Q, \boldsymbol{x}(\boldsymbol{\xi})) J(\boldsymbol{\xi}) \, \mathrm{d}\boldsymbol{\xi} \\ A_{ki}(\boldsymbol{y}^Q, e, p) &= \int_{E_e} M_p(\boldsymbol{\xi}) T_i^k(\boldsymbol{y}^Q, \boldsymbol{x}(\boldsymbol{\xi})) J(\boldsymbol{\xi}) \, \mathrm{d}\boldsymbol{\xi} \\ \tilde{A}_{ki}(\boldsymbol{y}^Q, e, p) &= \int_{E_e} [M_p(\boldsymbol{\xi}) - M_p(\boldsymbol{\eta})] T_i^k(\boldsymbol{y}^Q, \boldsymbol{x}(\boldsymbol{\xi})) J(\boldsymbol{\xi}) \, \mathrm{d}\boldsymbol{\xi} \\ \hat{A}_{ki}(\boldsymbol{y}^Q, e) &= \int_{E_e} T_i^k(\boldsymbol{y}^Q, \boldsymbol{x}(\boldsymbol{\xi})) J(\boldsymbol{\xi}) \, \mathrm{d}\boldsymbol{\xi} \end{aligned}$$

where $\boldsymbol{\eta}$ denotes the antecedent of $\boldsymbol{y}^Q$ on Δ_e. The integration procedures for the calculation of these element matrices crucially depends on whether the collocation point is located on the integration element E_e or not; this distinction is emphasized in the above expressions by introducing the index subsets $I(\boldsymbol{y}) = \{e \in [1, N_\mathrm{E}], \boldsymbol{y} \in E_e\}$, and $\bar{I}(\boldsymbol{y}) = [1, N_\mathrm{E}] \backslash I(\boldsymbol{y})$.

The previously described discretization method is applicable, with straightforward adaptations, to many other types of BIEs.

3.1.1 Solution of the linear system of BEM equations

The linear system of equation (21) takes the form

$$[\boldsymbol{A}]\{\boldsymbol{u}\} + [\boldsymbol{B}]\{\boldsymbol{t}\} = \boldsymbol{0} \tag{22}$$

where $[\boldsymbol{A}]$ and $[\boldsymbol{B}]$ are fully populated $N \times N$ matrices (where $N = 3N_\mathrm{N}$) and $\{\boldsymbol{u}\} = \{u_i^m\}$, and $\{\boldsymbol{t}\} = \{t_i^m\}$ combined gather $2N$ scalar degrees of freedom (DOFs). The latter are constrained by N additional relations expressing the boundary conditions. Appropriate column swapping between the matrices $[\boldsymbol{A}]$ and $[\boldsymbol{B}]$ allows the separation of knowns (sent to the right-hand side) and unknowns (kept in the left-hand side). Equation (22) thus becomes a square linear system of equations:

$$[\boldsymbol{K}]\{\boldsymbol{X}\} = \{\boldsymbol{Y}\} \tag{23}$$

where $\{\boldsymbol{X}\}$ denotes an N-"vector" gathering all the scalar components of $\{\boldsymbol{u}\}, \{\boldsymbol{t}\}$ that remain unknown, the matrix $\boldsymbol{K}$, of size $N \times N$, is made of the columns $[\boldsymbol{A}], [\boldsymbol{B}]$ associated to the DOFs in $\{\boldsymbol{X}\}$, and $\{\boldsymbol{Y}\}$ is the right-hand side equal to (minus) the sum of those columns of $[\boldsymbol{A}], [\boldsymbol{B}]$ associated to known components of $\{\boldsymbol{u}\}, \{\boldsymbol{t}\}$ multiplied by the value taken by these components. In practice, the actual construction of the matrices $[\boldsymbol{A}], [\boldsymbol{B}]$ is best avoided, and the assembly procedure will directly produce $[\boldsymbol{K}]$ and $\{\boldsymbol{Y}\}$. Furthermore, the incorporation of the boundary data need not make explicit use of nodal values, but results instead from a direct integration of the relevant contributions of equation (17) when the prescribed data is analytically known as a function of the point coordinates. The assembly CPU time is $O(N^2)$.

The matrix $[\boldsymbol{K}]$ in (23) is fully populated and nonsymmetric. Therefore, equation (23) is usually solved by means of either an LU decomposition-based direct solver [an $O(N^3/3)$ procedure] or a generalized minimal residual (GMRES) iterative algorithm (Saad and Schultz, 1986); see **Linear Algebraic Solvers and Eigenvalue Analysis**. Both memory and CPU time requirements make BEM equations difficult and expensive to solve for large numbers of DOFs, using the standard approach as described in this section. This has prompted the development of fast solution techniques (Section 5) for large problems.

3.2 Numerical integration

The element matrices are usually evaluated using numerical integration techniques, which are selected

according to whether the integral is nonsingular, singular, or nearly singular. Additionally, significant effort has been directed toward analytical integrations when possible (Aimi and Diligenti, 2002; Carini and Salvadori, 2002; Nintcheu Fata, 2009; Niu *et al.*, 2005; Salvadori, 2001, 2002).

3.2.1 *Nonsingular integrals*

They occur when the collocation point is located away from the element. Standard quadrature techniques, usually of Gaussian type, are used. They are described in many books on numerical integration (Davis and Rabinowitz, 1975; Stroud and Secrest, 1966) or on computational mechanics. Owing to the $O(|\boldsymbol{y}^Q - \boldsymbol{x}|^{-1})$ or $O(|\boldsymbol{y}^Q - \boldsymbol{x}|^{-2})$ behavior of the fundamental solutions, it is advisable to adjust the number of Gauss points used according to the distance of $\boldsymbol{y}^Q$ to E_e (in relative terms, that is, compared to the element characteristic length). Criteria are proposed for that purpose in Lachat and Watson (1976) and Rezayat *et al.* (1986), among others.

3.2.2 *Singular integrals*

They occur when the collocation point is located on the element; in the isoparametric case, it is then located at one of the element nodes. When the BEM equations are obtained from a regularized integral equation like (17), the singular element integrals [here $\tilde{A}_{ki}(\boldsymbol{y}^Q, e, p)$ and $B_{ki}(\boldsymbol{y}^Q, e, p)$ of equation (21)] are convergent. Still, their accurate numerical computation requires their transformation into nonsingular integrals. This is usually done using a variable transformation in the parametric coordinates $\boldsymbol{\xi}$. The two most commonly used transformations are based on polar coordinates or Duffy triangular coordinates, respectively. Details can be found in textbooks on BEM, for example, Aliabadi (2001), Bonnet (1999a), and Kane (1994). If Δ_e is the unit square $\boldsymbol{\xi} \in [-1, 1]^2$, such transformations have the form

$$\begin{cases} \xi_1 = \eta_1 + u\cos v \\ \xi_2 = \eta_2 + u\sin v \end{cases} \quad \text{(polar)}$$

$$\begin{cases} \xi_1 = u + \eta_1(1-u) \\ \xi_2 = uv + \eta_2(1-u) \end{cases} \quad \text{(Duffy)} \qquad (24)$$

Note that the above Duffy coordinates map the triangle of vertices $\{\boldsymbol{\eta}, \boldsymbol{\xi} = (-1, 1), \boldsymbol{\xi} = (1, 1)\}$, that is, one of the four possible triangles sharing the vertex $\boldsymbol{\eta}$, onto the set $\{0 \le u \le 1, -1 \le v \le 1\}$ (Figure 3); similar transformations must be derived for the three other triangular subregions of Δ_e. In both cases, one has

$$|\boldsymbol{x}(\boldsymbol{\xi}) - \boldsymbol{y}^Q| = u\hat{\boldsymbol{r}}(u, v) \qquad \text{with} \quad \hat{\boldsymbol{r}}(0, v) \neq 0$$

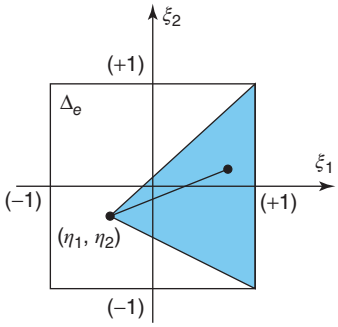

Figure 3. Eight-noded quadrilateral element: notation for the singular integration. The shaded triangular area corresponds to the Duffy coordinate mapping (24). (Reproduced with permission from Bonnet, 2003. © Springer 2003.)

so that the singular behavior of the fundamental solution is described in terms of the coordinate u. Furthermore, both choices also lead to

$$\mathrm{d}\boldsymbol{\xi} = ug(u, v))\ \mathrm{d}u\ \mathrm{d}v \quad \text{with} \quad g(0, v) \neq 0$$

Finally, for all the usual polynomial interpolations, there exist smooth functions $\hat{M}_p(u, v)$ such that

$$M_p(\boldsymbol{\xi}) - M_p(\boldsymbol{\eta}_e) = u\hat{M}_p(u, v)$$

Therefore, either mapping $\boldsymbol{\xi}(u, v)$ is readily seen to transform the integrals $\tilde{A}_{ki}(\boldsymbol{y}^Q, e, p)$ and $B_{ki}(\boldsymbol{y}^Q, e, p)$, or any similar weakly singular element integral arising in the BEM, into nonsingular integrals in (u, v), which can therefore be computed numerically using standard schemes, for example, Gaussian quadrature, in the (u, v) coordinates.

For other singular integration strategies, for example, the direct algorithm, the same transformations in $\boldsymbol{\xi}$-space are used in order to evaluate the singular contributions and perform the subsequent limiting processes analytically.

3.2.3 *Nearly singular integrals*

Integrals on an element E are *nearly singular* when the observation point $\boldsymbol{y}$ lies outside E but very close to it; the corresponding integrand, although nonsingular, presents a sharp and narrow peak, which makes accurate numerical integration very difficult. Such integrals occur in the case of adjacent elements of very dissimilar sizes, or when attempting to evaluate interior representation formulas such as (7) or (12) at observation points very close to the boundary. Standard numerical integration techniques usually yield poor results when applied to nearly singular integrals, and special techniques have therefore been proposed. Telles (1987) introduces a transformation of the parametric

element Δ_e onto itself so as to concentrate Gauss points near the orthogonal projection of $\boldsymbol{y}$ on E. An algorithm based on (orthogonal) projection (of the observation point) and angular and radial (variable) transformation (PART) is presented by Hayami and Matsumoto (1994) and refined in further papers. Adaptive techniques have been proposed by Schwab (1994), among others.

3.3 Computation of domain integrals

When nonzero body forces are present, the domain integral

$$\int_\Omega \rho F_i(\boldsymbol{x}) U_i^k(\boldsymbol{y},\boldsymbol{x})\ \mathrm{d}V_x \tag{25}$$

appears on the right-hand side in the integral equation, as in (11). Although it can conceivably be computed numerically (at the expense of introducing *integration cells*, that is, finite element–like domain subdivisions), it is obviously desirable, if at all possible, to convert it into boundary integrals, which is possible in several situations outlined below. The case of domain integrals involving initial strains is deferred to Section 7.

3.3.1 Isotropic elasticity and body forces deriving from a potential

Any fundamental solution $\boldsymbol{U}(\boldsymbol{y},\boldsymbol{x})$ for isotropic elasticity is representable in terms of the *Galerkin tensor* $\boldsymbol{G}(\boldsymbol{y},\boldsymbol{x})$ as

$$U_i^k(\boldsymbol{y},\boldsymbol{x}) = 2(1-\nu)G_{i,jj}^k(\boldsymbol{y},\boldsymbol{x}) - G_{j,ji}^k(\boldsymbol{y},\boldsymbol{x}) \tag{26}$$

where, for the three-dimensional Kelvin fundamental solution, $\boldsymbol{G}(\boldsymbol{y},\boldsymbol{x})$ is given by

$$G_i^k(\boldsymbol{y},\boldsymbol{x}) = F(\boldsymbol{y},\boldsymbol{x})\delta_{ik} = \frac{1}{16\pi(1-\nu)\mu} r\delta_{ik} \tag{27}$$

Also, assume the existence of a potential Φ and a constant b such that $\rho\boldsymbol{F} = \boldsymbol{\nabla}\,\Phi$ with $\Delta\Phi = b$. Then, the domain integral (25) can be converted by means of integrations by parts into a sum of boundary integrals

$$\begin{aligned}\int_\Omega \rho F_i U_i^k\ \mathrm{d}V_x = \int_{\partial\Omega} \{&(1+\chi)\Phi[G_{j,ii}^k - G_{i,ij}^k]n_j \\ &+ \chi\Phi_{,j} n_j G_{i,i}^k\}\ \mathrm{d}S_x - \chi b\int_{\partial\Omega} G_i^k n_i\ \mathrm{d}S_x\end{aligned} \tag{28}$$

(with $\chi = 1-2\nu$). This result includes several important situations: gravity forces (with $\Phi = -\rho g y_3$ and $b = 0$), centrifugal inertia [with $\Phi(\boldsymbol{x}) = (1/2)\rho\omega^2 R^2(\boldsymbol{x})$, $b = 2\rho\omega^2$, $\omega/2\pi$ being the rotation frequency and $R(\boldsymbol{x})$ the distance between $\boldsymbol{x}$ and rotation axis], and thermal loading induced by a steady-state temperature field T verifying $\Delta T = r$ (usually $r = 0$).

3.3.2 Multiple reciprocity method

Again in the context of using the three-dimensional Kelvin solution, introduce

$$G_i^{k(N)}(\boldsymbol{y},\boldsymbol{x}) = \frac{1}{16\pi\mu(1-\nu)}\delta_{ik}\frac{r^{2N+1}}{(2N+2)!}$$

Then, the sequence $\boldsymbol{U}^{(N)}(\boldsymbol{y},\boldsymbol{x}), N \geq 0$ of fundamental solutions defined by applying (26) to $\boldsymbol{G}^{(N)}(\boldsymbol{y},\boldsymbol{x})$ thus defined is such that $\boldsymbol{U}^{(0)}(\boldsymbol{y},\boldsymbol{x}) = \boldsymbol{U}(\boldsymbol{y},\boldsymbol{x})$ and $\boldsymbol{U}^{(N)}(\boldsymbol{y},\boldsymbol{x}) = \boldsymbol{\Delta U}^{(N+1)}(\boldsymbol{y},\boldsymbol{x})$. Repeated applications of the third Green identity to (25) then yield

$$\begin{aligned}\int_\Omega \boldsymbol{F}\cdot\boldsymbol{U}^k\ \mathrm{d}V_x = &\int_\Omega \boldsymbol{\Delta}^N\boldsymbol{F}\cdot\boldsymbol{U}^{k(N)}\ \mathrm{d}V_x \\ &+ \sum_{p=0}^{N-1}\int_{\partial\Omega}(\boldsymbol{U}_{,n}^{k(p+1)}\cdot\boldsymbol{\Delta}^p\boldsymbol{F} - \boldsymbol{U}^{k(p+1)}\cdot(\boldsymbol{\Delta}^p\boldsymbol{F})_{,n})\ \mathrm{d}S_x\end{aligned}$$

for an arbitrary value of N ($\boldsymbol{\Delta}^p$ denotes the vector Laplace operator iterated p times).

3.4 Miscellaneous issues

3.4.1 Interpolation of the traction vector

The traction vector is usually discontinuous across edges or at corners, whereas usual interpolation of the conformal type enforces continuity. This apparent contradiction can be addressed in several ways, depending on the particular situation at hand.

When all faces adjacent to an edge or corner except one support *prescribed* tractions, the prescribed contributions contribute directly to the r.h.s. of (23) and the nodal DOFs refer to the face supporting unknown tractions. When at least two adjacent faces support unknown tractions (a not-so-frequent situation), several options are available:

- Use discontinuous elements for the tractions, that is, elements for which *all* traction nodes are interior. Two drawbacks of this approach are (i) unwanted traction discontinuities are introduced, and (ii) there is a sharp increase in the number of traction DOFs.
- Treat the nodes located on edges or corners as double or multiple nodes, that is, consider them as separate nodes (one per face) that happen to be located at the same geometrical point (see Sladek and Sladek, 1991 for a critical discussion of this approach).

- Use selectively discontinuous elements, as proposed by Patterson and Sheikh (1984), where only nodes originally located on edges or corners are moved away from them, so as to enforce or relax traction continuity as needed. This is similar to the multiple-node approach, except that the relevant nodes are geometrically distinct as well due to shifting. It is best to avoid shifting by too small an amount in order to avoid nearly singular integrations when traction nodes are also collocation points.

3.4.2 *Postprocessing: computation of elastic field values at interior points*

The evaluation of interior representation formulas such as (7) or (12) is a straightforward task, except (as mentioned before) for observation points very close to the boundary. The computational cost is $O(N)$ for each observation point, $\tilde{\boldsymbol{x}}$, because all integrals must be recomputed when $\tilde{\boldsymbol{x}}$ is changed. Therefore, evaluating, for example, the stress distribution over a grid of observation points, can be computationally expensive, and benefit greatly from the kind of acceleration techniques presented in Section 5.

3.4.3 *Postprocessing: evaluation of stresses on the boundary*

Once the BEM equations are solved, the displacement and traction distributions on the boundary are known. In principle, the stress tensor can be computed at any point of the boundary from this information. Writing the displacement gradient $\boldsymbol{\nabla u}$ in its tangential and normal parts $\boldsymbol{\nabla}_S \boldsymbol{u}$ and $\boldsymbol{u}_{,n}$, one has

$$\boldsymbol{\sigma}(\boldsymbol{y}) = \boldsymbol{C} : (\boldsymbol{\nabla}_S \boldsymbol{u} + \boldsymbol{u}_n \otimes \boldsymbol{n})(\boldsymbol{y}) \qquad (\boldsymbol{y} \in \partial\Omega) \tag{29}$$

The tangential gradient $\boldsymbol{\nabla}_S \boldsymbol{u}$ can be computed by means of a differentiation of the displacement interpolation (20), while the normal derivative $\boldsymbol{u}_{,n}$ is expressible in terms of $\boldsymbol{t}$ and $\boldsymbol{\nabla}_S \boldsymbol{u}$ from the relation

$$\boldsymbol{t} = \boldsymbol{n} \cdot \boldsymbol{C} : (\boldsymbol{\nabla}_S \boldsymbol{u} + \boldsymbol{u}_n \otimes \boldsymbol{n}) \tag{30}$$

This method is computationally economical but not always accurate (Guiggiani, 1994). A better but more expensive approach consists of evaluating the integral representation formula for the stress on the boundary, either in a regularized form such as (13) or by means of the direct algorithm for hypersingular integrals (Guiggiani, 1994, 1998). Each stress evaluation is then an $O(N)$ computation, so the cost using standard methods can become significant for a large number of evaluation points.

4 THE BOUNDARY ELEMENT METHOD IN ELASTICITY: SYMMETRIC GALERKIN

As emphasized in the previous section, the standard (collocation) approach to BEM leads to matrix equations whose matrix has, in general, no symmetry. Since (assuming the use of direct solvers and keeping the problem size fixed) both storage and computing time requirements for a symmetric BEM formulation would be half those for a nonsymmetric BEM formulation, there is a strong practical incentive to derive symmetric BEM formulations. In addition, formulations based on symmetric operators are more amenable to mathematical justification (existence, uniqueness, and convergence properties of the numerical scheme). Since the fundamental variational principles of solid mechanics involve symmetric energy bilinear operators, the possibility of deriving symmetric BEM formulations is to be expected.

The collocation BEM is based on displacement integral equations like (17) or traction integral equations like the inner product of (13) by $n_j(\boldsymbol{y})$, which have the form of pointwise residuals set equal to zero: $r_k^{\mathrm{U}}(\boldsymbol{y}) = 0$ or $r_i^{\mathrm{T}}(\boldsymbol{y}) = 0$, respectively. It is natural to consider weighted residual forms of such equations, in analogy with the weak formulations on which FEMs are based, in the form

$$\int_{\partial\Omega} \tilde{t}_k(\boldsymbol{y}) r_k^{\mathrm{U}}(\boldsymbol{y})\, \mathrm{d}S_y = 0 \quad \text{and} \quad \int_{\partial\Omega} \tilde{u}_i(\boldsymbol{y}) r_i^{\mathrm{T}}(\boldsymbol{y})\, \mathrm{d}S_y = 0$$

where $\tilde{t}_k(\boldsymbol{y})$ and $\tilde{u}_i(\boldsymbol{y})$ are trial functions, their notations being chosen so that the weighted residuals are work-like. They are usually referred to as Galerkin boundary element method (GBEM) formulations. In particular, GBEM formulations lead to relaxed smoothness requirements on the unknowns compared to the collocation of residuals. This constitutes a substantial practical advantage for the traction integral equation, which, among other things, is an essential component of BEM formulations for fracture mechanics (Section 6). SGBEM formulations are also useful for multidomain configurations, as shown by, for example, Kallivokas *et al.* (2005).

Although GBEM formulations need not be symmetric (Parreira and Guiggiani, 1989), most of the research on GBEM formulations has been directed toward symmetric Galerkin boundary element method (SGBEM) formulations. Mathematical expositions of SGBEMs can be found in books by, for example, Sauter and Schwab (2011) and Steinbach (2008), whereas general references on SGBEMs for solid mechanics include the review article by Bonnet *et al.* (1998a) and the book by Sutradhar *et al.* (2008). The symmetry in

the GBEM formulation is achieved by selecting the trial functions in a manner that is dependent on the boundary condition structure of the problem at hand. For the sake of definiteness, assume that $\partial\Omega$ is split into two disjoint and complementary components S_u and S_t on which displacements and tractions, respectively, are prescribed, that is

$$\boldsymbol{u} = \bar{\boldsymbol{u}} \text{ (on } S_u), \qquad \boldsymbol{t} = \bar{\boldsymbol{t}} \text{ (on } S_t) \tag{31}$$

Representative examples of the implementation of SGBEMs for solid mechanics problems include (Burgardt, 1999; Haas and Kuhn, 2002; Frangi *et al.*, 2001). The indeterminacy of SGBEM formulations where whole internal connected components of the boundary support traction-free conditions (e.g., for solids containing voids) has been analyzed and solved by Freddi and Royer-Carfagni (2006).

4.1 Variational formulation

It is interesting to see that the SGBEM formulation for linear elasticity (assuming the absence of body forces and initial strains) is not merely a weighted residual statement, but can be established from fundamental variational principles of linear elasticity. To that purpose, consider the augmented potential energy

$$E(\boldsymbol{v}) = \int_\Omega \boldsymbol{\varepsilon}(\boldsymbol{v}) : \boldsymbol{C} : \boldsymbol{\varepsilon}(\boldsymbol{v}) \, \mathrm{d}V - \int_{S_t} \bar{\boldsymbol{t}} \cdot \boldsymbol{v} \, \mathrm{d}S - \int_{S_u} \boldsymbol{t}(\boldsymbol{u}) \cdot (\boldsymbol{v} - \bar{\boldsymbol{u}}) \, \mathrm{d}S \tag{32}$$

where the prescribed displacement appears explicitly as a constraint term. Letting $\boldsymbol{v} = \boldsymbol{u} + \delta\boldsymbol{u}$, the stationarity condition is

$$\delta E(\boldsymbol{u}) = \int_\Omega \boldsymbol{\varepsilon}(\boldsymbol{u}) : \boldsymbol{C} : \boldsymbol{\varepsilon}(\delta\boldsymbol{u}) \, \mathrm{d}V - \int_{S_t} \bar{\boldsymbol{t}} \cdot \delta\boldsymbol{u} \, \mathrm{d}S - \int_{S_u} \boldsymbol{t}(\boldsymbol{u}) \cdot \delta\boldsymbol{u} \, \mathrm{d}S = 0 \quad (\forall \delta\boldsymbol{u})$$

where the variations $\delta\boldsymbol{u}$ are unconstrained and the boundary condition (31a) must be enforced additionally. Restricting the stationarity equation to trial functions $\delta\boldsymbol{u}$, which satisfy the elastic equilibrium field equation (i.e., $\operatorname{div}(\boldsymbol{C} : \boldsymbol{\varepsilon}(\delta\boldsymbol{u})) = \boldsymbol{0}$), an integration by parts leads to

$$\delta E(\boldsymbol{u}) = \int_{S_t} \bar{\boldsymbol{u}} \cdot \boldsymbol{t}(\delta\boldsymbol{u}) \, \mathrm{d}S + \int_{S_u} \boldsymbol{u} \cdot \boldsymbol{t}(\delta\boldsymbol{u}) \, \mathrm{d}S - \int_{S_t} \bar{\boldsymbol{t}} \cdot \delta\boldsymbol{u} \, \mathrm{d}S - \int_{S_u} \boldsymbol{t}(\boldsymbol{u}) \cdot \delta\boldsymbol{u} \, \mathrm{d}S = 0 \quad (\forall \delta\boldsymbol{u}, \operatorname{div}(\boldsymbol{C} : \boldsymbol{\varepsilon}(\delta\boldsymbol{u})) = \boldsymbol{0}) \tag{33}$$

Any such trial functions can be expressed using (7) and (12) in the form of integral representations:

$$\delta u_k(\tilde{\boldsymbol{x}}) = \int_{S_t} \tilde{u}_i(\boldsymbol{x}) T_i^k(\tilde{\boldsymbol{x}}, \boldsymbol{x}) \, \mathrm{d}S_x - \int_{S_u} \tilde{t}_i(\boldsymbol{x}) U_i^k(\tilde{\boldsymbol{x}}, \boldsymbol{x}) \, \mathrm{d}S_x \tag{34}$$

$$\delta t_k(\tilde{\boldsymbol{x}}) = \int_{S_t} \tilde{u}_i(\boldsymbol{x}) D_{ijk\ell}(\tilde{\boldsymbol{x}}, \boldsymbol{x}) n_j(\tilde{\boldsymbol{x}}) n_\ell(\boldsymbol{x}) \, \mathrm{d}S_x - \int_{S_u} \tilde{t}_i(\boldsymbol{x}) T_i^k(\boldsymbol{x}, \tilde{\boldsymbol{x}}) \, \mathrm{d}S_x \tag{35}$$

Inserting (34) and (35) into the stationarity equation (33), in principle, yields the desired SGBEM formulation. However, owing to the presence of the strongly singular kernel $T_i^k(\boldsymbol{x}, \tilde{\boldsymbol{x}}) = O(1/r^2)$ and the hypersingular kernel $D_{ijab}(\tilde{\boldsymbol{x}}, \boldsymbol{x}) = O(1/r^3)$, a more careful approach is called for, involving a limiting process. This technical step is well documented and can be performed using either a limit-to-the-boundary approach (Gray, 1998), an extension to SGBEM of the direct algorithm (Bonnet and Guiggiani, 2003), or a regularization (Bonnet, 1995c). All three strategies aim at formulating mathematically well-defined sets of SGBEM equations that are amenable to numerical implementation. The various SGBEM formulations thus obtained may be superficially different but are equivalent. The SGBEM formulation obtained following the regularization approach is as follows:

Find $\hat{\boldsymbol{u}} \in \mathcal{V}_u, \boldsymbol{t} \in \mathcal{V}_t$ such that

$$\begin{cases} \mathcal{B}_{uu}(\hat{\boldsymbol{u}}, \tilde{\boldsymbol{u}}) + \mathcal{B}_{tu}(\boldsymbol{t}, \tilde{\boldsymbol{u}}) = \mathcal{L}_u(\tilde{\boldsymbol{u}}; \bar{\boldsymbol{t}}) \\ \mathcal{B}_{ut}(\hat{\boldsymbol{u}}, \tilde{\boldsymbol{t}}) + \mathcal{B}_{tt}(\boldsymbol{t}, \tilde{\boldsymbol{t}}) = \mathcal{L}_t(\tilde{\boldsymbol{t}}; \bar{\boldsymbol{u}}) \end{cases} \quad \forall \tilde{\boldsymbol{u}} \in \mathcal{V}_u, \forall \tilde{\boldsymbol{t}} \in \mathcal{V}_t \tag{36}$$

where the sets $\mathcal{V}_u, \mathcal{V}_t$ of admissible functions are

$$\mathcal{V}_u = \{\tilde{\boldsymbol{u}} \mid \tilde{\boldsymbol{u}} \in C^{0,\alpha}(S_t) \text{ and } \tilde{\boldsymbol{u}} = \boldsymbol{0} \text{ on } \partial S_t\}$$
$$\mathcal{V}_t = \{\tilde{\boldsymbol{t}} \mid \tilde{\boldsymbol{t}} \text{ piecewise continuous on } S_u\}$$

while the bilinear operators are given by

$$\mathcal{B}_{uu}(\hat{\boldsymbol{u}}, \tilde{\boldsymbol{u}}) = \int_{S_t}\int_{S_t} R_q \hat{u}_i(\boldsymbol{x}) R_s \tilde{u}_k(\tilde{\boldsymbol{x}}) \times B_{ikqs}(\tilde{\boldsymbol{x}}, \boldsymbol{x}) \, \mathrm{d}S_x \, \mathrm{d}S_{\tilde{x}} \tag{37}$$

$$\mathcal{B}_{tu}(\boldsymbol{t}, \tilde{\boldsymbol{u}}) = -\int_{S_u}\int_{S_t} t_k(\boldsymbol{x}) \tilde{u}_i(\tilde{\boldsymbol{x}}) T_i^k(\boldsymbol{x}, \tilde{\boldsymbol{x}}) \, \mathrm{d}S_x \, \mathrm{d}S_{\tilde{x}} = \mathcal{B}_{ut}(\tilde{\boldsymbol{u}}, \boldsymbol{t}) \tag{38}$$

$$\mathcal{B}_{tt}(\boldsymbol{t},\tilde{\boldsymbol{t}}) = \int_{S_u}\int_{S_u} t_k(\boldsymbol{x})\tilde{t}_i(\tilde{\boldsymbol{x}})U_i^k(\boldsymbol{x},\tilde{\boldsymbol{x}})\ \mathrm{d}S_x\ \mathrm{d}S_{\tilde{x}} \tag{39}$$

and the linear operators are given by

$$\begin{aligned}\mathcal{L}_u(\tilde{\boldsymbol{u}}) = &\int_{S_t}(\bar{\kappa}(\boldsymbol{x})-1)\bar{t}_k(\boldsymbol{x})\tilde{u}_k(\boldsymbol{x})\ \mathrm{d}S_{\tilde{x}}\\ &-\int_{\partial\Omega}\int_{S_u} R_q\hat{\tilde{u}}_i(\boldsymbol{x})R_s\tilde{u}_k(\tilde{\boldsymbol{x}})B_{iqks}(\tilde{\boldsymbol{x}},\boldsymbol{x})\ \mathrm{d}S_x\ \mathrm{d}S_{\tilde{x}}\\ &+\int_{S_t}\int_{S_t}\bar{t}_k(\boldsymbol{x})[\tilde{u}_i(\tilde{\boldsymbol{x}})-\tilde{u}_i(\boldsymbol{x})]T_i^k(\boldsymbol{x},\tilde{\boldsymbol{x}})\ \mathrm{d}S_x\ \mathrm{d}S_{\tilde{x}}\\ &-\int_{S_t}\int_{S_u}\bar{t}_k(\boldsymbol{x})\tilde{u}_i(\boldsymbol{x})T_i^k(\boldsymbol{x},\tilde{\boldsymbol{x}})\ \mathrm{d}S_x\ \mathrm{d}S_{\tilde{x}}\end{aligned} \tag{40}$$

$$\begin{aligned}\mathcal{L}_t(\tilde{\boldsymbol{t}}) = &\int_{S_u}\bar{\kappa}(\boldsymbol{x})\tilde{t}_k(\boldsymbol{x})\bar{u}_k(\boldsymbol{x})\ \mathrm{d}S_{\tilde{x}}\\ &+\int_{S_u}\int_{\partial\Omega}\tilde{t}_k(\tilde{\boldsymbol{x}})[\hat{\tilde{u}}_i(\boldsymbol{x})-\hat{\tilde{u}}_i(\tilde{\boldsymbol{x}})]T_i^k(\tilde{\boldsymbol{x}},\boldsymbol{x})\ \mathrm{d}S_{\tilde{x}}\ \mathrm{d}S_x\\ &-\int_{S_u}\int_{S_t}\bar{t}_k(\boldsymbol{x})\tilde{t}_i(\tilde{\boldsymbol{x}})U_i^k(\boldsymbol{x},\tilde{\boldsymbol{x}})\ \mathrm{d}S_x\ \mathrm{d}S_{\tilde{x}}\end{aligned} \tag{41}$$

In equations (40) and (41), the function $\bar{\kappa}(\boldsymbol{x})$ is such that either $\bar{\kappa}(\boldsymbol{x}) = 0$ (if $\boldsymbol{n}$ is exterior to $\partial\Omega$ at $\boldsymbol{x}$, e.g., when $\partial\Omega$ is the external boundary of a bounded body) or $\bar{\kappa}(\boldsymbol{x}) = 1$ (if $\boldsymbol{n}$ is interior to $\partial\Omega$ at $\boldsymbol{x}$, e.g., when $\partial\Omega$ is the boundary of an unbounded medium or of a cavity).

One key identity in obtaining this result, due to Nedelec (1982), reads

$$D_{ijk\ell}(\tilde{\boldsymbol{x}},\boldsymbol{x})n_j(\tilde{\boldsymbol{x}})n_\ell(\boldsymbol{x}) = R_q^x R_s^{\tilde{x}} B_{ikqs}(\tilde{\boldsymbol{x}},\boldsymbol{x})$$

where $R_a f \equiv e_{abc}n_b f_{,c}$ is the *surface curl* operator and

$$\begin{aligned}B_{ikqs}(\tilde{\boldsymbol{x}},\boldsymbol{x}) = \frac{\mu}{4\pi(1-\nu)r}[&\delta_{qs}r_{,i}r_{,k}+\delta_{ik}\delta_{qs}\\ &-2\nu\delta_{is}\delta_{qk}-(1-\nu)\delta_{iq}\delta_{ks}]\end{aligned}$$

This identity, together with a variant of the Stokes formula, allows the transformation of the integral containing the hypersingular kernel $D_{ijk\ell}(\tilde{\boldsymbol{x}},\boldsymbol{x})n_j(\tilde{\boldsymbol{x}})n_\ell(\boldsymbol{x})$ into one involving the weakly singular kernel $B_{ikqs}(\tilde{\boldsymbol{x}},\boldsymbol{x}) = O(1/r)$ instead. The symmetric character of the GBEM formulation (36–41) can be checked by close inspection. In particular, a new unknown $\hat{\boldsymbol{u}}$ defined by

$$\hat{\boldsymbol{u}} = \boldsymbol{u} - \hat{\tilde{\boldsymbol{u}}} \qquad \text{on } S_t$$

has been introduced, so that both $\hat{\boldsymbol{u}}$ and $\tilde{\boldsymbol{u}}$ are in the same function space $\mathcal{V}_u$.

4.2 Solution of the linear system of SGBEM equations

Interpolating the boundary and the unknowns in the manner described in Section 3, a system of linear equations of the form

$$\begin{bmatrix}\boldsymbol{B}_{uu} & -\boldsymbol{B}_{tu}\\ -\boldsymbol{B}_{ut} & \boldsymbol{B}_{tt}\end{bmatrix}\begin{Bmatrix}\boldsymbol{U}\\ \boldsymbol{T}\end{Bmatrix} = \begin{Bmatrix}\boldsymbol{L}_u\\ \boldsymbol{L}_t\end{Bmatrix} \tag{42}$$

is eventually reached. It is important to note that the matrix is symmetric but not sign-definite (except for the special cases of pure Dirichlet and pure Neumann problems). Thus, Cholesky decomposition does not apply except for the special cases. However, direct linear solvers for indefinite symmetric matrices are expounded in Golub and Van Loan (1989), and codes are provided, for example, in software libraries like LAPACK (Anderson *et al.*, 1995). Such direct solvers, as well as the Cholesky algorithm for sign-definite symmetric matrices, need $O(N^3)/6$ arithmetic operations. In addition, iterative solvers like biconjugate gradient or GMRES can also be applied to (42). Iterative solvers are discussed in Greenbaum (1997) in general terms, and in (Hackbusch and Wittum, 1996; Wendland, 1997) in connection with SGBEM.

4.3 Numerical integration

The SGBEM involves *double* element integrals. For example, the bilinear operator $\mathcal{B}_{tt}$ gives rise to

$$\int_E\int_{E'} N_p(\boldsymbol{\xi})N_{\tilde{p}}(\tilde{\boldsymbol{\xi}})U_i^k(\boldsymbol{x}(\boldsymbol{\xi}),\tilde{\boldsymbol{x}}(\tilde{\boldsymbol{\xi}}))J(\boldsymbol{\xi})J(\tilde{\boldsymbol{\xi}})\ \mathrm{d}\boldsymbol{\xi}\ \mathrm{d}\tilde{\boldsymbol{\xi}}$$

There are four kinds of double element integrals, with singularity of increasing severity:

(i) Disjoint integrations, where E and E' are separated; they are nonsingular and can be computed using, for example, Gauss quadrature formulas (either Cartesian products of 1D Gaussian rules or 4D Gaussian rules; see Stroud, 1971).

(ii) Vertex-adjacent integrals, where E and E' share a common vertex.

(iii) Edge-adjacent integrals, where E and E' share a common edge.

(iv) Coincident integrals, where $E = E'$.

In cases (ii), (iii), and (iv), it is best to treat the integrals as Four dimensional rather than a succession of two-dimensional integrals (in the latter case, situations (ii) and (iii) may give rise to nearly singular integrals over E' for Gauss points in E close to a vertex or edge, for which care must be exercised). Variable transformations such as

generalizations of Duffy coordinates for the 4D $(\xi, \tilde{\xi})$-space (Frangi *et al.*, 2001) then allow recasting of all these singular integrals into nonsingular integrals.

Analytical integration approaches have also been developed for the double element integrals arising in the SGBEM, see, for example, Carini *et al.* (1999) or Lenoir and Salles (2012).

5 FAST SOLUTION TECHNIQUES

As mentioned in Sections 3 and 4, the fully populated character of the governing matrix operator in the discretized BEM equations (23) or (42) creates severe limitations in the size of BEM discretizations (typically to around 10 000 DOFs), because of both memory space and computing time requirements, when conventional methods such as these previously discussed are used. In particular, recall that the solution using direct algorithms is an $O(N^3)$ computation.

To improve this situation, the main remedy consists of using iterative solvers. Algorithms such as GMRES (Saad and Schultz, 1986) for general (possibly unsymmetric) invertible matrices or the conjugate gradient for symmetric positive-definite matrices require repeated calculations of matrix–vector products $[\boldsymbol{K}]\{\boldsymbol{X}\}$, where $\{\boldsymbol{X}\}$ assumes various trial values for the unknown DOFs until convergence is reached. In particular, the governing matrix $[\boldsymbol{K}]$ need not be stored. Computing one matrix–vector product is an $O(N^2)$ task. Hence, solving the BEM equations iteratively is an $O(KN^2)$ task, where K depends on parameters such as the iteration count, preconditioning methods, and accuracy requested for convergence, and usually increases slowly with N (i.e., $K(N)/N = o(1)$ for large N). This is a step in the right direction, but the $O(N^2)$ cost of matrix–vector products still remains a significant obstacle. Furthermore, storage of the governing matrix $[\boldsymbol{K}]$ is avoided only at the cost of recomputing it each time, a lengthy $O(N^2)$ computation because of the high cost of numerical integration.

To significantly accelerate BEM algorithms for large-sized problems, it is therefore essential that the matrix–vector products be computable, at least in an approximate way, with a complexity better than $O(N^2)$; (see **Multigrid Methods for FEM and BEM Applications**, **Panel Clustering Techniques and Hierarchical Matrices for BEM and FEM**). Several approaches, outlined in the remainder of this section, are available for doing so. In the interest of a compact exposition, it is worth noting that all matrix–vector products relevant to the BEM arise from the discretization of integral operators having the generic form

$$[\mathcal{K}u](\tilde{\boldsymbol{x}}) \equiv \int_{\partial\Omega} K(\tilde{\boldsymbol{x}}, \boldsymbol{x}) u(\boldsymbol{x}) \, \mathrm{d}S_x \tag{43}$$

leading to a generic discretized form $[\boldsymbol{K}]\{\boldsymbol{u}\}$, via either a collocation or a Galerkin formulation.

5.1 The fast multipole method

The evaluation of $[\boldsymbol{K}]\{\boldsymbol{u}\}$ by classical methods is a $O(N^2)$ task because the kernel $K(\tilde{\boldsymbol{x}}, \boldsymbol{x})$ is a two-point function; thus all element integrals must be recomputed each time a new location of $\tilde{\boldsymbol{x}}$ is used. The fast multipole method (FMM) relies on a series expansion of $K(\tilde{\boldsymbol{x}}, \boldsymbol{x})$ in the form

$$K(\tilde{\boldsymbol{x}}, \boldsymbol{x}) = \sum_{n \geq 0} k_n^{(1)}(\tilde{\boldsymbol{x}}, \boldsymbol{x}_0) k_n^{(2)}(\boldsymbol{x}, \boldsymbol{x}_0) \tag{44}$$

with $|\boldsymbol{x} - \boldsymbol{x}_0| < |\tilde{\boldsymbol{x}} - \boldsymbol{x}_0|$. The functions $k_n^{(1)}(\tilde{\boldsymbol{x}}, \boldsymbol{x}_0)$ are singular at $\tilde{\boldsymbol{x}} = \boldsymbol{x}_0$, while $k_n^{(2)}(\boldsymbol{x}, \boldsymbol{x}_0)$ are smooth at $\boldsymbol{x} = \boldsymbol{x}_0$. The truncation error bound of the series for a truncation level $n = p$ is known and typically depends on the ratio $|\boldsymbol{x} - \boldsymbol{x}_0|/|\tilde{\boldsymbol{x}} - \boldsymbol{x}_0|$ (a smaller ratio requiring a lower p to achieve a given level of accuracy). Expansions of the form (44) can be found by means of a Taylor expansion w.r.t. $\boldsymbol{x}$ about $\boldsymbol{x}_0$ ($k_n^{(2)}(\boldsymbol{x}, \boldsymbol{x}_0)$ being, in that case, polynomials), like in Fu *et al.* (1998). For kernels related to Laplace, elastostatics, or Stokes flow problems (among others), expansions (44) can also be formulated from that of $1/|\boldsymbol{x} - \tilde{\boldsymbol{x}}|$ involving spherical harmonics. The value at $\tilde{\boldsymbol{x}}$ of $K(\tilde{\boldsymbol{x}}, \boldsymbol{x})$ then takes the form of a superposition of the effects of monopoles, dipoles, quadrupoles, and so on, located at $\boldsymbol{x}$, that is, multipoles.

One essential feature of (44) is the reformulation of $K(\tilde{\boldsymbol{x}}, \boldsymbol{x})$ into a sum of products of functions of $\tilde{\boldsymbol{x}}$ and functions of $\boldsymbol{x}$, which means that integrations w.r.t. $\boldsymbol{x}$ performed for one choice of $\tilde{\boldsymbol{x}}$ can be reused for another $\tilde{\boldsymbol{x}}$, thus enabling a complexity better than $O(N^2)$. However, since (44) holds only for integration points closer to the origin $\boldsymbol{x}_0$ than the collocation point $\tilde{\boldsymbol{x}}$, the same origin $\boldsymbol{x}_0$ cannot be used for all the element integrations. One idea is to divide the BE mesh into M regions S_m $(1 \leq m \leq M)$. The contribution of S_m to the integral (43) is then evaluated by standard (singular or nonsingular) procedures if $\tilde{\boldsymbol{x}}$ lies on S_m or a region adjacent to S_m, and invoke (44) with $\boldsymbol{x}_0 = \boldsymbol{x}_0^m \in S_m$ when $\tilde{\boldsymbol{x}}$ lies on a non-adjoining region. An operation count evaluation shows that the optimal choice $m = O(N^{2/3})$ leads to a $O(N^{4/3})$ complexity for the overall matrix–vector evaluation (Nishimura, 2002).

The FMM, first introduced in Rokhlin (1985) and Greengard and Rokhlin (1987), improves on this idea. Contributions to the evaluation of (43) of elements containing $\tilde{\boldsymbol{x}}$ or close to $\tilde{\boldsymbol{x}}$ are evaluated using the traditional element integration methods (this is a $O(N)$ contribution to the overall matrix–vector computation). Other contributions are evaluated on the basis of the kernel expansion (44) recast

in the form

$$K(\tilde{\boldsymbol{x}},\boldsymbol{x}) = \sum_{m\geq 0}\sum_{n\geq 0} h_m^{(1)}(\tilde{\boldsymbol{x}},\tilde{\boldsymbol{x}}_0)T_{mn}(\tilde{\boldsymbol{x}}_0,\boldsymbol{x}_0)k_n^{(2)}(\boldsymbol{x},\boldsymbol{x}_0) \qquad (45)$$

where the new origin $\tilde{\boldsymbol{x}}_0$ is closer to $\tilde{\boldsymbol{x}}$ than to $\boldsymbol{x}$. Then, one has

$$\int_{S_{\tilde{x}}} K(\tilde{\boldsymbol{x}},\boldsymbol{x})u(\boldsymbol{x})\,\mathrm{d}S_x = \sum_{m\geq 0} h_m^{(1)}(\tilde{\boldsymbol{x}},\tilde{\boldsymbol{x}}_0)L_m(\tilde{\boldsymbol{x}}_0)$$

where $S_{\tilde{x}}$ denotes a subset of $\partial\Omega$ such that $\tilde{\boldsymbol{x}} \notin S_{\tilde{x}}$, and with the *local expansion* $L_m(\tilde{\boldsymbol{x}}_0)$ given by

$$L_m(\tilde{\boldsymbol{x}}_0) = \sum_{n\geq 0} T_{mn}(\tilde{\boldsymbol{x}}_0,\boldsymbol{x}_0)M_n(\boldsymbol{x}_0)$$

in terms of the *multipole moments* $M_n(\boldsymbol{x}_0)$:

$$M_n(\boldsymbol{x}_0) = \int_{S_{\tilde{x}}} k_n^{(2)}(\boldsymbol{x},\boldsymbol{x}_0)u(\boldsymbol{x})\,\mathrm{d}S_x$$

One sees that the local expansions $L_m(\tilde{\boldsymbol{x}}_0)$ allow the computation of $[\mathcal{K}u](\tilde{\boldsymbol{x}})$ for all $\tilde{\boldsymbol{x}}$ sufficiently close to $\tilde{\boldsymbol{x}}_0$.

In addition, a hierarchical tree structure of elements is introduced. For that purpose, a cube containing the whole boundary $\partial\Omega$, called level-0 cell, is divided into eight cubes (level-1 cells), each of which is divided in the same fashion. A level-ℓ cell is divided into level-$(\ell+1)$ cells unless it contains less than a preset (relatively small) number of boundary elements. The FMM algorithm then consists of the following:

- An *upward pass* where multipole moments are first computed for the lowest level cells and then recursively aggregated by moving upward in the tree until level 2 (for which there are $4\times4\times4$ cells overall) is reached. This operation requires identities of the form

$$k_n^{(2)}(\boldsymbol{x},\boldsymbol{x}_1) = \sum_{n'\geq 0} c_{nn'}(\boldsymbol{x}_1,\boldsymbol{x}_0)k_{n'}^{(2)}(\boldsymbol{x},\boldsymbol{x}_0)$$

  where the coefficients $c_{nn'}(\boldsymbol{x}_1,\boldsymbol{x}_0)$ are known for the usual fundamental solutions, which allow shifting of the origin from the center of a level-$(\ell+1)$ cell to the center of a level-ℓ cell (*multipole-to-multipole*, or M2M, translation).
- A *downward pass* where local expansions are first computed at level $\ell = 2$ and then evaluated at selected lower level cells by tracing the tree structure downwards. This operation requires identities allowing shifting the origin from the center of a level-ℓ cell to the center of a level-$(\ell+1)$ cell (*local-to-local*, or L2L, translation), which have the form

$$h_m^{(1)}(\tilde{\boldsymbol{x}},\tilde{\boldsymbol{x}}_1) = \sum_{m'\geq 0} b_{mm'}(\tilde{\boldsymbol{x}}_1,\tilde{\boldsymbol{x}}_0)h_{m'}^{(1)}(\tilde{\boldsymbol{x}},\tilde{\boldsymbol{x}}_0)$$

  where the coefficients $b_{mm'}(\tilde{\boldsymbol{x}}_1,\tilde{\boldsymbol{x}}_0)$ are known for the usual fundamental solutions. At all levels, only interaction between well-separated cells are so evaluated.
- A direct calculation, which includes all singular integrations, where the near-field contributions to the integral operator are evaluated using conventional integration methods.

Detailed descriptions of FMM algorithms can be found in Greengard and Rokhlin (1987, 1997), and Nishimura (2002). For BEM associated with static problems, the FMM is found to be an $O(N)$ task, which is a considerable improvement. Thus, the iterative solution of a system of BEM equations is in this context, an $O(KN)$ computation. Yoshida *et al.* (2001) present many-crack elastostatic computations where problems with $N \sim 10^5$ DOFs are solved in 1–2 h using a 500-MHz computer (the extrapolated solution time using traditional methods would have been measured in weeks). Fast multipole SGBEM implementations are described in Margonari and Bonnet (2005) or Of *et al.* (2006) and, for crack problems, in Trinh *et al.* (2015), while numerical homogenization computations involving thousands of fibers embedded in a 3D matrix and millions of BE DOFs are presented in Liu *et al.* (2005). Applications to MEMS are described in Frangi *et al.* (2006). Many of the recent developments in FMMs address wave propagation and the computation of time-harmonic or transient responses, see the survey by Chaillat and Bonnet (2013) and for example, Chaillat *et al.* (2008) or Kager and Schanz (2015). Finally, a kernel-independent approach of the FMM is proposed by Ying *et al.* (2004).

5.2 Other methods

5.2.1 Panel clustering method

The panel clustering method was first proposed in Hackbusch and Nowak (1989), and its elastostatic version can be found in Hayami and Sauter (1997). It has many similarities with the FMM, in that it is based on a tree structure of elements (or "panels") and on an expansion of the kernel. The latter has the form

$$K(\tilde{\boldsymbol{x}},\boldsymbol{x}) = \sum_{n\geq 0} k'^{(1)}_n(\tilde{\boldsymbol{x}},\boldsymbol{x}_0)k'^{(2)}_n(\boldsymbol{x})$$

rather than (44); this decomposition can be derived, for example, by means of a Taylor expansion of $K(\tilde{\boldsymbol{x}},\boldsymbol{x})$ about

$\boldsymbol{x} = \boldsymbol{x}_0$. Apparently, the panel clustering method has not been the subject of as many investigations and developments as the FMM. The complexity of the matrix–vector product is found in this case to be $O(N(\ln\ N)^{d+2})$, where d is the spatial dimensionality of the problem (see **Panel Clustering Techniques and Hierarchical Matrices for BEM and FEM**).

5.2.2 *Adaptive cross approximation*

The adaptive cross approximation (ACA) technique consists of a sequence of decompositions $[\boldsymbol{K}] = [\boldsymbol{S}_k] + [\boldsymbol{E}_k]$ $(k = 1, 2, \cdots)$, where $[\boldsymbol{S}_k]$ is a low-rank approximation of $[\boldsymbol{K}]$, with $\mathrm{Rank}([\boldsymbol{S}_k]) \leq k$, and $[\boldsymbol{E}_k]$ is the approximation error. The corresponding algorithm can be found in Kurz *et al.* (2002), where it is reported to define an $O(r^2 N)$ computation (r: rank of the final approximant $[\boldsymbol{S}]$). Numerical examples for the 3D Laplace equation and a FEM–BEM coupled approach for 3D electromagnetic problems are presented in the same reference. Bebendorf and Grzhibovskis (2006) present an ACA-based formulation for linear elasticity.

5.2.3 *Wavelet BEM*

This method assumes a hierarchical sequence of meshes, that is, one for which the mesh of level $\ell + 1$ is created by subdividing the elements of the mesh of level ℓ. The bases of interpolation functions are defined so that all new basis functions at level $\ell + 1$ (i.e., those not representable with the level ℓ basis functions) have vanishing moments. This property, combined with the decay of the kernel $K(\tilde{\boldsymbol{x}}, \boldsymbol{x})$ with increasing distances $|\boldsymbol{x} - \tilde{\boldsymbol{x}}|$, ensures that many coefficients of the matrix $[\boldsymbol{K}]$ expressed in the wavelet interpolation base are very small, and thus neglectable. A sparse approximation of $[\boldsymbol{K}]$ is thus constructed. Lage and Schwab (1999) report a wavelet BEM algorithm for which a sparse approximation of $[\boldsymbol{K}]$ containing $O(N(\ln\ N)^2)$ entries is generated in an $O(N(\ln\ N)^4)$ operation for three-dimensional Laplace-type problems (see **Adaptive Wavelet Techniques in Numerical Simulation**).

6 THE BOUNDARY ELEMENT METHOD FOR FRACTURE MECHANICS

Boundary element methods are quite well suited to fracture mechanics analyses. This is in large part due to the ease in creating boundary meshes for cracked solids, the crack being modeled as one of the component surfaces of the mesh (for elastic problems), whereas producing domain meshes of three-dimensional cracked solids is a much more labor-intensive task, especially since mesh refinement is needed in the vicinity of the crack front. The meshing issue is particularly sensitive for the simulation of crack propagation, where repeated remeshings are needed. A substantial body of published work on the application of BEMs to fracture mechanics is available (see the survey by Aliabadi, 1997) (see **Computational Fracture Mechanics**).

6.1 BEM formulations

For definiteness, consider a bounded elastic body $\Omega \in \mathbb{R}^3$ of finite extension, externally bounded by the closed surface S and containing a crack modeled by the open surface Γ (i.e., $\partial\Omega = S \cup \Gamma$), see Figure 4. The displacement $\boldsymbol{u}$, strain $\boldsymbol{\epsilon}$, and stress $\boldsymbol{\sigma}$ are related by the field equation (5) without body forces (i.e., with $\boldsymbol{f} = \boldsymbol{0}$). Besides, displacements and tractions are prescribed on the portions S_u and $S_t = S \backslash S_u$ of S and the crack surface Γ is stress-free, that is

$$\boldsymbol{u} = \bar{\boldsymbol{u}} \ (\text{on}\ \ S_u), \qquad \boldsymbol{t} = \bar{\boldsymbol{t}} \ (\text{on}\ \ S_t), \qquad \boldsymbol{t} = \boldsymbol{0} \ (\text{on}\ \ \Gamma) \quad (46)$$

It is important to emphasize that crack problems cannot be solved solely on the basis of the single-region displacement integral equation (17), or any equivalent variant. Indeed, when a traction-free crack is buried in Ω, equation (17) becomes

$$\int_S \left\{ T_i^k(\boldsymbol{y}, \boldsymbol{x})[u_i(\boldsymbol{x}) - u_i(\boldsymbol{y})] - U_i^k(\boldsymbol{y}, \boldsymbol{x}) t_i(\boldsymbol{x}) \right\} \, \mathrm{d}S_x - \int_\Gamma T_i^k(\boldsymbol{y}, \boldsymbol{x}) \phi_i(\boldsymbol{x}) \, \mathrm{d}S_x = 0 \quad (\boldsymbol{y} \in S) \quad (47)$$

where $\boldsymbol{\phi} = \boldsymbol{u}^+ - \boldsymbol{u}^-$ is the crack opening displacement (COD) and the $\pm$ signs refer to an arbitrarily chosen orientation of Γ such that the unit normal $\boldsymbol{n}$ is directed from Γ^- to Γ^+. A simple argument – namely the fact that subtracting from (47) equation (17) for the problem with the same boundary data but *without* crack results in a *homogeneous* equation, which therefore has either zero or infinitely many solutions – leads to the conclusion that equation (47) applied to the boundary value problem (5), (46) is not uniquely

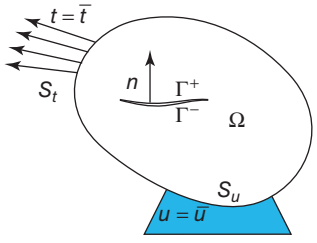

Figure 4. Cracked elastic solid: notation.

solvable (Cruse, 1988). Therefore, alternative BEM formulations are needed to solve crack problems, and the most common ones are now briefly described. With the exception of the multizone formulation, they all involve a combination of displacement and traction integral equations.

6.1.1 *Multizone formulation*

This approach consists of dividing Ω into two subregions Ω^+ and Ω^-, so that the crack surface Γ lies in the interface between Ω^+ and Ω^-. Then, the displacement integral equation (17) is invoked separately for each subdomain. The traction-free condition on Γ is then applied on each side Ω^+ and Ω^-, together with the perfect bonding conditions on the non-crack part of the interface, through which the two sets of BEM equations are coupled.

This approach has the advantage of relying only on the displacement BEM formulation, but at the expense of a substantial increase of the problem size. Besides, the interface has also an adverse effect on meshing simplicity, especially for the simulation of crack propagation where the crack surface must be iteratively updated. For problems involving planar cracks lying on a plane of symmetry, the situation is better, as one needs only to solve the BEM equations on one of the subregions. For problems involving interface cracks between dissimilar materials, the multizone approach is more attractive.

6.1.2 *Displacement discontinuity formulation: collocation*

Avoiding both the above-mentioned degeneracy and unwanted new interfaces, the displacement discontinuity formulation is based on an association of equation (47) for collocation points $\boldsymbol{y} \in S$ and a traction integral equation for collocation points $\boldsymbol{y} \in \Gamma$. The latter can be obtained as a variant of (13), and reads

$$t_i(\boldsymbol{y}) = -n_j(\boldsymbol{x})C_{ijk\ell}\left\{ D_{\ell b}u_a(\boldsymbol{y})A^k_{ab}(\boldsymbol{y},\partial\Omega) + \int_\Gamma [D_{\ell b}\phi_a(\boldsymbol{x}) - D_{\ell b}\phi_a(\boldsymbol{y})]\Sigma^k_{ab}(\boldsymbol{y},\boldsymbol{x})\ \mathrm{d}S_x \right\} \mathrm{d}S_x + \int_S \left\{ n_j(\boldsymbol{x})C_{ijk\ell} \times \Sigma^k_{ab}(\boldsymbol{y},\boldsymbol{x})D_{\ell b}u_a(\boldsymbol{x}) - t_a(\boldsymbol{x})T^k_i(\boldsymbol{x},\boldsymbol{y}) \right\}\ \mathrm{d}S_x \quad (\boldsymbol{y} \in \Gamma) \tag{48}$$

where $\boldsymbol{t}(\boldsymbol{y})$, the traction at the collocation point $\boldsymbol{y} \in \Gamma$, is here set to zero on account of (46). Formulations equivalent to (48) but involving finite part integrals are also available, together with well-defined techniques (notably the direct algorithm, see Guiggiani, 1998) for the numerical computation of hypersingular element integrals.

Equation (48) requires that $\boldsymbol{\phi}$ possess $C^{1,\alpha}$ Hölder regularity at $\boldsymbol{x} = \boldsymbol{y}$. Defining conformal $C^{1,\alpha}$ interpolations for $\boldsymbol{\phi}$ is relatively easy for plane problems (boundary elements are curvilinear segments), for example, using Hermite shape functions or Overhauser elements (Camp and Gipson, 1991), but much more difficult for three-dimensional situations (boundary elements are surface patches). Besides, failing to enforce the $C^{1,\alpha}$ smoothness at $\boldsymbol{y}$ of the interpolation of $\boldsymbol{\phi}$ may lead to inaccurate numerical evaluation of singular integrals (Krishnasamy *et al.*, 1992).

When an interpolation of the usual form (20) is used for $\boldsymbol{\phi}$, no collocation point $\boldsymbol{y}$ is allowed to lie on interelement edges; on the other hand, any usual interpolation of $\boldsymbol{\phi}$ has $C^{1,\alpha}$ regularity at any point interior to an element. One thus has to choose between

- Using conformal interpolations, but collocating (48) at element interior points only. This may lead to overdetermined linear systems of equations, to be solved in the least square sense. Alternatively, equations may be added together so as to obtain a square system of equations.
- Using nonconformal interpolations for $\boldsymbol{\phi}$, that is, discontinuous elements, and collocate (48) at the interpolation nodes (all are interior to an element). The required $C^{1,\alpha}$ smoothness at the collocation points is thus enforced, and a square system of equations is usually obtained. On the other hand, this procedure increases significantly the number of DOFs supported by the crack surface.
- Using simultaneously a $C^{0,\alpha}$ interpolation for $\boldsymbol{\phi}$ and another $C^{0,\alpha}$ interpolation for its tangential derivatives $D_{ij}\boldsymbol{\phi}$ (Polch *et al.*, 1987).

Implementation issues are discussed in many papers, for example, Watson (2006).

6.1.3 *Dual formulation*

In the displacement discontinuity method, the unknown on Γ is $\boldsymbol{\phi} = \boldsymbol{u}^+ - \boldsymbol{u}^-$, not the individual displacements $\boldsymbol{u}^+, \boldsymbol{u}^-$ on the crack faces. This is usually of no consequence, as the usual fracture mechanics parameters, for example, stress intensity factors (SIFs) (Section 6.2) or energy release rate, depend on $\boldsymbol{\phi}$ and not on $\boldsymbol{u}^+, \boldsymbol{u}^-$ separately.

Nevertheless, in a variant called the *dual boundary element method for fracture mechanics problems* (Mi and Aliabadi, 1992), the individual displacements $\boldsymbol{u}^+, \boldsymbol{u}^-$, not the COD $\boldsymbol{\phi}$, are taken as unknowns on Γ. In that case, the system (47, 48) becomes underdetermined and is supplemented for collocation points $\boldsymbol{y} \in \Gamma$ with the displacement integral equation

$$u_k^+(\boldsymbol{y}) + \int_S \left\{ u_i(\boldsymbol{x}) T_i^k(\boldsymbol{y},\boldsymbol{x}) - t_i(\boldsymbol{x}) U_i^k(\boldsymbol{y},\boldsymbol{x}) \right\} \, \mathrm{d}S_y - \int_\Gamma [\phi_i(\boldsymbol{x}) - \phi_i(\boldsymbol{y})] T_i^k(\boldsymbol{y},\boldsymbol{x}) \, \mathrm{d}S_y = 0 \tag{49}$$

6.1.4 *Displacement discontinuity formulation: symmetric Galerkin*

The Galerkin formulation for cracks embedded in finite bodies can be established from equations (36) by dividing Ω into two subregions Ω^+ and Ω^-, so that the crack surface Γ lies in the interface $\tilde{\Gamma}$ thus defined, and then combining the formulation (36) for each subdomain (e.g., by considering the tractions on $\tilde{\Gamma}$ as prescribed for both subdomains, and subtracting the two SGBEM equations $\mathcal{B}_{uu}(\hat{\boldsymbol{u}},\tilde{\boldsymbol{u}}) + \mathcal{B}_{tu}(\boldsymbol{t},\tilde{\boldsymbol{u}}) = \mathcal{L}_u(\tilde{\boldsymbol{u}})$) and enforcing the perfect bonding conditions ($\boldsymbol{\phi} = \boldsymbol{0}$ and $\boldsymbol{t}^+ + \boldsymbol{t}^- = \boldsymbol{0}$ on $\tilde{\Gamma}\backslash\Gamma$) and the traction-free conditions on Γ. This leads to a set of SGBEM equations of the form

$$\text{Find } \hat{\boldsymbol{u}} \in \mathcal{V}_u, \boldsymbol{\phi} \in \mathcal{V}_\phi, \boldsymbol{t} \in \mathcal{V}_t \quad \text{such that}$$

$$\begin{cases} \mathcal{B}_{uu}(\hat{\boldsymbol{u}},\tilde{\boldsymbol{u}}) + \mathcal{B}_{tu}(\boldsymbol{t},\tilde{\boldsymbol{u}}) \\ +\mathcal{B}_{\phi u}(\boldsymbol{\phi},\tilde{\boldsymbol{u}}) = \mathcal{L}_u(\tilde{\boldsymbol{u}};\bar{\boldsymbol{t}}) \\ \mathcal{B}_{ut}(\hat{\boldsymbol{u}},\tilde{\boldsymbol{t}}) + \mathcal{B}_{tt}(\boldsymbol{t},\tilde{\boldsymbol{t}}) \\ +\mathcal{B}_{\phi t}(\boldsymbol{\phi},\tilde{\boldsymbol{t}}) = \mathcal{L}_t(\tilde{\boldsymbol{t}};\bar{\boldsymbol{u}}) \forall \tilde{\boldsymbol{u}} \in \mathcal{V}_u, \forall \tilde{\boldsymbol{\phi}} \in \mathcal{V}_\phi, \forall \tilde{\boldsymbol{t}} \in \mathcal{V}_t \\ \mathcal{B}_{u\phi}(\hat{\boldsymbol{u}},\tilde{\boldsymbol{\phi}}) + \mathcal{B}_{t\phi}(\boldsymbol{t},\tilde{\boldsymbol{\phi}}) \\ +\mathcal{B}_{\phi\phi}(\boldsymbol{\phi},\tilde{\boldsymbol{\phi}}) = 0 \end{cases} \tag{50}$$

where the new set $\mathcal{V}_\phi$ of admissible functions is $\mathcal{V}_\phi = \{\tilde{\boldsymbol{\phi}} \mid \tilde{\boldsymbol{\phi}} \in C^{0,\alpha}(\Gamma)\text{and } \tilde{\boldsymbol{\phi}} = \boldsymbol{0} \text{ on } \partial\Gamma\}$. One thus sees that ordinary C^0 interpolations for $\boldsymbol{\phi}$ can be used, whereas collocation formulations of the traction integral equation requires, as already mentioned, stronger $C^{1,\alpha}$ smoothness at the collocation points. This is a definite advantage for the GBEM approach as applied to crack problems (regardless of its symmetry).

In the simpler case of a crack embedded in an infinite elastic body with a symmetric load $\bar{\boldsymbol{t}}$ on both crack faces, the SGBEM formulation takes the simpler form

$$\text{Find } \boldsymbol{\phi} \in \mathcal{V}_\phi \quad \text{such that}$$

$$\int_\Gamma \int_\Gamma R_q \psi_i(\boldsymbol{x}) B_{ikqs}(\boldsymbol{y},\boldsymbol{x}) R_s \phi_k(\boldsymbol{y}) \, \mathrm{d}S_y \, \mathrm{d}S_x = -\int_\Gamma \tilde{\boldsymbol{\phi}} \cdot \bar{\boldsymbol{t}} \, \mathrm{d}S \quad (\forall \tilde{\boldsymbol{\phi}} \in \mathcal{V}_\phi) \tag{51}$$

Investigations and numerical implementations of (51), or variants of it, are presented in Bui (1977), Gu and Yew (1988), and Xu *et al.* (1995), while mathematical foundations are given in Costabel and Stephan (1987). Three-dimensional implementations of the finite-body formulation (50) by Li *et al.* (1998) and Frangi *et al.* (2001) were found to provide very accurate results even with relatively coarse meshes. Among other applications of SGBEMs to the modeling of fracture and damage, cohesive interface problems are considered in Salvadori (2003) and Vodička (2016). The extension of SGBEM formulations to cracked anisotropic solids is treated in Rungamornrat and Mear (2008). FMMs have been developed in Lai and Rodin (2003) and Trinh *et al.* (2015), among others, for SGBEM formulations of crack problems.

6.2 Computation of stress intensity factors and energy release rate

Quantities of interest for fracture mechanics analyses can be evaluated by postprocessing the boundary field variables computed by means of one of the above-described formulations. They notably include the SIFs, which characterize the intensity of the well-known $d^{-1/2}$ singular behavior of strains and stresses near the crack front $\partial\Gamma$ (see **Computational Fracture Mechanics**):

$$u_i(\boldsymbol{x}) = \frac{1+\nu}{E}\left(\frac{2d}{\pi}\right)^{1/2} K_\alpha(s) f_i(\theta) + O(d)$$

$$\sigma_{ij}(\boldsymbol{x}) = \left(\frac{1}{2\pi d}\right)^{-1/2} K_\alpha(s) g_{ij}(\theta) + O(1)$$

$$(\alpha = \mathrm{I}, \mathrm{II}, \mathrm{III})$$

where s is the arc length along $\partial\Gamma$; $d = \mathrm{Distance}(\boldsymbol{x}, \partial\Gamma)$ and d, θ are polar coordinates in the plane orthogonal to $\partial\Gamma$ containing $\boldsymbol{x}$; and $f_i(\theta)$ and $g_{ij}(\theta)$ are known universal dimensionless functions of θ. An SIF is associated to each of the three basic deformation modes: opening (K_I), sliding (K_II), tearing (K_III). In the BEM, the SIFs are most often evaluated from the interpolated COD $\boldsymbol{\phi} = \boldsymbol{u}|_{\theta=\pi} - \boldsymbol{u}|_{\theta=0}$:

- Extrapolation consists of finding the best fit (e.g., using quadratic regression) between the COD interpolation on elements adjacent to the crack front and the theoretical asymptotic expression;
- Quarter-node elements take advantage of the fact that, for three-noded quadratic interpolation on lines (used e.g., in BEM formulations for 2D crack problems), selecting the middle node location so that its distance to the crack tip is one-fourth of the element length ensures that the usual quadratic interpolation of $\boldsymbol{\phi}$ possesses the $d^{1/2}$ behavior (see, e.g., Cruse and Wilson, 1977 for early BEM implementations). The fact that the asymptotic behavior of $\boldsymbol{\phi}$ is correctly modeled enhances the accuracy in SIF evaluation. This approach has been refined by

Gray *et al.* (2003), where the introduction of a *cubic* interpolation for $\boldsymbol{\phi}$ supported by the usual three-noded element removes the unwanted $O(d)$ term in the interpolated $\boldsymbol{\phi}$; the SIFs are then evaluated by a simple formula in terms of the nodal values $\boldsymbol{\phi}^2, \boldsymbol{\phi}^3$ at nodes 2 and 3 (node 1 being the crack tip, n, and t, the normal and tangential directions, respectively):

$$K_{\mathrm{I}} \approx \frac{\mu}{12(1-\nu)}\left(\frac{2\pi}{\ell}\right)^{1/2}[8\phi_n^2 - \phi_n^3]$$

$$K_{\mathrm{II}} \approx \frac{\mu}{12(1-\nu)}(\frac{2\pi}{\ell})^{1/2}[8\phi_t^2 - \phi_t^3]$$

The quarter-node concept can be extended to eight-noded and nine-noded elements used for 3D problems, but there are constraints on the shape of elements adjacent to the crack front, which sometimes make them impractical with meshes generated by mesh generators.

- Special elements with interpolation functions including a correct representation of the asymptotic crack-front behavior have also been proposed in Cruse (1988), Luchi and Rizzuti (1987) or (for the SGBEM) Li *et al.* (1998), among others.

The energy release rate G, that is, (minus) the derivative of the potential energy at equilibrium in infinitesimal perturbations of the crack front is also of primary interest in fracture mechanics, as it is involved in usual crack propagation criteria. It is also obtained by postprocessing the BEM solution, by means of path-independent J integrals (Huber *et al.*, 1993), interaction integrals (Cisilino and Ortiz, 2005), or a shape sensitivity approach using the concepts outlined in Section 8 (Bonnet, 1999c).

6.3 Crack growth

BEMs are well suited to the simulation of crack growth. Repeated remeshings entailed by the incremental simulation of crack growth are much easier with surface BEM meshes than with domain FEM meshes, especially for three-dimensional situations and curved crack shapes that may evolve with growth. In addition, the BEM allows for accurate evaluations of quantities involved in crack growth criteria, such as SIFs, energy release rates, invariant integrals such as the J-integral, or field quantities close to the crack front. A number of studies have been devoted to the simulation of crack growth by the BEM. Three-dimensional situations are addressed by dell'Erba and Aliabadi (2000) for thermoelasticity, Frangi (2002) using the SGBEM, Cisilino and Aliabadi (1999) for elastoplasticity, and Xu *et al.* (1995) for crack propagation in fiber–matrix composite materials, among others.

6.4 Overview of other methods or situations

Traction-free cracks have been considered so far in this section for the sake of definiteness and convenience, but this is by no means a mandatory assumption. For instance, pressurized or otherwise loaded cracks can be considered. If the load is symmetric, that is, $\boldsymbol{t}^+ + \boldsymbol{t}^-$ holds, the displacement discontinuity method can be invoked with the minimal modification of setting $\boldsymbol{t}(\boldsymbol{y})$ in the traction BIE (48) equal to $\boldsymbol{t}^-(\boldsymbol{y})$, the traction applied on Γ_-, instead of zero. Similarly, the dual method for this case consists of using the same modified traction BIE together with equation (49). Other types of boundary conditions on the crack, such as Dirichlet conditions or coupling with thermal effects, may be considered along similar lines. In such cases, the load undergone by the crack faces is not necessarily symmetric. In that case, the term

$$-\int_\Gamma U_i^k(\boldsymbol{y},\boldsymbol{x})[t_i^+(\boldsymbol{x}) + t_i^+(\boldsymbol{x})]\ \mathrm{d}S_x$$

should be added to the left-hand side of (47), and equations such as (48) and (49) need to be modified accordingly. Partheymuller *et al.* (2000) provide further insight into the comparison of the displacement discontinuity method and the dual method for various cases of boundary conditions.

Also worth mentioning is that Green's functions, which satisfy suitable (usually traction-free) boundary conditions on the crack faces, are available for simple crack shapes, for example, straight cracks. The corresponding BIE formulations therefore involve only integrals on the external (i.e., noncrack) surface. For example, Snyder and Cruse (1975) introduced this concept for anisotropic cracked plates, and Telles *et al.* (1995) developed techniques for numerically calculating the crack Green's function. Fluid flow in fractured media is addressed by Vu *et al.* (2013), and damaged structures with bonded piezoelectric sensors in Benedetti *et al.* (2010). ACA acceleration techniques are applied to 3D fracture problems in Kolk *et al.* (2005).

7 BOUNDARY-DOMAIN INTEGRAL EQUATIONS FOR ELASTIC–PLASTIC PROBLEMS

In the framework of infinitesimal strain, it is usually assumed that the strain tensor can be decomposed additively into an elastic part and a plastic (or viscoplastic) part, that is

$$\boldsymbol{\varepsilon} = \boldsymbol{\varepsilon}^{\mathrm{E}} + \boldsymbol{\varepsilon}^{\mathrm{P}} \quad \text{where} \quad \boldsymbol{\sigma} = \boldsymbol{C} : \boldsymbol{\varepsilon}^{\mathrm{E}} \tag{52}$$

so that the elastic part of the constitutive equation reads

$$\boldsymbol{\sigma} = \boldsymbol{C} : (\boldsymbol{\varepsilon} - \boldsymbol{\varepsilon}^{\mathrm{P}}) \tag{53}$$

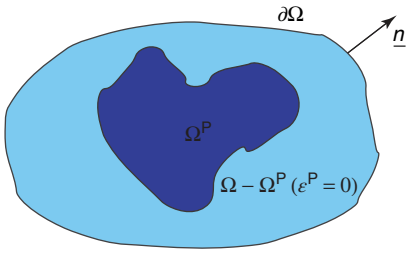

Figure 5. Subdivision of Ω into a potentially plastic region Ω^{P} and its elastic complement $\Omega \backslash \Omega^{\mathrm{P}}$.

Hence, BEM treatments for problems involving nonlinear constitutive properties are based on an integral identity governing elastic problems with distributions of (*a priori* unknown) initial strains (or stresses), which reads

$$\kappa(\tilde{\boldsymbol{x}}) u_k(\tilde{\boldsymbol{x}}) = \int_{\partial\Omega} \{ U_i^k(\tilde{\boldsymbol{x}}, \boldsymbol{x}) t_i(\boldsymbol{x}) - T_i^k(\tilde{\boldsymbol{x}}, \boldsymbol{x}) u_i(\boldsymbol{x}) \} \, \mathrm{d}S_x + \int_{\Omega^{\mathrm{P}}} \Sigma_{ab}^k(\tilde{\boldsymbol{x}}, \boldsymbol{x}) \varepsilon_{ab}^{\mathrm{P}}(\boldsymbol{x}) \, \mathrm{d}V_x \tag{54}$$

This is in fact a variant of equation (7) where the absence of body forces is assumed for simplicity and $\Omega^{\mathrm{P}} \subseteq \Omega$ denotes the potentially plastic region (Figure 5), that is, a region outside of which $\boldsymbol{\varepsilon}^{\mathrm{P}} = \mathbf{0}$ is assumed (keeping in mind that the true support of $\boldsymbol{\varepsilon}^{\mathrm{P}}$ is not known *a priori* and evolves with the load). The corresponding displacement BIE is then obtained in the same manner from (11).

7.1 Integral representation of strain or stress at interior points

If the initial strain field $\boldsymbol{\varepsilon}^{\mathrm{P}}$ is known, the displacement BIE (11) collocated at the BEM mesh nodes provides a suitable set of discretized equations for the unknown boundary DOFs. However, in nonlinear solid mechanics analyses by BEM, the field $\boldsymbol{\varepsilon}^{\mathrm{P}}$ is to be determined in addition to the usual boundary unknowns. Hence, another set of integral equations are needed, in the form of the integral representation of strain collocated at interior points. This new set of equations thus comes from differentiating the integral representation (54) with respect to coordinates of the observation point $\tilde{\boldsymbol{x}}$. A technical difficulty appears at this stage, namely that the differentiation of (7) with respect to $\tilde{x}_{\ell}$ involves the derivatives $\Sigma_{ij,\tilde{\ell}}^k(\tilde{\boldsymbol{x}}, \boldsymbol{x})$, which have a $|\boldsymbol{x} - \tilde{\boldsymbol{x}}|^{-3}$ singularity which is not integrable over Ω (the overbar in $()_{,\tilde{\ell}}$ denoting a partial derivative w.r.t. the ℓ-coordinate of $\tilde{\boldsymbol{x}}$). The derivation of the integral representation of strain is therefore not straightforward, as witnessed by the fact that incorrect expressions were found in the literature until Bui (1978) established the correct expression, which involves a free term and a CPV domain integral.

Another approach consists, with the help of an auxiliary integral identity, of performing an indirect regularization approach in order to reformulate the integral representation in an integrable form. Without going into the details of this derivation (Chandra and Mukherjee, 1997; Poon *et al.*, 1998b; Dong and Bonnet, 2002; Bonnet, 2003), the regularized integral representation formula for the displacement gradient at an interior point $\tilde{\boldsymbol{x}}$ is obtained (isolating $\tilde{\boldsymbol{x}}$ into a subregion $\Omega_e \subset \Omega^{\mathrm{P}}$) as

$$\begin{aligned} u_{k,\ell}(\tilde{\boldsymbol{x}}) = & \int_{\partial\Omega} \{ U_{i,\tilde{\ell}}^k(\tilde{\boldsymbol{x}}, \boldsymbol{x}) t_i(\boldsymbol{x}) - \Sigma_{ab,\tilde{\ell}}^k(\tilde{\boldsymbol{x}}, \boldsymbol{x}) u_a(\boldsymbol{x}) \\ & \times n_b(\boldsymbol{x}) \} \, \mathrm{d}S_x + \int_{\Omega^{\mathrm{P}} - \Omega_e} \Sigma_{ab,\tilde{\ell}}^k(\tilde{\boldsymbol{x}}, \boldsymbol{x}) \varepsilon_{ab}^{\mathrm{P}}(\boldsymbol{x}) \, \mathrm{d}V_x \\ & + \int_{\Omega_e} \Sigma_{ab,\tilde{\ell}}^k(\tilde{\boldsymbol{x}}, \boldsymbol{x}) [\varepsilon_{ab}^{\mathrm{P}}(\boldsymbol{x}) - \varepsilon_{ab}^{\mathrm{P}}(\tilde{\boldsymbol{x}})] \, \mathrm{d}V_x + \varepsilon_{ab}^{\mathrm{P}}(\tilde{\boldsymbol{x}}) C_{ijab} \\ & \times \int_{\partial\Omega_e} U_{i,\tilde{\ell}}^k(\tilde{\boldsymbol{x}}, \boldsymbol{x}) n_j(\boldsymbol{x}) \, \mathrm{d}S_x \end{aligned} \tag{55}$$

Note that the boundary integrals in (55) are nonsingular if $\tilde{\boldsymbol{x}} \in \Omega^{\mathrm{P}}$ is chosen inside Ω. In particular, they are always nonsingular if $\Omega^{\mathrm{P}} \cap \partial\Omega = \emptyset$, that is, when the potentially plastic region does not reach the external boundary. If $\Omega^{\mathrm{P}} \cap \partial\Omega \neq \emptyset$, it may be necessary or useful to invoke the integral representation of strain at collocation points $\tilde{\boldsymbol{x}} \in \partial\Omega$. This gives rise to hypersingular boundary integrals (Section 2.3), to which either a direct approach or an indirect regularization can be applied. The specific issue of indirect regularization of (55) is addressed in, for example, Bonnet *et al.* (1998b) and Poon *et al.* (1998b).

Equations (11) and (55) are the two integral identities upon which BEM techniques for nonlinear problems are built. In fact, since the formulation involves domain integrals over the potentially plastic region and collocation at internal points, the ensuing discretization technique is referred to as a domain-boundary element method (D/BEM) rather than a BEM. To exploit (11) and (55), the nonlinear part of the constitutive property, which up to now has been left unspecified, must be invoked (see **Elastoplastic and Viscoplastic Deformations in Solids and Structures**).

7.2 D/BEM treatment of small-strain elastoplasticity

Since the early paper by Swedlow and Cruse (1971), D/BEM treatments of quasi-static elastoplasticity have been investigated by Telles and Brebbia (1981), Banerjee and Raveendra (1986), Mukherjee and Chandra (1987), Telles and Carrer

(1991, 1994), Comi and Maier (1992), Maier *et al.* (1993), and Huber *et al.* (1996), among others. Elastic–plastic constitutive behavior gives rise to history-dependent evolution problems. In quasi-static situations, there is no physical time scale, and the evolution is described by a kinematical parameter t (e.g., a proportionality factor of the loading), called *time* for simplicity. Elastic–plastic analyses generally consist of prescribing an incremental load history and finding the corresponding incremental history of mechanical variables (displacements, strains, stresses, etc.). Implicit integration algorithms, based on the concept of *consistent tangent operator* (*CTO*) and originally introduced for the finite element method (see Nguyen, 1977; Simo and Taylor, 1985, as well as Simo and Hugues, 1998 for a comprehensive exposition), are now widely used by the FEM community. Using this approach, the Newton iterative method used for each load step converges quadratically, allowing for a reduction of the number of iterations as well as for larger load steps than other integration strategies. Implicit integration algorithms can also be developed in a D/BEMs framework (Bonnet and Mukherjee, 1996; Poon *et al.*, 1998a), and similar robustness properties have been demonstrated (see, e.g., the comparative study by Paulino and Liu, 1999). Hence, the D/BEM treatment of small-strain elastoplasticity presented in this section is based on an implicit integration algorithm (see **Elastoplastic and Viscoplastic Deformations in Solids and Structures**).

7.2.1 Incremental formulation

Basically, the boundary element approach to elastic–plastic analysis is based on the integral equation (11) and the integral representation (55) of strain. These equations are discretized using boundary elements for the boundary unknowns $\boldsymbol{u}, \boldsymbol{t}$ and integration cells for the domain integrals containing $\boldsymbol{\varepsilon}^{\mathrm{P}}$. Since the plastic region, that is, the geometrical support of $\boldsymbol{\varepsilon}^{\mathrm{P}}$, is not known *a priori*, a *potentially plastic* subset Ω^{P} of Ω, outside of which no plastic strain is expected, must be defined *a priori*. Interpolation functions for the plastic strain $\boldsymbol{\varepsilon}^{\mathrm{P}}$ or the total strain $\boldsymbol{\varepsilon}$ are defined on the cells. The resulting matrix equations associated to (11) and (55) have the form

$$[\boldsymbol{A}]\{\boldsymbol{u}\} + [\boldsymbol{B}]\{\boldsymbol{t}\} = [\boldsymbol{Q}]\{\boldsymbol{C} : \boldsymbol{\varepsilon}^{\mathrm{P}}\} \tag{56}$$

$$\{\boldsymbol{\varepsilon}\} = -[\boldsymbol{A}']\{\boldsymbol{u}\} - [\boldsymbol{B}']\{\boldsymbol{t}\} + [\boldsymbol{Q}']\{\boldsymbol{C} : \boldsymbol{\varepsilon}^{\mathrm{P}}\} \tag{57}$$

or, after separation of known and unknown DOFs in $\{\boldsymbol{u}\}, \{\boldsymbol{t}\}$ and appropriate column-switching in the matrices $[\boldsymbol{A}], [\boldsymbol{B}]$ and $[\boldsymbol{A}'], [\boldsymbol{B}']$, the form

$$[\boldsymbol{K}]\{\boldsymbol{X}\} = \{\boldsymbol{Y}\} + [\boldsymbol{Q}]\{\boldsymbol{C} : \boldsymbol{\varepsilon}^{\mathrm{P}}\} \tag{58}$$

$$\{\boldsymbol{\varepsilon}\} = \{\boldsymbol{Y}'\} - [\boldsymbol{K}']\{\boldsymbol{X}\} + [\boldsymbol{Q}']\{\boldsymbol{C} : \boldsymbol{\varepsilon}^{\mathrm{P}}\} \tag{59}$$

where $\{\boldsymbol{Y}\}, \{\boldsymbol{Y}'\}$ incorporate the boundary data. Equations (56), (57) or (58), (59) may also be viewed as a symbolic form of the continuous integral equations (11) and (55).

Solving (58) for $\{\boldsymbol{X}\}$ and substituting the result into (59), one obtains

$$\{\boldsymbol{\varepsilon}\} = \{\boldsymbol{\varepsilon}^{\mathrm{L}}\} + [\boldsymbol{S}]\{\boldsymbol{C} : \boldsymbol{\varepsilon}^{\mathrm{P}}\}$$
$$\text{with} \quad \begin{cases} \{\boldsymbol{\varepsilon}^{\mathrm{L}}\} = \{\boldsymbol{f}'\} - [\boldsymbol{K}'][\boldsymbol{K}]^{-1}\{\boldsymbol{f}\} \\ [\boldsymbol{S}] = [\boldsymbol{Q}'] - [\boldsymbol{K}'][\boldsymbol{K}]^{-1}[\boldsymbol{Q}] \end{cases} \tag{60}$$

To take into account the incremental nature of the problem, the evolution between the time instants t_n and $t_{n+1} = t_n + \Delta t$ is considered. Equation (60) thus takes the incremental form

$$\{\Delta\boldsymbol{\varepsilon}_n\} = \{\Delta\boldsymbol{\varepsilon}_n^{\mathrm{L}}\} + [\boldsymbol{S}]\{\boldsymbol{C} : \Delta\boldsymbol{\varepsilon}_n^{\mathrm{P}}\} \tag{61}$$

using the notation $\Delta(\,)_n = (\,)_{n+1} - (\,)_n$. The variables $(\boldsymbol{u}_n, \boldsymbol{t}_n)$ on $\partial\Omega$ and $(\boldsymbol{\varepsilon}_n, \boldsymbol{\sigma}_n, \bar{e}_n^{\mathrm{P}})$ are assumed to be known. In particular, initial conditions must be provided at the starting time t_0. Solving the nth increment of the time-discretized elastic–plastic problem then consists in finding all mechanical variables at $t = t_{n+1}$, or, equivalently, in finding all the increments $\Delta\boldsymbol{\varepsilon}_n$, and so on.

The plastic part of the constitutive behavior still remains to be accounted for. Following the approach of Simo and Taylor (1985), the *radial return algorithm* (*RRA*), symbolically denoted by $\bar{\boldsymbol{\sigma}}$, outputs the stress $\boldsymbol{\sigma}_{n+1}$ given a strain increment $\Delta\boldsymbol{\varepsilon}_n$ and the mechanical variables $(\boldsymbol{\varepsilon}_n, \boldsymbol{\sigma}_n, \bar{e}_n^{\mathrm{P}})$ at $t = t_n$:

$$\boldsymbol{\sigma}_{n+1} = \bar{\boldsymbol{\sigma}}(\boldsymbol{\varepsilon}_n, \boldsymbol{\sigma}_n, \bar{e}_n^{\mathrm{P}}, \Delta\boldsymbol{\varepsilon}_n) \tag{62}$$

where $\bar{e}^{\mathrm{P}}$ denotes the cumulative plastic equivalent strain

$$\bar{e}^{\mathrm{P}} = \int_0^t \sqrt{\frac{2}{3}}(\boldsymbol{d}^p : \boldsymbol{d}^p)^{1/2} \colon \mathrm{d}\tau$$

In view of (2), the new plastic strain $\boldsymbol{\varepsilon}_{n+1}^{\mathrm{P}} = \bar{\boldsymbol{\varepsilon}}^{\mathrm{P}}(\boldsymbol{\varepsilon}_n, \boldsymbol{\sigma}_n, \bar{e}_n^{\mathrm{P}}, \Delta\boldsymbol{\varepsilon}_n)$ follows at once through

$$\boldsymbol{C} : \bar{\boldsymbol{\varepsilon}}^{\mathrm{P}}(\boldsymbol{\varepsilon}_n, \boldsymbol{\sigma}_n, \bar{e}_n^{\mathrm{P}}, \Delta\boldsymbol{\varepsilon}_n) = \bar{\boldsymbol{\sigma}}(\boldsymbol{\varepsilon}_n, \boldsymbol{\sigma}_n, \bar{e}_n^{\mathrm{P}}, \Delta\boldsymbol{\varepsilon}_n) - \boldsymbol{C} : \boldsymbol{\varepsilon}_{n+1} \tag{63}$$

Substituting (62) into (61), one obtains a nonlinear system of equations

$$\{G(\Delta\boldsymbol{\varepsilon}_n)\} \equiv [\boldsymbol{S}]\{\bar{\boldsymbol{\sigma}}(\boldsymbol{\varepsilon}_n, \boldsymbol{\sigma}_n, \bar{e}_n^{\mathrm{P}}, \Delta\boldsymbol{\varepsilon}_n) - \boldsymbol{\sigma}_n - \boldsymbol{C} : \Delta\boldsymbol{\varepsilon}_n\}$$
$$- \{\Delta\boldsymbol{\varepsilon}_n^{\mathrm{L}}\} + \{\Delta\boldsymbol{\varepsilon}_n\} = \{\boldsymbol{0}\} \tag{64}$$

whose primary unknown is $\{\Delta\boldsymbol{\varepsilon}_n\}$, which is the strain increment compatible with both the elastic equilibrium and the

plastic constitutive behavior (left unspecified at this point). Equation (64) is then solved by means of an iterative procedure. For example, using the Newton method, the additive correction $\delta\boldsymbol{\varepsilon}_n^i = \Delta\boldsymbol{\varepsilon}_n^{i+1} - \Delta\boldsymbol{\varepsilon}_n^i$ to $\Delta\boldsymbol{\varepsilon}_n^i$ solves the linear system of equations

$$([\boldsymbol{S}][\boldsymbol{D}_{n+1}^i] - [\boldsymbol{I}])\{\delta\boldsymbol{\varepsilon}_n^i\} = \{G(\Delta\boldsymbol{\varepsilon}_n^i)\} \tag{65}$$

where

$$\begin{aligned} \boldsymbol{D}_{n+1}^i &= \boldsymbol{C} - \boldsymbol{C}_{n+1}^i \\ \text{with} \quad \boldsymbol{C}_{n+1}^i &\equiv \frac{\partial\bar{\boldsymbol{\sigma}}}{\partial\Delta\boldsymbol{\varepsilon}_n}(\boldsymbol{\varepsilon}_n, \boldsymbol{\sigma}_n, \bar{e}_n^{\mathrm{P}}, \Delta\boldsymbol{\varepsilon}_n^i) \end{aligned} \tag{66}$$

$\boldsymbol{C}_{n+1}^i$ is the *local consistent tangent operator* (local CTO) and $([\boldsymbol{S}][\boldsymbol{D}_{n+1}^i] - [\boldsymbol{I}])$ is the global CTO. The iterative procedure is carried out until convergence, and the value of $\{\Delta\boldsymbol{\varepsilon}_n\}$ thus obtained is used to update the mechanical variables:

$$\boldsymbol{\varepsilon}_{n+1} = \boldsymbol{\varepsilon}_n + \Delta\boldsymbol{\varepsilon}_n \qquad \boldsymbol{\sigma}_{n+1} = \overline{\boldsymbol{\sigma}}(\boldsymbol{\varepsilon}_n, \boldsymbol{\sigma}_n, \bar{e}_n^{\mathrm{P}}, \Delta\boldsymbol{\varepsilon}_n)$$

It is interesting to note that the Newton step (65) involves the difference $[\boldsymbol{C} - \boldsymbol{C}_{n+1}^i]$ between the elastic tensor and the local CTO, rather than the local CTO itself; this is entirely consistent with the fact that (61) accounts for equilibrium as well as the elastic constitutive law.

Observe that $\boldsymbol{C} - \boldsymbol{C}_{n+1}^i = \boldsymbol{0}$ at points where the incremental deformation is purely elastic. The implication is that the block-diagonal matrix $[\boldsymbol{C} - \boldsymbol{C}_{n+1}^i]$ can have zero blocks on the diagonal, leading to corresponding zero block columns in the matrix $[\boldsymbol{S}][\boldsymbol{D}_{n+1}^i]$. This can be used to reduce the size of the system (65) to that of the plastically deforming zone, with significant savings in computer time.

7.2.2 Radial return algorithm

For completeness, the RRA is now explicitly given for a specific constitutive behavior, namely isotropic elasticity, a von Mises yield criterion with isotropic linear hardening, and an associative flow rule. The elastic domain $\mathbb{E}$ in the stress space is thus defined by

$$\begin{aligned} \mathbb{E} &= \{\boldsymbol{\sigma} | f(\boldsymbol{\sigma}) \leq 0\} \\ \text{with} \quad f(\boldsymbol{\sigma}; \bar{e}^{\mathrm{P}}) &\equiv \sqrt{\boldsymbol{s} : \boldsymbol{s}} - \sqrt{\frac{2}{3}}(\sigma_0 + h\bar{e}^{\mathrm{P}}) \end{aligned} \tag{67}$$

where $\boldsymbol{s} = \boldsymbol{\sigma} - 1/3\mathrm{Tr}(\boldsymbol{\sigma})$ is the deviatoric stress, σ_0 is the initial yield stress, and h is the hardening modulus. Incompressibility of plastic strain is assumed. The constitutive equations are then the elastic stress–strain equation (2), the evolution equations

$$\dot{\boldsymbol{\varepsilon}}^{\mathrm{P}} = \gamma\hat{\boldsymbol{n}} \qquad \dot{\bar{e}}^{\mathrm{P}} = \gamma\sqrt{\frac{2}{3}}$$

(where $\hat{\boldsymbol{n}} \equiv \partial f/\partial\boldsymbol{\sigma} = \boldsymbol{s}/|\boldsymbol{s}|$), and the complementarity Kuhn–Tucker conditions

$$f(\boldsymbol{\sigma}; \bar{e}^{\mathrm{P}}) \leq 0 \qquad \gamma \geq 0 \qquad \gamma f(\boldsymbol{\sigma}; \bar{e}^{\mathrm{P}}) = 0$$

The plastic multiplier γ is found from enforcing the *consistency condition*

$$\gamma\dot{f}(\boldsymbol{\sigma}; \bar{e}^{\mathrm{P}}) = 0$$

The RRA consists of the following steps. First, the (elastic) trial stress $\boldsymbol{\sigma}_{n+1}^{\mathrm{T}}$ is defined by

$$\begin{aligned} \boldsymbol{s}_{n+1}^{\mathrm{T}} &= \boldsymbol{s}_n + 2\mu\Delta\boldsymbol{e}_n \\ \boldsymbol{\sigma}_{n+1}^{\mathrm{T}} &= \boldsymbol{\sigma}_n + K\Delta\boldsymbol{\varepsilon}_n : (\boldsymbol{1} \otimes \boldsymbol{1}) + 2\mu\Delta\boldsymbol{e}_n \end{aligned} \tag{68}$$

($\boldsymbol{e}$: deviatoric strain). If $f(\boldsymbol{\sigma}_{n+1}^{\mathrm{T}}; \bar{e}_n^{\mathrm{P}}) \leq 0$, that is, $\boldsymbol{\sigma}_{n+1}^{\mathrm{T}}$ is in the elastic domain, one has

$$\bar{\boldsymbol{\sigma}} = \boldsymbol{\sigma}_{n+1}^{\mathrm{T}} \qquad \boldsymbol{\varepsilon}_{n+1}^{\mathrm{P}} = \boldsymbol{\varepsilon}_n^{\mathrm{P}} \qquad \bar{e}_{n+1}^{\mathrm{P}} = \bar{e}_n^{\mathrm{P}}$$

On the other hand, if $f(\boldsymbol{\sigma}_{n+1}^{\mathrm{T}}; \bar{e}_n^{\mathrm{P}}) > 0$, $\bar{\boldsymbol{\sigma}}$ is given by the following equations, which constitute the RRA (Simo and Taylor, 1985):

$$\begin{aligned} \hat{\boldsymbol{n}} &= \frac{\boldsymbol{s}_{n+1}^{\mathrm{T}}}{|\boldsymbol{s}_{n+1}^{\mathrm{T}}|} \qquad \boldsymbol{s}_{n+1} = \boldsymbol{s}_{n+1}^{\mathrm{T}} - 2\mu\gamma\Delta t\hat{\boldsymbol{n}} \\ \bar{e}_{n+1}^{\mathrm{P}} &= \bar{e}_n^{\mathrm{P}} + \sqrt{\frac{2}{3}}\gamma\Delta t \quad \bar{\boldsymbol{\sigma}} = K\boldsymbol{\varepsilon}_{n+1} : (\boldsymbol{1} \otimes \boldsymbol{1}) + \boldsymbol{s}_{n+1} \end{aligned} \tag{69}$$

where $K = 2\mu(1+\nu)/(3-6\nu)$ is the compressibility modulus. The scalar $\gamma\Delta t$ solves the equation $f(\bar{\sigma}) = 0$, which is solvable in closed form:

$$2\mu\gamma\Delta t = \frac{|\boldsymbol{\xi}^{\mathrm{T}}| - \sqrt{\frac{2}{3}}(\sigma_0 + h\bar{e}_n^{\mathrm{P}})}{1 + (H+h)/(3\mu)}$$

In general, the equation governing $\gamma\Delta t$ is nonlinear and must be solved numerically. Finally, the local CTO is given in this case by Simo and Taylor (1985)

$$\boldsymbol{C}_{n+1} = \boldsymbol{C} - 2\mu\left[(\beta - \delta)\hat{\boldsymbol{n}} \otimes \hat{\boldsymbol{n}} + (1-\beta)\left(\boldsymbol{I} - \frac{1}{3}\boldsymbol{1} \otimes \boldsymbol{1}\right)\right] \tag{70}$$

where $\mathbf{1}$ and $\boldsymbol{I}$ are the second-order and symmetric fourth-order identity tensors, respectively, and

$$\beta = \frac{|\boldsymbol{s}_{n+1}|}{|\boldsymbol{s}^{\mathrm{T}}_{n+1}|} \qquad \delta = \frac{h}{h + 3\mu}$$

For more general versions of this algorithm, see Simo and Hugues (1998).

7.3 Elastic–plastic analysis based on symmetric Galerkin D/BEM

Elastic–plastic analyses can also be developed on the basis of the SGBEM; see, for example, Maier and Polizzotto (1987), Polizzotto (1988), Maier *et al.* (1995), Frangi and Maier (1999), and Burgardt (1999). For this purpose, one first needs to set up a symmetric set of governing SGBEM equations for the boundary unknowns $\boldsymbol{u}, \boldsymbol{t}$, and the plastic strains $\boldsymbol{\varepsilon}^{\mathrm{P}}$. This can be achieved following the path outlined in Section 4 but with the potential energy now given by

$$E(\boldsymbol{v}, \boldsymbol{\varepsilon}^{\mathrm{P}}) = \int_{\Omega} [\boldsymbol{\varepsilon}(\boldsymbol{v}) - \boldsymbol{\varepsilon}^{\mathrm{P}}] : \boldsymbol{C} : [\boldsymbol{\varepsilon}(\boldsymbol{v}) - \boldsymbol{\varepsilon}^{\mathrm{P}}] \, \mathrm{d}V - \int_{S_t} \bar{\boldsymbol{t}} \cdot \boldsymbol{v} \, \mathrm{d}S - \int_{S_u} \boldsymbol{t}(\boldsymbol{u}) \cdot (\boldsymbol{v} - \bar{\boldsymbol{u}}) \, \mathrm{d}S$$

instead of (32), which leads to the stationarity equation

$$\begin{aligned} \delta E(\boldsymbol{u}, \boldsymbol{\varepsilon}^{\mathrm{P}}) = {} & \int_{\Omega^{\mathrm{P}}} [\boldsymbol{\varepsilon} : \boldsymbol{C} : \tilde{\boldsymbol{\varepsilon}} - \boldsymbol{\varepsilon}^{\mathrm{P}} : \boldsymbol{C} : \delta\boldsymbol{\varepsilon}] + \int_{S_t} \bar{\boldsymbol{u}} \cdot \boldsymbol{t}(\delta\boldsymbol{u}) \, \mathrm{d}S \\ & + \int_{S_u} \boldsymbol{u} \cdot \boldsymbol{t}(\delta\boldsymbol{u}) \, \mathrm{d}S - \int_{S_t} \bar{\boldsymbol{t}} \cdot \delta\boldsymbol{u} \, \mathrm{d}S \\ & - \int_{S_u} \boldsymbol{t}(\boldsymbol{u}) \cdot \boldsymbol{u} \, \mathrm{d}S = 0 \quad (\forall \delta\boldsymbol{u}, \mathrm{div}\,(\boldsymbol{C} : \boldsymbol{\varepsilon}(\delta\boldsymbol{u})) = \boldsymbol{0}) \end{aligned} \tag{71}$$

upon assuming that all trial functions $\delta\boldsymbol{u}$ satisfy div $(\boldsymbol{C} : [\boldsymbol{\varepsilon}(\delta\boldsymbol{u}) - \tilde{\boldsymbol{\varepsilon}}) = \boldsymbol{0})$, with $\tilde{\boldsymbol{\varepsilon}} = \boldsymbol{0}$ outside of Ω^{P}. Any such trial functions can be expressed in the form of integral representations:

$$\delta u_k(\tilde{\boldsymbol{x}}) = \int_{\Omega^{\mathrm{P}}} \tilde{\varepsilon}_{ij}(\boldsymbol{x}) \Sigma^k_{ij}(\tilde{\boldsymbol{x}}, \boldsymbol{x}) \, \mathrm{d}V_x + \int_{S_t} \tilde{u}_i(\boldsymbol{x}) T^k_i(\tilde{\boldsymbol{x}}, \boldsymbol{x}) \, \mathrm{d}S_x - \int_{S_u} \tilde{t}_i(\boldsymbol{x}) U^k_i(\tilde{\boldsymbol{x}}, \boldsymbol{x}) \, \mathrm{d}S_x$$

As a result, the set of continuous SGBEM equations has the structure (Bonnet *et al.*, 1998a)

$$\begin{aligned} \mathcal{B}_{tt}(\boldsymbol{t}, \tilde{\boldsymbol{t}}) + \mathcal{B}_{ut}(\boldsymbol{u}, \tilde{\boldsymbol{t}}) + \mathcal{B}_{\varepsilon t}(\boldsymbol{\varepsilon}^{\mathrm{P}}, \tilde{\boldsymbol{t}}) &= \mathcal{L}_t(\tilde{\boldsymbol{t}}; \bar{\boldsymbol{u}}) \\ \mathcal{B}_{tu}(\boldsymbol{t}, \tilde{\boldsymbol{u}}) + \mathcal{B}_{uu}(\boldsymbol{u}, \tilde{\boldsymbol{u}}) + \mathcal{B}_{\varepsilon u}(\boldsymbol{\varepsilon}^{\mathrm{P}}, \tilde{\boldsymbol{u}}) &= \mathcal{L}_u(\tilde{\boldsymbol{u}}; \bar{\boldsymbol{t}}) \\ \mathcal{B}_{t\varepsilon}(\boldsymbol{t}, \tilde{\boldsymbol{\varepsilon}}) + \mathcal{B}_{u\varepsilon}(\boldsymbol{u}, \tilde{\boldsymbol{\varepsilon}}) + \mathcal{B}_{\varepsilon\varepsilon}(\boldsymbol{\varepsilon}^{\mathrm{P}}, \tilde{\boldsymbol{\varepsilon}}) &= -\mathcal{A}(\boldsymbol{\varepsilon}, \tilde{\boldsymbol{\varepsilon}}) \end{aligned} \tag{72}$$

where $\mathcal{B}_{uu}$, $\mathcal{B}_{ut}$, and $\mathcal{B}_{tt}$ are as defined by (37), (38), and (39); the new bilinear operator $\mathcal{B}_{\varepsilon\varepsilon}$ is symmetric while $\mathcal{B}_{u\varepsilon}$, $\mathcal{B}_{t\varepsilon}$ are transposes of $\mathcal{B}_{\varepsilon u}$, $\mathcal{B}_{\varepsilon t}$, respectively; the linear operators $\mathcal{L}_u$ and $\mathcal{L}_t$ are as defined by (40) and (41); and the bilinear operator $\mathcal{A}$ is defined by

$$\mathcal{A}(\boldsymbol{\varepsilon}, \tilde{\boldsymbol{\varepsilon}}) = \int_{\Omega^{\mathrm{P}}} \boldsymbol{\varepsilon} : \boldsymbol{C} : \tilde{\boldsymbol{\varepsilon}} \, \mathrm{d}V \tag{73}$$

Upon introducing standard BE interpolations for $(\boldsymbol{u}, \tilde{\boldsymbol{u}})$ on S_t and $(\boldsymbol{t}, \tilde{\boldsymbol{t}})$ on S_u, and standard (continuous) interpolations for $(\boldsymbol{\varepsilon}^{\mathrm{P}}, \tilde{\boldsymbol{\varepsilon}})$ on Ω^{P} (and using the same interpolation bases for the associated unknown and test functions, in keeping with the SGBEM approach), equation (72) takes the form

$$\begin{bmatrix} \boldsymbol{B}_{tt} & \boldsymbol{B}_{ut} & \boldsymbol{B}_{\varepsilon t} & \boldsymbol{0} \\ \boldsymbol{B}_{tu} & \boldsymbol{B}_{uu} & \boldsymbol{B}_{\varepsilon u} & \boldsymbol{0} \\ \boldsymbol{B}_{t\varepsilon} & \boldsymbol{B}_{u\varepsilon} & \boldsymbol{B}_{\varepsilon\varepsilon} & \boldsymbol{A} \end{bmatrix} \begin{Bmatrix} \boldsymbol{t} \\ \boldsymbol{u} \\ \boldsymbol{\varepsilon}^{\mathrm{P}} \\ \boldsymbol{\varepsilon} \end{Bmatrix} = \begin{Bmatrix} \boldsymbol{F}_t \\ \boldsymbol{F}_u \\ \boldsymbol{0} \end{Bmatrix} \tag{74}$$

with obvious notations and noting that $\boldsymbol{A}$ is a stiffness-like symmetric matrix. Next, in preparation of the time-stepping process, equation (74) is written in incremental form (noting that the time-dependent loading is contained in $\boldsymbol{F}_t$ and $\boldsymbol{F}_u$):

$$\begin{bmatrix} \boldsymbol{B}_{tt} & \boldsymbol{B}_{ut} & \boldsymbol{B}_{\varepsilon t} & \boldsymbol{0} \\ \boldsymbol{B}_{tu} & \boldsymbol{B}_{uu} & \boldsymbol{B}_{\varepsilon u} & \boldsymbol{0} \\ \boldsymbol{B}_{t\varepsilon} & \boldsymbol{B}_{u\varepsilon} & \boldsymbol{B}_{\varepsilon\varepsilon} & \boldsymbol{A} \end{bmatrix} \begin{Bmatrix} \Delta\boldsymbol{t}_n \\ \Delta\boldsymbol{u}_n \\ \Delta\boldsymbol{\varepsilon}^{\mathrm{P}}_n \\ \Delta\boldsymbol{\varepsilon}_n \end{Bmatrix} = \begin{Bmatrix} \Delta\boldsymbol{F}^n_t \\ \Delta\boldsymbol{F}^n_u \\ \boldsymbol{0} \end{Bmatrix} \tag{75}$$

Using the first two equations to eliminate the increments $(\Delta\boldsymbol{u}_n, \Delta\boldsymbol{t}_n)$, the third equation yields a relationship between $(\Delta\boldsymbol{\varepsilon}^{\mathrm{P}}, \Delta\boldsymbol{\varepsilon})$ of the form

$$[\boldsymbol{R}]\{\Delta\boldsymbol{\varepsilon}^{\mathrm{P}}_n\} + [\boldsymbol{A}]\{\Delta\boldsymbol{\varepsilon}_n\} = \{\Delta\boldsymbol{F}_n\} \tag{76}$$

As before, all variables at time t_n, collectively denoted as $\mathcal{S}_n$, are assumed to be known (which requires imposing initial conditions at time t_0), and the increments $\Delta\boldsymbol{\varepsilon}^{\mathrm{P}}_n, \Delta\boldsymbol{\varepsilon}_n$ are sought.

The plastic part of the constitutive behavior still remains to be accounted for. This is again done using the implicit algorithm based on the RRA, described in Section 7.2, and with the same notations. Here, substituting definition (62) of $\bar{\boldsymbol{\sigma}}$, that is, $\boldsymbol{\sigma}_{n+1} = \bar{\boldsymbol{\sigma}}(\Delta\boldsymbol{\varepsilon}_n, \mathcal{S}_n)$, into the elastic constitutive equation (2) written in incremental form yields

$$\bar{\boldsymbol{\sigma}}(\Delta\boldsymbol{\varepsilon}_n, \mathcal{S}_n) - \boldsymbol{\sigma}_n = \boldsymbol{C} : (\Delta\boldsymbol{\varepsilon}^{\mathrm{P}}_n - \Delta\boldsymbol{\varepsilon}_n) \tag{77}$$

which allows expressing $\Delta\boldsymbol{\varepsilon}^{\mathrm{P}}_n$ in terms of $\Delta\boldsymbol{\varepsilon}_n$ and $\bar{\boldsymbol{\sigma}}(\Delta\boldsymbol{\varepsilon}_n, \mathcal{S}_n)$.

Doing so directly for the nodal unknowns in (76) and performing the subsequent Newton iteration is feasible but leads to unsymmetric tangent matrices for the Newton steps. In order to formulate a symmetric Newton step, equation (77) is multiplied (in the tensor inner-product sense) by a trial strain $\tilde{\boldsymbol{\varepsilon}}$ and then integrated over Ω^{P}, to obtain

$$\int_{\Omega^{\mathrm{P}}} \bar{\boldsymbol{\sigma}}(\Delta\boldsymbol{\varepsilon}_n, \mathcal{S}_n) : \tilde{\boldsymbol{\varepsilon}} \, \mathrm{d}V - \mathcal{A}(\Delta\boldsymbol{\varepsilon}_n, \tilde{\boldsymbol{\varepsilon}}) + \mathcal{A}(\Delta\boldsymbol{\varepsilon}_n^{\mathrm{P}}, \tilde{\boldsymbol{\varepsilon}}) = \int_{\Omega^{\mathrm{P}}} \boldsymbol{\sigma}_n : \tilde{\boldsymbol{\varepsilon}} \, \mathrm{d}V$$

Then, putting $\Delta\boldsymbol{\varepsilon}_n^{i+1} = \Delta\boldsymbol{\varepsilon}_n^i + \delta\boldsymbol{\varepsilon}_n^i$ and expanding the above equality to first order in $\delta\boldsymbol{\varepsilon}_n^i$ in anticipation of the Newton iteration to be implemented, one gets

$$\mathcal{A}_{n+1}^i(\delta\boldsymbol{\varepsilon}_n^i, \tilde{\boldsymbol{\varepsilon}}) - \mathcal{A}(\delta\boldsymbol{\varepsilon}_n^i, \tilde{\boldsymbol{\varepsilon}}) + \mathcal{A}(\delta\boldsymbol{\varepsilon}_n^{\mathrm{P},i}, \tilde{\boldsymbol{\varepsilon}}) + \mathcal{H}(\Delta\boldsymbol{\varepsilon}_n^i) = 0$$

$$\mathcal{H}(\Delta\boldsymbol{\varepsilon}_n) \equiv \int_{\Omega^{\mathrm{P}}} \bar{\boldsymbol{\sigma}}(\Delta\boldsymbol{\varepsilon}_n, \mathcal{S}_n) : \tilde{\boldsymbol{\varepsilon}} \, \mathrm{d}V - \mathcal{A}(\Delta\boldsymbol{\varepsilon}_n, \tilde{\boldsymbol{\varepsilon}}) + \mathcal{A}(\Delta\boldsymbol{\varepsilon}_n^{\mathrm{P}}, \tilde{\boldsymbol{\varepsilon}}) - \int_{\Omega^{\mathrm{P}}} \boldsymbol{\sigma}_n : \tilde{\boldsymbol{\varepsilon}}$$

where $\mathcal{A}_{n+1}^i$ is defined by (73) but using the local CTO $\boldsymbol{C}_{n+1}^i(\Delta\boldsymbol{\varepsilon}_n, \mathcal{S}_n)$ instead of the elastic Hooke tensor $\boldsymbol{C}$. In discretized form, this equation becomes

$$[\boldsymbol{A}_n^i - \boldsymbol{A}]\{\delta\boldsymbol{\varepsilon}_n^i\} + [\boldsymbol{A}]\{\delta\boldsymbol{\varepsilon}_n^{\mathrm{P},i}\} + \boldsymbol{H}_n = \{\boldsymbol{0}\} \tag{78}$$

where $\boldsymbol{S}_n$ is the discretized $\mathcal{S}_n$ and $\boldsymbol{H}_n$ incorporates the known stress field $\boldsymbol{\sigma}_n$. In combination with the linear equation (76) put in a similar iterative form, each correction $\{\delta\boldsymbol{\varepsilon}_n^i, \delta\boldsymbol{\varepsilon}_n^{\mathrm{P},i}\}$ is finally found to be governed by the following symmetric system of linear equations:

$$\begin{bmatrix} \boldsymbol{R} & \boldsymbol{A} \\ \boldsymbol{A} & \boldsymbol{A}_n^i - \boldsymbol{A} \end{bmatrix} \begin{Bmatrix} \delta\boldsymbol{\varepsilon}_n^{\mathrm{P},i} \\ \delta\boldsymbol{\varepsilon}_n^i \end{Bmatrix} = \begin{Bmatrix} -\boldsymbol{G}_n^i \\ -\boldsymbol{H}_n^i \end{Bmatrix} \tag{79}$$

with

$$\boldsymbol{G}_n^i \equiv [\boldsymbol{R}]\{\delta\boldsymbol{\varepsilon}_n^{\mathrm{P},i}\} + [\boldsymbol{A}]\{\Delta\boldsymbol{\varepsilon}_n\} - \{\Delta\boldsymbol{F}_n\}$$

This scheme has been implemented for three-dimensional problems in Burgardt (1999). It is worth mentioning that setting up the discretized bilinear operators of (74) involves numerical integrations in four dimensions (for $\boldsymbol{B}_{tt}$, $\boldsymbol{B}_{ut}$, $\boldsymbol{B}_{uu}$), five dimensions (for $\boldsymbol{B}_{\varepsilon t}, \boldsymbol{B}_{\varepsilon u}$), and six dimensions (for $\boldsymbol{B}_{\varepsilon\varepsilon}$), including weakly singular integrations. In the latter case, various types of coordinate changes in the parameter space are available, so that these singular integrations do not raise serious conceptual difficulties. From a more practical viewpoint, the calculation of the operators $\boldsymbol{B}_{\varepsilon\varepsilon}$ and, to a lesser extent, $\boldsymbol{B}_{\varepsilon t}, \boldsymbol{B}_{\varepsilon u}$ using Cartesian products of one-dimensional Gaussian rules was found to be extremely time consuming. Outside of other possibilities for code optimization, which have not been explored as of now, much can be gained by employing well-chosen quadrature rules devised for the n-cube instead of n-fold Cartesian products of one-dimensional rules. A collection of such rules are given in Stroud (1971). For instance, the sixfold product of the 3-point rule (i.e., 729 quadrature points in all) can be replaced by a six-dimensional 125-point rule, among several possibilities. For now, this high computational cost means that only a moderate number of (20-noded brick-shaped) domain cells could be used in numerical examples.

7.4 Finite strains

Extensions of D/BEM to problems with both geometrical and material nonlinearities are also proposed by Mukherjee and Chandra (1991), Zhang *et al.* (1992), Leu and Mukherjee (1993), and Foerster and Kuhn (1994), among others, and in the book by Chandra and Mukherjee (1997).

When geometrical nonlinearities, in the form of finite strains, are present, the governing equations must be formulated in rate form. A detailed presentation of this subject is not attempted here (the reader is referred to the above-mentioned references). However, some insight into how D/BEM formulations are developed for this class of problems can be obtained by looking at the governing displacement DBIE (or, more appropriately here, the velocity DBIE):

$$\bar{\kappa} v_k(\tilde{\boldsymbol{x}}) + \int_{\partial\Omega} \{T_i^k(\tilde{\boldsymbol{x}}, \boldsymbol{x})[v_i(\boldsymbol{x}) - v_i(\tilde{\boldsymbol{x}})] - U_i^k(\tilde{\boldsymbol{x}}, \boldsymbol{x}) t_i^s(\boldsymbol{x})\} \, \mathrm{d}S_x = \int_{\Omega} \Sigma_{ij}^k(\tilde{\boldsymbol{x}}, \boldsymbol{x}) \boldsymbol{d}_{ij}^{\mathrm{P}}(\boldsymbol{x}) \, \mathrm{d}V_x + \int_{\Omega} U_{i,j}^k(\tilde{\boldsymbol{x}}, \boldsymbol{x}) \boldsymbol{g}_{ji}(\boldsymbol{x}) \, \mathrm{d}V_x \tag{80}$$

where $\boldsymbol{v}$ is the velocity field, $\boldsymbol{d} = (\boldsymbol{\nabla v} + \boldsymbol{\nabla v}^{\mathrm{T}})/2$ is the total strain rate, $\boldsymbol{d}^{\mathrm{P}}$ is the inelastic strain rate, $\boldsymbol{g}$ is defined by the formula

$$\boldsymbol{g} = \boldsymbol{\sigma} \cdot \boldsymbol{\omega} + \boldsymbol{d} \cdot \boldsymbol{\sigma} - (\mathrm{Tr}(\boldsymbol{d}))\boldsymbol{\sigma}$$

(where $\boldsymbol{\omega} = (\boldsymbol{\nabla v} - \boldsymbol{\nabla v}^{\mathrm{T}})/2$ is the antisymmetric part of the velocity gradient), and $\boldsymbol{t}^s$ is the scaled Lagrange traction rate defined by

$$\boldsymbol{t}^s = \boldsymbol{n} \cdot (\dot{\boldsymbol{\sigma}} + \boldsymbol{\sigma} \cdot \boldsymbol{\omega} - \boldsymbol{\omega} \cdot \boldsymbol{\sigma} - \boldsymbol{g})$$

The stress–strain rate relationship is of the form

$$\boldsymbol{\sigma} = \lambda \mathrm{Tr}(\boldsymbol{d}) + 2\mu(\boldsymbol{d} - \boldsymbol{d}^{\mathrm{P}}) \quad \mathrm{Tr}(\boldsymbol{d}^{\mathrm{P}}) = 0$$

which defines the inelastic strain rate $\boldsymbol{d}^{\mathrm{P}}$.

Regularized strain rate representation formulas can be established from (80), providing the foundation for incremental and iterative solution algorithms. Contrary to small-strain plasticity, which in some cases may affect only a small part of the domain Ω under consideration, geometric nonlinearities are expected to spread over the entire region, thus entailing a significant computational burden in terms of numerical integration and solution procedures, since fully populated matrices over domain unknowns arise in the process.

For completeness, one can also mention the work of Bigoni and Capuani (2002), where a Green's function approach for the incremental problem of finite elasticity in plane strain is proposed.

8 SHAPE SENSITIVITY ANALYSIS

The consideration of sensitivity analysis of integral functionals with respect to shape parameters arises in many situations in which a geometrical domain plays a primary role; shape optimization and inverse problems are the most obvious, as well as possibly the most important, of such instances (see **Identification of Material Parameters for Constitutive Equations**).

It is well known that apart from resorting to approximative techniques such as finite differences, shape sensitivity evaluation can be dealt with using either the direct differentiation approach or the adjoint variable approach (Burczyński, 1993b). Besides, consideration of shape changes in otherwise (i.e., for fixed shape) linear problems makes BEMS very attractive, as they constitute the minimal modeling as far as the geometrical support of unknown field variables is concerned.

Typical applications concern shape optimization and inverse problems, see, for example, Brancati *et al.* (2012), Guzina *et al.* (2003, 2009), and Rus and Gallego (2007) in the context of vibrations or wave propagation. However, shape sensitivity analysis also has important applications in fracture mechanics, see, for example, Bonnet (1999c).

8.1 Differentiation with respect to shape perturbations

To consider shape perturbations, the shape of Ω is assumed to depend on a parameter t (a fictitious, nonphysical "time") through a continuum kinematics-type Lagrangian description. The unperturbed, "initial" configuration Ω is conventionally associated with $t = 0$:

$$\boldsymbol{x} \in \Omega \to \boldsymbol{x}^t = \boldsymbol{\Phi}(\boldsymbol{x}, t) \in \Omega(t) \qquad \boldsymbol{\Phi}(\boldsymbol{x}, 0) = \boldsymbol{x} \tag{81}$$

All "time" derivatives are here implicitly taken at $t = 0$, that is, the first-order effect of infinitesimal perturbations of $\Omega \equiv \Omega(0)$ is considered. The *geometrical transformation* $\boldsymbol{\Phi}(\cdot\,; t)$ must possess a strictly positive Jacobian for $t \geq 0$. A given domain evolution considered as a whole admits infinitely many different representations (81).

8.1.1 Differentiation of scalar or tensor fields

Differentiation of field variables and integrals in a domain perturbation is a well-documented subject (Petryk and Mróz, 1986; Sokolowski and Zolesio, 1992); a few basic concepts and results are recalled now. The *initial transformation velocity* $\boldsymbol{\theta}$ is defined by

$$\boldsymbol{\theta}(\boldsymbol{x}) = \frac{\partial \boldsymbol{\Phi}}{\partial t}\Big|_{t=0} \tag{82}$$

The "material" (or "Lagrangian") derivative at $t = 0$ of a field quantity $f(\boldsymbol{x}, t)$ in a geometrical transformation, denoted by $\overset{\star}{f}$, is defined by

$$\begin{aligned} \overset{\star}{f} &= \lim_{t\to 0} \frac{1}{t}[f(\boldsymbol{x}^t, t) - f(\boldsymbol{x}, 0)] = \frac{\partial f}{\partial t} + \boldsymbol{\nabla} f \cdot \boldsymbol{\theta} \\ &= f' + \boldsymbol{\nabla} f \cdot \boldsymbol{\theta} \end{aligned} \tag{83}$$

(where f' is used as a shorthand notation for the partial "time" derivative). The material derivative of the gradient of a field quantity is given by

$$(\boldsymbol{\nabla} f)^\star = \boldsymbol{\nabla} \overset{\star}{f} - \boldsymbol{\nabla} f \cdot \boldsymbol{\nabla}\, \boldsymbol{\theta} \tag{84}$$

8.1.2 Differentiation of integrals

First, recall that the derivative of the volume differential element $\mathrm{d}V$ is given by

$$\overset{\star}{\mathrm{d}V} = (\mathrm{div}\ \theta)\mathrm{d}V$$

so that the derivative of a generic volume integral

$$I(f, D; t) = \int_{D(t)} f(\boldsymbol{x}, t)\mathrm{d}V$$

is given by the well-known formula

$$\frac{\mathrm{d}I}{\mathrm{d}t} = \overset{\star}{I} = \int_D \{\overset{\star}{f} + f\,\mathrm{div}\ \boldsymbol{\theta}\}\mathrm{d}V \tag{85}$$

where $\theta_n = \boldsymbol{\theta} \cdot \boldsymbol{n}$. The material derivatives of the unit normal $\boldsymbol{n}$ and the surface differential element $\mathrm{d}S$ on a material

surface $S_t = \mathbf{\Phi}(S;t)$ are given (Petryk and Mróz, 1986) by

$$\overset{\star}{\mathrm{d}S} = \mathrm{div}_S\boldsymbol{\theta}\,\mathrm{d}S = D_r\theta_r\,\mathrm{d}S$$
$$\overset{\star}{\boldsymbol{n}} = -\boldsymbol{n}\cdot\boldsymbol{\nabla}_S\boldsymbol{\theta} = -n_bD_a\theta_b\boldsymbol{e}_a \tag{86}$$

in terms of the surface gradient $\boldsymbol{\nabla}_S$ and the surface divergence div_S:

$$\boldsymbol{\nabla}_S f = \boldsymbol{\nabla} f - (\boldsymbol{\nabla} f\cdot\boldsymbol{n})\boldsymbol{n} = (f_{,i} - n_i f_{,n})\boldsymbol{e}_i \equiv (D_i f)\boldsymbol{e}_i \tag{87}$$
$$\mathrm{div}_S\boldsymbol{u} = \mathrm{div}\,\boldsymbol{u} - (\boldsymbol{\nabla}\boldsymbol{u}\cdot\boldsymbol{n})\cdot\boldsymbol{n} = D_iu_i \tag{88}$$

Then, for a generic surface integral $J(t)$

$$J(f,S;t) = \int_{S(t)} f(\boldsymbol{x},t)\,\mathrm{d}S$$

one has, using (86)

$$\frac{\mathrm{d}J}{\mathrm{d}t} = \overset{\star}{J} = \int_S\left\{\overset{\star}{f}\mathrm{d}S + f(\,\mathrm{d}S)^{\star}\right\} = \int_S\left\{\overset{\star}{f} + f\mathrm{div}_S\boldsymbol{\theta}\right\}\,\mathrm{d}S \tag{89}$$

8.2 Direct differentiation of boundary integral equations

In the BIE context, the direct differentiation approach rests primarily upon the material differentiation of the governing integral equations. This step has been studied by many researchers, from BIE formulation in either singular form (Barone and Yang, 1989; Mellings and Aliabadi, 1995) or regularized form (Bonnet, 1995b; Matsumoto *et al.*, 1993; Nishimura *et al.*, 1992; Nishimura, 1995). For instance, the integral equation governing the elastic shape sensitivities, obtained from the BIE formulation (17), reads (Bonnet, 1995b)

$$\bar{\kappa}\overset{\star}{u}_k(\boldsymbol{y}) + \int_{\partial\Omega}\left\{T_i^k(\boldsymbol{y},\boldsymbol{x})[\overset{\star}{u}_i(\boldsymbol{x}) - \overset{\star}{u}_i(\boldsymbol{y})] - U_i^k(\boldsymbol{y},\boldsymbol{x})\overset{\star}{t}_i(\boldsymbol{x})\right\}\mathrm{d}S_x = -\int_{\partial\Omega}[\theta_r(\boldsymbol{y}) - \theta_r(\boldsymbol{x})] \times D_{rj}u_i(\boldsymbol{x})\Sigma_{ij}^k(\boldsymbol{y},\boldsymbol{x})\,\mathrm{d}S_x + \int_{\partial\Omega}t_i(\boldsymbol{x})\left\{\overset{\star}{U}_i^k(\boldsymbol{y},\boldsymbol{x}) + U_i^k(\boldsymbol{y},\boldsymbol{x})D_r\theta_r(\boldsymbol{x})\right\}\mathrm{d}S_x \quad (\boldsymbol{y}\in\partial\Omega) \tag{90}$$

Following this approach, the process of sensitivity computation needs the solution of as many new boundary value problems as the numbers of shape parameters present. The fact that they all involve the same, original, governing operator reduces the computational effort to the building of new right-hand sides and the solution of linear systems by backsubstitution. The usual material differentiation formula for surface integrals is shown in Bonnet (1997) to be still valid when applied to strongly singular or hypersingular formulations. Thus, the direct differentiation approach is, in particular, applicable in the presence of cracks.

8.3 Adjoint solution method

Another approach to shape sensitivity (and to other sensitivity calculations as well), namely the adjoint solution method, is useful when the sensitivity of some state-dependent objective function is required. In that case, the desired sensitivity can be expressed in terms of the original solution $(\boldsymbol{u},\boldsymbol{t})$ and an *adjoint solution* $(\tilde{\boldsymbol{u}},\tilde{\boldsymbol{t}})$, and the calculation of the Lagrangian derivatives $\overset{\star}{\boldsymbol{u}},\overset{\star}{\boldsymbol{t}}$ can be avoided. In connection with BEMs, the adjoint solution method has been the subject of many investigations by, for example, Bonnet (1995a,b) Bonnet *et al.* (2002), Burczyński (1993a), Burczyński and Fedelinski (1992), Burczyński *et al.* (1995), and Choi and Kwak (1988). In this section, the adjoint solution method is presented for the model problem where a buried cavity or crack is to be identified from elastostatic boundary measurements (this kind of inverse problem is considered by, e.g., Nishimura and Kobayashi (1995), Kassab *et al.* (1994), and Eller (1996)), but sensitivity formulations can be developed on similar lines for many other situations.

Consider an elastic body $\Omega\in\mathbb{R}^3$ of finite extension, externally bounded by the closed surface S and containing a defect bounded by the surface Γ (i.e., $\partial\Omega = S\cup\Gamma$). For the sake of definiteness, the defect is taken to be either a cavity (i.e., Γ is a closed surface and the interior region bounded by Γ is nonempty) or a crack (i.e., Γ is an open surface across which displacement jumps are expected). The displacement $\boldsymbol{u}$, strain $\boldsymbol{\varepsilon}$, and stress $\boldsymbol{\sigma}$ are related by the field equation (5) without body forces (i.e., with $\boldsymbol{f}=\boldsymbol{0}$). Besides, boundary conditions of the form (46) are assumed, that is, displacements and tractions are prescribed on the portions S_u and $S_t = S\backslash S_u$ of S, and the crack surface Γ is stress-free. Equations (46) and (5) define the *direct problem*.

Consider the problem of determining the shape and position of an unknown defect embedded in the elastic body using elastostatic measurements. The lack of information about Γ must be compensated by some extra knowledge about the field quantities on S (redundant boundary data). Assume, for example, that a measurement $\hat{\boldsymbol{u}}(\boldsymbol{x})$ of $\boldsymbol{u}$ (resp. $\hat{\boldsymbol{t}}(\boldsymbol{x})$ of $\boldsymbol{t}$) is available for $\boldsymbol{x}\in S_t$ (resp. $\boldsymbol{x}\in S_u$). The defect identification is then usually formulated as the minimization of a cost function. The most obvious choice for the latter is a least-squared

misfit function, for example

$$\mathcal{J}(\Gamma) = J(\boldsymbol{u}_\Gamma, \boldsymbol{t}_\Gamma) = \frac{1}{2}\int_{S_t} |\hat{\boldsymbol{u}} - \boldsymbol{u}_\Gamma|^2 \, \mathrm{d}S + \frac{1}{2}\int_{S_u} |\hat{\boldsymbol{t}} - \boldsymbol{t}_\Gamma|^2 \, \mathrm{d}S \tag{91}$$

where $(\boldsymbol{u}_\Gamma, \boldsymbol{t}_\Gamma)$ refer to the solution of problem (5, 46) for a given Γ. For the sake of generality, generic objective functions of the form

$$\mathcal{J}(\Gamma) = J(\boldsymbol{u}_\Gamma, \boldsymbol{t}_\Gamma, \Gamma) = \int_{S_t} \varphi_u(\boldsymbol{u}_\Gamma, \boldsymbol{x}) \, \mathrm{d}S + \int_{S_u} \varphi_p(\boldsymbol{t}_\Gamma, \boldsymbol{x}) \, \mathrm{d}S + \int_\Gamma \psi(\boldsymbol{x}) \, \mathrm{d}S \tag{92}$$

which obviously generalize (91), are considered. Minimizing $\mathcal{J}$ with respect to Γ using classical gradient-based methods is computationally much more efficient if a procedure for computing the gradient of $\mathcal{J}$ with respect to shape perturbations of Γ, in addition to $\mathcal{J}(\Gamma)$ itself, is available.

8.3.1 Adjoint formulations for shape sensitivity

Any sufficiently small perturbation of Γ can be described by means of a domain transformation (81), which does not affect the external boundary S, that is, such that $\boldsymbol{\theta} = \boldsymbol{0}$ on S.

It is customary to derive the adjoint problem by means of an optimal control approach whereby the variables in the objective function $J(\boldsymbol{u}, \boldsymbol{t}, \Gamma)$ are formally considered as independent ones and the direct problem (5, 46) is treated as an explicit constraint. The following Lagrangian is thus introduced:

$$\mathcal{L}(\boldsymbol{u}, \tilde{\boldsymbol{u}}, \boldsymbol{t}, \tilde{\boldsymbol{t}}, \Gamma) = J(\boldsymbol{u}, \boldsymbol{t}, \Gamma) + \int_\Omega \boldsymbol{\sigma} : \boldsymbol{\nabla}\tilde{\boldsymbol{u}} \, \mathrm{d}V - \int_{S_u} (\boldsymbol{u} - \bar{\boldsymbol{u}}) \cdot \tilde{\boldsymbol{t}} \, \mathrm{d}S - \int_{S_u} \boldsymbol{t} \cdot \tilde{\boldsymbol{u}} \, \mathrm{d}S - \int_{S_t} \bar{\boldsymbol{t}} \cdot \tilde{\boldsymbol{u}} \, \mathrm{d}S \tag{93}$$

where $(\tilde{\boldsymbol{u}}, \tilde{\boldsymbol{t}})$, the test functions of the direct problem in weak form, act as Lagrange multipliers.

Using formulas (85) and (89), noticing that $(\boldsymbol{C} : \boldsymbol{\nabla}\overset{\star}{\boldsymbol{u}}) : \boldsymbol{\nabla}\tilde{\boldsymbol{u}} = \tilde{\boldsymbol{\sigma}} : \boldsymbol{\nabla}\overset{\star}{\boldsymbol{u}}$, and ignoring the terms containing $\tilde{\boldsymbol{u}}^\star, \tilde{\boldsymbol{t}}^\star$ arising in this calculation (they merely reproduce the direct problem constraint and thus vanish), the total derivative of $\mathcal{L}$ with respect to a given domain perturbation is given by

$$\overset{\star}{\mathcal{L}}(\boldsymbol{u}, \tilde{\boldsymbol{u}}, \boldsymbol{t}, \tilde{\boldsymbol{t}}, \Gamma) = \int_\Omega \{(\boldsymbol{\sigma} : \boldsymbol{\nabla}\tilde{\boldsymbol{u}})\mathrm{div}\ \boldsymbol{\theta} - [\boldsymbol{\sigma} \cdot \boldsymbol{\nabla}\tilde{\boldsymbol{u}} + \tilde{\boldsymbol{\sigma}} \cdot \boldsymbol{\nabla}\boldsymbol{u}] : \boldsymbol{\nabla}\boldsymbol{\theta}\} \, \mathrm{d}V + \int_\Gamma [\boldsymbol{\nabla}\psi \cdot \boldsymbol{\theta} + \psi \mathrm{div}_S \boldsymbol{\theta}] \, \mathrm{d}S + \int_\Omega \tilde{\boldsymbol{\sigma}} : \boldsymbol{\nabla}\overset{\star}{\boldsymbol{u}} \, \mathrm{d}V - \int_{S_u} (\tilde{\boldsymbol{u}} - \frac{\partial \varphi_p}{\partial \boldsymbol{t}}) \cdot \overset{\star}{\boldsymbol{t}} \, \mathrm{d}S - \int_{S_u} \tilde{\boldsymbol{t}} \cdot \overset{\star}{\boldsymbol{u}} \, \mathrm{d}S + \int_{S_t} \frac{\partial \varphi_u}{\partial \boldsymbol{u}} \cdot \overset{\star}{\boldsymbol{u}} \, \mathrm{d}S \tag{94}$$

When Γ is an open surface (i.e., a crack), the partial derivative $(\boldsymbol{\nabla}u)_{,\eta}$ has usually a $d^{-3/2}$ singularity along the crack edge $\partial\Gamma$, while $\boldsymbol{\nabla}\overset{\star}{\boldsymbol{u}}$ and $\boldsymbol{\nabla}\boldsymbol{u}$ have the same $d^{-1/2}$ singularity (d: distance to $\partial\Gamma$); this explains our using Lagrangian derivatives $\overset{\star}{\boldsymbol{u}}$.

Now, the multipliers $\tilde{\boldsymbol{u}}, \tilde{\boldsymbol{t}}$ are chosen specifically so that all terms containing $\overset{\star}{\boldsymbol{u}}$ and $\overset{\star}{\boldsymbol{t}}$ in (94) combine to zero for any $\overset{\star}{\boldsymbol{u}}$ and $\overset{\star}{\boldsymbol{t}}$. The weak formulation of an *adjoint problem*, of a form similar to the direct problem in (93) but with $\overset{\star}{\boldsymbol{u}}, \overset{\star}{\boldsymbol{t}}$ now acting as test functions, is thus defined. Its *adjoint solution* $\tilde{\boldsymbol{u}}_\Gamma, \tilde{\boldsymbol{t}}_\Gamma$ is therefore found (by analogy to (93)) to solve the field equations of elastic equilibrium (5), together with the following boundary conditions:

$$\tilde{\boldsymbol{t}} = -\frac{\partial \varphi_u}{\partial \boldsymbol{u}} \ (\text{on } S_t) \quad \tilde{\boldsymbol{u}} = \frac{\partial \varphi_p}{\partial \boldsymbol{t}} \ (\text{on } S_u) \quad \tilde{\boldsymbol{t}} = \boldsymbol{0} \ \ (\text{on } \Gamma^\pm) \tag{95}$$

Finally, equation (94) allows expressing the derivative of J in terms of the direct and adjoint solutions:

$$\begin{aligned} \overset{\star}{\mathcal{J}}(\Gamma) &= \overset{\star}{\mathcal{L}}(\boldsymbol{u}_\Gamma, \tilde{\boldsymbol{u}}_\Gamma, \boldsymbol{t}_\Gamma, \tilde{\boldsymbol{t}}_\Gamma, \Gamma) \\ &= \int_\Omega \{(\boldsymbol{\sigma}_\Gamma : \boldsymbol{\nabla}\tilde{\boldsymbol{u}}_\Gamma)\mathrm{div}\ \boldsymbol{\theta} - [\boldsymbol{\sigma}_\Gamma \cdot \boldsymbol{\nabla}\tilde{\boldsymbol{u}}_\Gamma + \tilde{\boldsymbol{\sigma}}_\Gamma \cdot \boldsymbol{\nabla}\boldsymbol{u}_\Gamma] : \boldsymbol{\nabla}\boldsymbol{\theta}\} \, \mathrm{d}V \\ &\quad + \int_\Gamma [\boldsymbol{\nabla}\psi \cdot \boldsymbol{\theta} + \psi \mathrm{div}_S \boldsymbol{\theta}] \, \mathrm{d}S \end{aligned} \tag{96}$$

This formula allows an efficient computation of the directional derivative of $\mathcal{J}(\Gamma)$ in any perturbation velocity $\boldsymbol{\theta}$. It is well suited to domain discretization techniques (e.g., finite elements) for the solution of the direct and adjoint problems.

8.3.2 Sensitivity to cavity shape in terms of boundary integrals

Both the direct and the adjoint problems can be easily formulated using the BIE (17) and solved with the BEM. In addition, a BEM-based defect identification algorithm requires a sensitivity formula written in terms of boundary integrals rather than (96).

A transformation of (96) is achieved by noting that any elastostatic states $(\boldsymbol{u}, \boldsymbol{\sigma})$ and $(\tilde{\boldsymbol{u}}, \tilde{\boldsymbol{\sigma}})$ verify

$$\{(\boldsymbol{\sigma} : \tilde{\boldsymbol{\varepsilon}})\mathrm{div}\ \boldsymbol{\theta} - [\boldsymbol{\sigma} \cdot \boldsymbol{\nabla}\tilde{\boldsymbol{u}} + \tilde{\boldsymbol{\sigma}} \cdot \boldsymbol{\nabla}\boldsymbol{u}] : \boldsymbol{\nabla}\boldsymbol{\theta}\} = \mathrm{div}\,((\boldsymbol{\sigma} : \tilde{\boldsymbol{\varepsilon}})\boldsymbol{\theta} - [\boldsymbol{\sigma} \cdot \boldsymbol{\nabla}\tilde{\boldsymbol{u}} + \tilde{\boldsymbol{\sigma}} \cdot \boldsymbol{\nabla}\boldsymbol{u}] \cdot \boldsymbol{\theta}) \tag{97}$$

If Γ is a closed surface, that is, a cavity, this identity directly leads to the boundary-only version of (96):

$$\overset{\star}{\mathcal{J}}(\Gamma) = \int_\Gamma \{(\boldsymbol{\sigma} : \tilde{\boldsymbol{\varepsilon}})\theta_n - [\boldsymbol{t}_\Gamma \cdot \boldsymbol{\nabla}\tilde{\boldsymbol{u}}_\Gamma + \tilde{\boldsymbol{t}}_\Gamma \cdot \boldsymbol{\nabla}\boldsymbol{u}_\Gamma] \cdot \boldsymbol{\theta}\} \, \mathrm{d}S + \int_\Gamma [\boldsymbol{\nabla}\psi \cdot \boldsymbol{\theta} + \psi \mathrm{div}_S \boldsymbol{\theta}] \, \mathrm{d}S \tag{98}$$

To ensure that formula (98) can actually be evaluated using only the boundary traces of the direct and adjoint solutions, the bilinear form $\boldsymbol{\sigma} : \boldsymbol{\nabla}\tilde{\boldsymbol{u}}$ must be expressed in terms of $\boldsymbol{\nabla}_S \boldsymbol{u}, \boldsymbol{\nabla}_S \tilde{\boldsymbol{u}}$, taking $\boldsymbol{t} = \tilde{\boldsymbol{t}} = \boldsymbol{0}$ into account in the process:

$$\boldsymbol{\sigma} : \boldsymbol{\nabla}\tilde{\boldsymbol{u}} = \mu \left\{ \frac{2\nu}{1-\nu} \mathrm{div}_S \boldsymbol{u} \, \mathrm{div}_S \tilde{\boldsymbol{u}} + \frac{1}{2}(\boldsymbol{\nabla}_S \boldsymbol{u} + \boldsymbol{\nabla}^{\mathrm{T}}{}_S \boldsymbol{u}) : (\boldsymbol{\nabla}_S \tilde{\boldsymbol{u}} + \boldsymbol{\nabla}^{\mathrm{T}}{}_S \tilde{\boldsymbol{u}}) - (\boldsymbol{n} \cdot \boldsymbol{\nabla}_S \boldsymbol{u}) \cdot (\boldsymbol{n} \cdot \boldsymbol{\nabla}_S \tilde{\boldsymbol{u}}) \right\} \tag{99}$$

8.3.3 Sensitivity to crack shape in terms of boundary integrals

If Γ is a crack, the well-known singular behavior of strains and stresses at the crack front prevents a direct application of the divergence formula to (96) for the entire cracked domain Ω because the r.h.s. of (97) is not integrable near the crack front $\partial\Gamma$. To circumvent this difficulty, a tubular neighborhood D_ε of $\partial\Gamma$ of radius ε is introduced, the well-known expansions of the mechanical fields near the *fixed* crack front are invoked inside D_ε, while identity (97) is invoked outside D_ε. Carrying out this limiting process (see Bonnet, 1999b; Bonnet *et al.*, 2002 for elastodynamics) results in the following shape sensitivity expression for $\mathcal{J}(\Gamma)$:

$$\overset{\star}{\mathcal{J}}(\Gamma) = \int_\Gamma \theta_n(s) [\![\boldsymbol{\sigma} : \boldsymbol{\nabla}\tilde{\boldsymbol{u}}]\!] \, \mathrm{d}S - \frac{1}{\mu} \int_{\partial\Gamma} \theta_\nu(s) \{(1-\nu)[K_{\mathrm{I}}\tilde{K}_{\mathrm{I}} + K_{\mathrm{II}}\tilde{K}_{\mathrm{II}}] + K_{\mathrm{III}}\tilde{K}_{\mathrm{III}}\}(s) \, \mathrm{d}s + \frac{1-\nu}{\mu} \int_{\partial\Gamma} \theta_n(s)(K_{\mathrm{I}}\tilde{K}_{\mathrm{II}} + K_{\mathrm{II}}\tilde{K}_{\mathrm{I}})(s) \, \mathrm{d}s \tag{100}$$

where $\boldsymbol{\nu}(s)$ denotes the unit outward normal to $\partial\Gamma$ lying in the tangent plane to Γ at $\boldsymbol{x}(s)$, and $\theta_\nu = \boldsymbol{\theta} \cdot \boldsymbol{\nu}$. Again, the identity (99) is useful. Equation (100) is well suited to the computation of the sensitivity of objective functions (92) with respect to crack shape perturbations in the context of boundary element methods. In particular (Section 6), the direct and adjoint SIFs can be computed from the BEM solution using, for example, any of the techniques mentioned in Section 6.2. BE-based formulations for crack shape sensitivity analysis are surveyed in Bonnet (2001).

9 FEM–BEM COUPLING

The idea of coupling BEM and FEM is not new (see, e.g., Barth, 1974; Zienkiewicz *et al.*, 1977; Johnson and Nedelec, 1980; Belytschko *et al.*, 1989; and **Coupling of Boundary Element Methods and Finite Element Methods**), and is particularly appealing in, for example, fluid structure, soil structure, and soil-fluid structure analyses; see, for example, Clouteau and Aubry (1993). FEM–BEM coupling is also an attractive option for problems where complex (and in particular nonlinear) phenomena are confined within a finite region surrounded by large elastic zones.

BEM–FEM coupling procedures can be either simultaneous (the complete set of equations for the coupled problem being formulated and solved as a whole) or iterative (alternating FEM solutions with data coming from previous BEM solution and BEM solutions with data coming from previous FEM solution). The iterative approach presents the advantage of allowing the coupling of BEM and FEM programs externally, that is, using them as "black boxes", whereas the simultaneous approach requires specific coding. It is also worth mentioning that simultaneous BEM–FEM coupling approach can be used with either direct or iterative solvers. In particular, the recent progress in fast iterative BEM solvers such as the FMM (Section 5) can be applied in the context of BEM–FEM coupling.

Coupling collocation BEM with the FEM, which is the most straightforward approach, breaks the symmetry of the resulting set of equations. Although this drawback is by no means fatal, it is often better for several reasons (optimization of memory resources and of computing time, availability of powerful iterative solvers for symmetric systems in the FEM packages) to derive symmetric coupled formulations, as in Ben Mariem and Hamdi (1987) or Bielak *et al.* (1995) for fluid–structure interaction. Additional relevant references include Springhetti *et al.* (2006), Rüberg and Schanz (2008), and El-Gebeily *et al.* (2002, 2003) for formulations involving a relaxation parameter, and Vu and Steinmann (2012) and van Opstal and van Brummelen (2013) for problems with nonlinearities.

Since the topic of FEM–BEM coupling is addressed in another chapter of this encyclopedia, this section is limited to the presentation of a symmetric BEM–FEM coupling procedure based on the construction of the stiffness matrix of a 3D elastic domain without any body forces (Mouhoubi *et al.*, 2002) in terms of nodal displacements on the boundary. This approach uses the BEM stiffness computation as a "slave" process, which in effect, computes the stiffness of a super element. To put it another way, the proposed operation essentially corresponds to a condensation on the boundary of a 3D FEM stiffness, but without ever having to discretize the interior of that region. A similar viewpoint

is adopted in Haas and Kuhn (2003) and Helldörfer *et al.* (2008).

9.1 Boundary energy and symmetric Galerkin formulations

Let Ω denote a three-dimensional, homogeneous elastic region. In the absence of body forces, the elastic strain energy associated with $(\boldsymbol{u}, \boldsymbol{t})$ can be expressed in *boundary energy* form (Clapeyron formula):

$$W = \frac{1}{2}\int_{\Omega} \boldsymbol{\sigma}(\tilde{\boldsymbol{x}}) : \boldsymbol{\varepsilon}(\tilde{\boldsymbol{x}})\, \mathrm{d}\Omega = \frac{1}{2}\int_{\Gamma} \boldsymbol{t}(\tilde{\boldsymbol{x}}) \cdot \boldsymbol{u}(\tilde{\boldsymbol{x}})\, \mathrm{d}S \qquad (101)$$

Since $(\boldsymbol{u}, \boldsymbol{t})$ are assumed to be compatible (i.e., to correspond to each other through the field equations of elastic equilibrium), the boundary energy is in fact a function of either $\boldsymbol{u}$ or $\boldsymbol{t}$ alone. In order to build a stiffness operator in the usual sense, the displacement $\boldsymbol{u}$ is taken as the primary variable and $W \equiv W(\boldsymbol{u})$ in equation (101). The explicit form of the mathematical link between $\boldsymbol{u}$ and $\boldsymbol{t}$ on Γ is either the displacement boundary integral equation (Somigliana identity) or, equivalently, the traction boundary integral equation. Here, both integral equations are invoked in Galerkin forms using the results of Section 4.

First, consider the traction $\boldsymbol{t}$ as being induced by $\boldsymbol{u}$ prescribed over $\partial\Omega$ (Dirichlet problem). In that case, the SGBEM formulation (36) reduces to

$$\text{Find } \boldsymbol{t} \in \mathcal{V}_t \quad \text{such that } \mathcal{B}^{\mathrm{D}}(\boldsymbol{t}, \tilde{\boldsymbol{t}}) = \mathcal{L}^{\mathrm{D}}(\tilde{\boldsymbol{t}}; \boldsymbol{u}) \quad \forall \tilde{\boldsymbol{t}} \in \mathcal{V}_t \qquad (102)$$

where $\mathcal{B}^{\mathrm{D}}(\boldsymbol{t}, \tilde{\boldsymbol{t}})$ and $\mathcal{L}^{\mathrm{D}}(\tilde{\boldsymbol{t}}; \boldsymbol{u})$ are given by (39) and (41) with $S_u = \partial\Omega, S_t = \emptyset$, the set $\mathcal{V}_t$ of admissible functions being defined by $\mathcal{V}_t = \{\tilde{\boldsymbol{t}} \mid \tilde{\boldsymbol{t}} \text{ piecewise continuous on } \partial\Omega\}$.

Next, consider the displacement $\boldsymbol{u}$ as being induced by $\boldsymbol{t}$ prescribed over $\partial\Omega$ (Neumann problem). In that case,

$$\text{Find } \boldsymbol{u} \in \mathcal{V}_u \quad \text{such that } \mathcal{B}^{\mathrm{N}}(\boldsymbol{u}, \tilde{\boldsymbol{u}}) = \mathcal{L}^{\mathrm{N}}(\tilde{\boldsymbol{u}}; \boldsymbol{t}) \quad \forall \tilde{\boldsymbol{u}} \in \mathcal{V}_u \qquad (103)$$

where $\mathcal{B}^{\mathrm{N}}(\boldsymbol{u}, \tilde{\boldsymbol{u}})$ and $\mathcal{L}^{\mathrm{N}}(\tilde{\boldsymbol{u}}; \boldsymbol{t})$ are given by (37) and (40) with $S_t = \partial\Omega, S_u = \emptyset$, the set $\mathcal{V}_u$ of admissible functions being defined by $\mathcal{V}_u = \{\tilde{\boldsymbol{u}} \mid \tilde{\boldsymbol{u}} \in C^{0,\alpha}(\partial\Omega)\}$.

Now, selecting the trial functions specifically as $\tilde{\boldsymbol{t}} = \boldsymbol{t}$ and $\tilde{\boldsymbol{u}} = \boldsymbol{u}$, one notices on inspecting (41) and (40) applied in the above-defined conditions that

$$\mathcal{L}^{\mathrm{D}}(\boldsymbol{t}; \boldsymbol{u}) - \mathcal{L}^{\mathrm{N}}(\boldsymbol{u}; \boldsymbol{t}) = \int_{\partial\Omega} \boldsymbol{t} \cdot \boldsymbol{u}\, \mathrm{d}S$$

Therefore, if $\boldsymbol{u}$ and $\boldsymbol{t}$ are compatible, that is, verify either (102) or (103), one finds that

$$2W(\boldsymbol{u}) = \mathcal{B}^{\mathrm{D}}(\boldsymbol{t}, \boldsymbol{t}) - \mathcal{B}^{\mathrm{N}}(\boldsymbol{u}, \boldsymbol{u}) \qquad (104)$$

9.2 Construction of the stiffness matrix

Assume now that the SGBEM equations (102) and (103) have been discretized using boundary element interpolations of the surface Γ, the boundary fields $(\boldsymbol{u}, \boldsymbol{t})$, and the associated test functions $(\tilde{\boldsymbol{u}}, \tilde{\boldsymbol{t}})$. Then, one has

$$2W(\boldsymbol{u}) = \{\boldsymbol{t}\}^{\mathrm{T}}[\boldsymbol{B}^{\mathrm{D}}]\{\boldsymbol{t}\} - \{\boldsymbol{u}\}^{\mathrm{T}}[\boldsymbol{B}^{\mathrm{N}}]\{\boldsymbol{u}\}$$

where $\boldsymbol{B}^{\mathrm{D}}$ and $\boldsymbol{B}^{\mathrm{N}}$ are the symmetric matrices obtained from the bilinear forms $\mathcal{B}^{\mathrm{D}}(\boldsymbol{t}, \tilde{\boldsymbol{t}})$ and $\mathcal{B}^{\mathrm{N}}(\boldsymbol{u}, \tilde{\boldsymbol{u}})$, and $\{\boldsymbol{u}\}, \{\boldsymbol{t}\}$ are constrained by the discretized version of (102), that is,

$$[\boldsymbol{B}^{\mathrm{D}}]\{\boldsymbol{t}\} = [\boldsymbol{L}^{\mathrm{D}}]\{\boldsymbol{u}\}$$

Combining the last two equations, the discretized boundary energy is expressed in terms of $\{\boldsymbol{u}\}$ as

$$W = \frac{1}{2}\{\boldsymbol{u}\}^{\mathrm{T}}[\boldsymbol{K}]\{\boldsymbol{u}\} \qquad (105)$$

where the stiffness matrix $[\boldsymbol{K}]$ of the subdomain is given by

$$[\boldsymbol{K}] = [\boldsymbol{L}^{\mathrm{D}}]^{\mathrm{T}}[\boldsymbol{B}^{\mathrm{D}}]^{-1}[\boldsymbol{L}^{\mathrm{D}}] - [\boldsymbol{B}^{\mathrm{N}}] \qquad (106)$$

Thus, the above equation provides the symmetric stiffness matrix for the subdomain Ω, which can be added to the stiffness matrix for the complementary subdomain, obtained, for example, by the FEM approach. It is, however, important to point out that equations (102) and (103), although exactly compatible as continuous equations, are not both exactly satisfied in discretized form by the same pair $\{\boldsymbol{u}\}, \{\boldsymbol{t}\}$ due to discretization errors (in other words, equations (105) and (106) hold only in an approximate sense for the discretized problem).

10 RELATED CHAPTERS

(*See also* **Boundary Element Methods: Foundation and Error Analysis**, **Coupling of Boundary Element Methods and Finite Element Methods**, **Multigrid Methods for FEM and BEM Applications**, **Panel Clustering Techniques and Hierarchical Matrices for BEM and FEM**, **Time-Dependent Problems with the Boundary Integral Equation Method**, **Finite Element Methods for Elasticity with Error-Controlled Discretization and Model Adaptivity**, **Models and Finite Elements for Thin-Walled Structures**, **Computational Contact Mechanics with the Finite Element Method**, **Elastoplastic and Viscoplastic Deformations in Solids and Structures**, **Computational Fracture Mechanics**)

REFERENCES

Aimi A and Diligenti M. Hypersingular kernel integration in 3D Galerkin boundary element method. *J. Comput. Appl. Math.* 2002; **138**:51–72.

Aliabadi MH. Boundary element formulations in fracture mechanics. *Appl. Mech. Rev.* 1997; **50**:83–96.

Aliabadi MH. *The Boundary Element Method: Applications in Solids and Structures*. John Wiley & Sons, Ltd., 2001.

Anderson E, Bai Z, Bischof C, Blackford S, Demmel J, Dongarra J, Du Croz J, Greenbaum Hammarlina S, McKenneu A and Sorónsen D, *Lapack Users' Guide* (2nd edn). SIAM: Philadelphia, PA, 1995.

Antes H and Panagiotopoulos PD. *The Boundary Integral Approach to Static and Dynamic Contact Problems*. Birkhäuser: Basel, 1992.

Balas J, Sladek J and Sladek V. *Stress Analysis by Boundary Element Methods*. Elsevier: Amsterdam, 1989.

Banerjee PK. *The Boundary Element Method in Engineering* (2nd edn). McGraw Hill: London, 1994.

Banerjee PK and Raveendra ST. Advanced boundary element analysis of two- and three-dimensional problems of elasto-plasticity. *Int. J. Numer. Methods Eng.* 1986; **23**:985–1002.

Barone MR and Yang RJ. A boundary element approach for recovery of shape sensitivities in three-dimensional elastic solids. *Comput. Methods Appl. Mech. Eng.* 1989; **74**:69–82.

Barth J. *Kombination eines Integralgleichungsverfahrens mit der Methode der Finiten Elemente zur Berechnung ebener Spannungkontentrationsprobleme*. PhD thesis, University of München, 1974.

Bebendorf M and Grzhibovskis R. Accelerating Galerkin BEM for linear elasticity using adaptive cross approximation. *Math. Methods Appl. Sci.* 2006; **29**:1721–1747.

Beer G, Smith I and Duenser C. *The Boundary Element Method with Programming*. Springer: New York, 2008.

Belytschko T, Chang HS and Lu YY. A variationally coupled finite element-boundary-element method. *Comput. Struct.* 1989; **33**:21–29.

Benedetti I, Aliabadi MH and Milazzo A. A fast bem for the analysis of damaged structures with bonded piezoelectric sensors. *Comput. Methods Appl. Mech. Eng.* 2010; **199**:490–501.

Ben Mariem J and Hamdi MA. A new boundary finite element method for fluid-structure interaction problems. *Int. J. Numer. Methods Eng.* 1987; **24**:1251–1267.

Benitez FG and Rosakis AJ. Three-dimensional elastostatics of a layer and a layered medium. *J. Elast.* 1987; **18**:3–50.

Beskos DE (ed.). *Boundary Element Analysis of Plates and Shells*. Springer-Verlag: Berlin, Heidelberg, 1991.

Bielak J, MacCamy RC and Zeng X. Stable coupling method for interface scattering problems by combined integral equations and finite elements. *J. Comput. Phys.* 1995; **119**:374–384.

Bigoni D and Capuani D. Green's function for incremental non-linear elasticity: shear bands and boundary integral formulation. *J. Mech. Phys. Solids* 2002; **50**:371–400.

Bonnet M. Regularized boundary integral equations for three-dimensional bounded or unbounded elastic bodies containing curved cracks of arbitrary shape under dynamic loading. In *Boundary Element Techniques: Applications in Engineering*, Brebbia NGZ CA (ed.). Computational Mechanics Publications: Southampton, 1989; 171–189.

Bonnet M. BIE and material differentiation applied to the formulation of obstacle inverse problems. *Eng. Anal. Bound. Elem.* 1995a; **15**:121–136.

Bonnet M. Regularized BIE formulations for first- and second-order shape sensitivity of elastic fields. *Comput. Struct.* 1995b; **56**:799–811.

Bonnet M. Regularized direct and indirect symmetric variational BIE formulations for three-dimensional elasticity. *Eng. Anal. Bound. Elem.* 1995c; **15**:93–102.

Bonnet M. Differentiability of strongly singular and hypersingular boundary integral formulations with respect to boundary perturbations. *Comput. Mech.* 1997; **19**:240–246.

Bonnet M. *Boundary Integral Equations Methods for Solids and Fluids*. John Wiley & Sons, Ltd.: Chichester, 1999a.

Bonnet M. A general boundary-only formula for crack shape sensitivity of integral functionals. *C.R. Acad. Sci. Paris, sér. II* 1999b; **327**:1215–1221.

Bonnet M. Stability of crack fronts under Griffith criterion: a computational approach using integral equations and domain derivatives of potential energy. *Comput. Methods Appl. Mech. Eng.* 1999c; **173**:337–364.

Bonnet M. Boundary element based formulations for crack shape sensitivity analysis. *Eng. Anal. Bound. Elem.* 2001; **25**:347–362.

Bonnet M. Materially nonlinear analysis. In *Advances in Boundary Element Methods*, CISM Courses and Lectures No. 440, Beskos DE and Maier G (eds). Springer Wien: New York, 2003; 55–114.

Bonnet M and Bui HD. Regularization of the displacement and traction BIE for 3D elastodynamics using indirect methods. In *Advances in Boundary Element Techniques*, Kane JH, Maier G, Tosaka N and Atluri SN (eds). Springer-Verlag, 1993; 1–29.

Bonnet M, Burczyński T and Nowakowski M. Sensitivity analysis for shape perturbation of cavity or internal crack using BIE and adjoint variable approach. *Int. J. Solids Struct.* 2002; **39**:2365–2385.

Bonnet M and Guiggiani M. Direct evaluation of double singular integrals and new free terms in 2D (symmetric) Galerkin BEM. *Comput. Methods Appl. Mech. Eng.* 2003; **22–24**:2565–2596.

Bonnet M and Guzina BB. Elastic-wave identification of penetrable obstacles using shape-material sensitivity framework. *J. Comput. Phys.* 2009; **228**:294–311.

Bonnet M, Maier G and Polizzotto C. Symmetric Galerkin boundary element method. *Appl. Mech. Rev.* 1998a; **51**:669–704.

Bonnet M, Poon H and Mukherjee S. Hypersingular formulation for boundary strain evaluation in the context of a CTO-based implicit BEM scheme for small strain elasto-plasticity. *Int. J. Plast.* 1998b; **14**:1033–1058.

Bonnet M and Mukherjee S. Implicit BEM formulations for usual and sensitivity problems in elasto-plasticity using the consistent tangent operator concept. *Int. J. Solids Struct.* 1996; **33**:4461–4480.

Brancati A, Aliabadi M and Mallardo V. A BEM sensitivity formulation for three-dimensional active noise control. *Int. J. Numer. Methods Eng.* 2012; **90**:1183–1206.

Bui HD. An integral equation method for solving the problem of a plane crack of arbitrary shape. *J. Mech. Phys. Solids* 1977; **25**:29–39.

Bui HD. Some remarks about the formulation of three-dimensional thermoelastoplastic problems by integral equations. *Int. J. Solids Struct.* 1978; **14**:935–939.

Bui HD, Loret B and Bonnet M. Régularisation des équations intégrales de l'élastostatique et de l'élastodynamique. *C.R. Acad. Sci. Paris, sér. II* 1985; **300**:633–636.

Burczyński T. Application of BEM in sensitivity analysis and optimization. *Comput. Mech.* 1993a; **13**:29–44.

Burczyński T. Recent advances in boundary element approach to design sensitivity analysis – a survey. In *Design Sensitivity Analysis*, Kleiber TH M (ed.). Atlanta Technology Publications, 1993b; 1–25.

Burczyński T and Fedelinski P. Boundary elements in shape design sensitivity analysis and optimal design of vibrating structures. *Eng. Anal. Bound. Elem.* 1992; **9**:195–201.

Burczyński T, Kane JH and Balakrishna C. Shape design sensitivity analysis via material derivative – adjoint variable approach. *Int. J. Numer. Methods Eng.* 1995; **38**:2839–2866.

Burgardt B. *Contribution à l'étude des méthodes des équations intégrales et à leur mise en œuvre numérique en élastoplasticité*. PhD thesis, Ecole centrale de Nantes, 1999.

Camp CV and Gipson GS. Overhauser elements in boundary element analysis. *Math. Comput. Modell.* 1991; **15**:59–69.

Carini A, Diligenti M, Maranesi P and Zanella M. Analytical integrations for two-dimensional elastic analysis by the symmetric Galerkin boundary element method. *Comput. Mech.* 1999; **23**:308–323.

Carini A and Salvadori A. Analytical integrations in 3D BEM: preliminaries. *Comput. Mech.* 2002; **28**:177–185.

Chaillat S. *Fast Multipole Method for 3-D elastodynamic boundary integral equations. Application to seismic wave propagation*. PhD thesis. Ecole Polytechnique, Palaiseau, France, 2008.

Chaillat S and Bonnet M. Recent advances on the fast multipole accelerated boundary element method for 3D time-harmonic elastodynamics. *Wave Motion* 2013; **50**:1090–1104.

Chaillat S, Bonnet M and Semblat JF. A multi-level fast multipole bem for 3-d elastodynamics in the frequency domain. *Comput. Methods Appl. Mech. Eng.* 2008; **197**:4233–4249.

Chan KS, Karasudhi P and Lee SL. Force at a point in the interior of a layered elastic half-space. *Int. J. Solids Struct.* 1974; **10**:1179–1199.

Chandra A and Mukherjee S. *Boundary Element Methods in Manufacturing*. Oxford University Press: Oxford, 1997.

Choi JO and Kwak BM. Boundary integral equation method for shape optimization of elastic structures. *Int. J. Numer. Methods Eng.* 1988; **26**:1579–1595.

Cisilino AP and Aliabadi MH. Three-dimensional boundary element analysis of fatigue crack growth in linear and non-linear fracture problems. *Eng. Fract. Mech.* 1999; **63**:713–733.

Cisilino AP and Ortiz J. Boundary element analysis of three-dimensional mixed-mode cracks via the interaction integral. *Comput. Methods Appl. Mech. Eng.* 2005; **194**:935–956.

Clouteau D and Aubry D. 3D seismic soil-fluid-structure interaction for arch dams including source and site effects. In *Proceedings of Eurodyn '93 International Conference*. Balkema: Rotterdam, 1993; 1217–1224.

Comi C and Maier G. Extremum, convergence and stability properties of the finite-increment problem in elastic-plastic boundary element analysis. *Int. J. Solids Struct.* 1992; **29**:249–270.

Costabel M and Stephan EP. An improved boundary element Galerkin method for three-dimensional crack problems. *Integr. Equ. Oper. Theory* 1987; **10**:467–504.

Cruse TA. Numerical solutions in three-dimensional elastostatics. *Int. J. Solids Struct.* 1969; **5**:1259–1274.

Cruse TA. *Boundary Element Analysis in Computational Fracture Mechanics*. Kluwer Academic Publishers, 1988.

Cruse TA and Richardson JD. Non-singular somigliana stress identities in elasticity. *Int. J. Numer. Methods Eng.* 1996; **39**:3273–3304.

Cruse TA and Wilson PM. Boundary Integral Equation Method for Elastic Fracture Mechanics Analysis. AFOSR-TR-780355. Pratt and Whitney Aircraft Group, 1977.

Davis JJ and Rabinowitz P. *Methods of Numerical Integration*. Academic Press: New York, 1975.

dell'Erba DN and Aliabadi MH. Three-dimensional thermo-mechanical fatigue grack growth using BEM. *Int. J. Fatigue* 2000; **22**:261–273.

Dong C and Bonnet M. An integral formulation for steady-state elastoplastic contact over a coated half-plane. *Comput. Mech.* 2002; **28**:105–121.

El-Gebeily M, Elleithy WM and Al-Gahtani HJ. Convergence of the domain decomposition finite element–boundary element coupling methods. *Comput. Methods Appl. Mech. Eng.* 2002; **191**:4851–4867.

Elleithy WM and Tanaka M. Interface relaxation algorithms for BEM–BEM coupling and FEM–BEM coupling. *Comput. Methods Appl. Mech. Eng.* 2003; **192**:2977–2992.

Eller M. Identification of cracks in three-dimensional bodies by many boundary measurements. *Inverse Prob.* 1996; **12**:395–408.

Fata SN. Explicit expressions for 3D boundary integrals in potential theory. *Int. J. Numer. Methods Eng.* 2009; **78**:32–47.

Foerster A and Kuhn G. A field boundary element formulation for material nonlinear problems at finite strains. *Int. J. Solids Struct.* 1994; **31**:1777–1792.

Frangi A. Fracture propagation in 3D by the symmetric Galerkin boundary element method. *Int. J. Fract.* 2002; **116**:313–330.

Frangi A and Guiggiani M. Boundary element analysis of Kirchhoff plates with direct evaluation of hypersingular integrals. *Int. J. Numer. Methods Eng.* 1999; **46**:1845–1863.

Frangi A and Guiggiani M. A direct approach for boundary integral equations with high-order singularities. *Int. J. Numer. Methods Eng.* 2000; **49**:871–898.

Frangi A and Guiggiani M. Free terms and compatibility conditions for 3D hypersingular boundary integral equations. *ZAMM* 2001; **81**:651–664.

Frangi A and Maier G. Dynamic elastic-plastic analysis by a symmetric Galerkin boundary element method with time-independent kernels. *Comput. Methods Appl. Mech. Eng.* 1999; **171**:281–308.

Frangi A, Novati G, Springhetti R and Rovizzi M. 3D fracture analysis by the symmetric Galerkin BEM. *Comput. Mech.* 2001; **28**:220–232.

Frangi A, Spinola G and Vigna B. On the evaluation of damping in MEMS in the slip–flow regime. *Int. J. Numer. Methods Eng.* 2006; **68**:1031–1051.

Freddi F and Royer-Carfagni G. Symmetric Galerkin BEM for bodies with unconstrained contours. *Comput. Methods Appl. Mech. Eng.* 2006; **195**:961–981.

Fu Y, Klimkowski KJ, Rodin GJ, Berger E, Browne JC, Singer JR, van der Greijn RA and Vemaganti KS. A fast solution method for the three-dimensional many-particle problems of linear elasticity. *Int. J. Numer. Methods Eng.* 1998; **42**:1215–1229.

Golub GH and Van Loan CF. *Matrix Computations* (2nd edn). Johns Hopkins University Press: Baltimore, MD, 1989.

Gray L. Evaluation of singular and hypersingular Galerkin integrals: direct limits and symbolic computation. In *Singular Integrals in Boundary Element Methods*, Sladek V and Sladek J (eds). Computational Mechanics Publications: Southampton, 1998; 45–84.

Gray LJ, Martha LF and Ingraffea AR. Hypersingular integrals in boundary element fracture analysis. *Int. J. Numer. Methods Eng.* 1990; **29**:1135–1158.

Gray LJ, Phan AV, Paulino GH and Kaplan T. Improved quarter-point crack-tip element. *Eng. Fract. Mech.* 2003; **70**:269–283.

Greenbaum A. *Iterative Methods for Solving Linear Systems*. SIAM: Philadelphia, PA, 1997.

Greengard L and Rokhlin V. A fast algorithm for particle simulations. *J. Comput. Phys.* 1987; **73**:325–348.

Greengard L and Rokhlin V. A new version of the fast multipole method for the Laplace equation in three dimensions. *Acta Numer.* 1997; **6**:229–270.

Gu H and Yew CH. Finite element solution of a boundary integral equation for mode I embedded three-dimensional fractures. *Int. J. Numer. Methods Eng.* 1988; **26**:1525–1540.

Guiggiani M. Hypersingular formulation for boundary stress evaluation. *Eng. Anal. Bound. Elem.* 1994; **14**:169–179.

Guiggiani M. Formulation and numerical treatment of boundary integral equations with hypersingular kernels. In *Singular Integrals in Boundary Element Methods*, Sladek V and Sladek J (eds). Computational Mechanics Publications: Southampton, 1998; 85–124.

Guiggiani M and Gigante A. A general algorithm for multidimensional Cauchy principal value integrals in the boundary element method. *ASME J. Appl. Mech.* 1990; **57**:906–915.

Guiggiani M, Krishnasamy G, Rudolphi TJ and Rizzo FJ. A general algorithm for the numerical solution of hypersingular boundary integral equations. *ASME J. Appl. Mech.* 1992; **59**:604–614.

Gumerov NA and Duraiswami R. *Fast Multipole Methods for the Helmholtz Equation in Three Dimensions*. Elsevier. 2005.

Guzina BB, Fata SN and Bonnet M. On the stress-wave imaging of cavities in a semi-infinite solid. *Int. J. Solids Struct.* 2003; **40**:1505–1523.

Guzina BB and Pak RYS. Static fundamental solutions for a bi-material full-space. *Int. J. Solids Struct.* 1999; **36**:493–516.

Haas M and Kuhn G. A symmetric Galerkin BEM implementation for 3D elastostatic problems with an extension to curved elements. *Comput. Mech.* 2002; **28**:250–259.

Haas M and Kuhn G. Mixed-dimensional, symmetric coupling of FEM and BEM. *Eng. Anal. Bound. Elem.* 2003; **27**:575–582.

Hackbusch W and Nowak ZP. On the fast matrix multiplication in the boundary element method by panel clustering. *Numer. Math.* 1989; **54**:463–491.

Hackbusch W and Wittum G (eds). *Boundary Elements: Implementation and Analysis of Advanced Algorithms*. Wieweg: Braunschweig, 1996.

Hayami K and Matsumoto H. A numerical quadrature for nearly singular boundary element integrals. *Eng. Anal. Bound. Elem.* 1994; **13**:143–154.

Hayami K and Sauter SA. Application of the panel clustering method to the three-dimensional elastostatics problem. In *Boundary Elements XIX*. Computational Mechanics Publications: Southampton, 1997; 625–634.

Helldörfer B, Haas M and Kuhn G. Automatic coupling of a boundary element code with a commercial finite element system. *Adv. Eng. Softw.* 2008; **39**:699–709.

Hildenbrand J and Kuhn G. Numerical computation of hypersingular integrals and application to the boundary integral equation for the stress tensor. *Eng. Anal. Bound. Elem.* 1992; **10**:209–218.

Huber O, Dallner R, Partheymuller P and Kuhn G. Evaluation of the stress tensor in 3D elastoplasticity by direct solving of hypersingular integrals. *Int. J. Numer. Methods Eng.* 1996; **39**:2555–2573.

Huber O, Nickel J and Kuhn G. On the decomposition of the J-integral for 3D problems. *Int. J. Fract.* 1993; **64**:339–348.

Johnson C and Nedelec JC. On the coupling of boundary integral and finite element methods. *Math. Comput.* 1980; **35**:1063–1079.

Kager B and Schanz M. Fast and data sparse time domain BEM for elastodynamics. *Eng. Anal. Bound. Elem.* 2015; **50**:212–223.

Kallivokas L, Juneja T and Bielak J. A symmetric Galerkin BEM variational framework for multi-domain interface problems. *Comput. Methods Appl. Mech. Eng.* 2005; **194**:3607–3636.

Kane JH. *Boundary Element Analysis in Engineering Continuum Mechanics*. Prentice Hall: Englewood Cliffs, NJ, 1994.

Kassab A, Moslehy FA and Daryapurkar AB. Nondestructive evaluation of cavities by an inverse elastostatics boundary element method. *Eng. Anal. Bound. Elem.* 1994; **13**:45–55.

Kellogg OD. *Foundations of Potential Theory*. Springer-Verlag: Berlin, Heidelberg, 1967.

Kolk K, Weber W and Kuhn G. Investigation of 3D crack propagation problems via fast BEM formulations. *Comput. Mech.* 2005; **37**:32–40.

Krishnasamy G, Rizzo FJ and Rudolphi TJ. Hypersingular boundary integral equations: their occurrence, interpretation, regularization and computation. In *Developments in Boundary Element Methods*, Advanced Dynamic Analysis, vol. 7, Banerjee PK and Kobayashi S (eds), Elsevier, 1992; 207–252.

Kupradze VD (ed.). *Three-dimensional Problems of the Mathematical Theory of Elasticity and Thermoelasticity*. North Holland: Amsterdam, 1979.

Kurz S, Rain O and Rjasanow S. The adaptive cross approximation technique for the 3D boundary element method. *IEEE Trans. Magn.* 2002; **38**:421–424.

Lachat JC and Watson JO. Effective numerical treatment of boundary integral equations: a formulation for three-dimensional elastostatics. *Int. J. Numer. Methods Eng.* 1976; **10**:991–1005.

Lage C and Schwab C. Wavelet Galerkin algorithms for boundary integral equations. *SIAM J. Sci. Comput.* 1999; **20**:2195–2222.

Lai Y-S and Rodin GJ. Fast boundary element method for three-dimensional solids containing many cracks. *Eng. Anal. Bound. Elem.* 2003; **27**:845–852.

Lenoir M and Salles N. Evaluation of 3-d singular and nearly singular integrals in Galerkin BEM for thin layers. *SIAM J. Sci. Comput.* 2012; **34**:A3057–A3078.

Leu LJ and Mukherjee S. Sensitivity analysis and shape optimization in nonlinear solid mechanics. *Eng. Anal. Bound. Elem.* 1993; **12**:251–260.

Li S, Mear ME and Xiao L. Symmetric weak-form integral equation method for three-dimensional fracture analysis. *Comput. Methods Appl. Mech. Eng.* 1998; **151**:435–459.

Liu Y, Nishimura N, Otani Y, Takahashi T, Chen XL and Munakata H. A fast boundary element method for the analysis of fiber-reinforced composites based on a rigid-inclusion model. *ASME J. Appl. Mech.* 2005; **72**:115–128.

Luchi M and Rizzuti S. Boundary elements for three-dimensional crack analysis. *Int. J. Numer. Methods Eng.* 1987; **24**:2253–2271.

Maier G, Miccoli S, Novati G and Perego U. Symmetric Galerkin boundary element method in plasticity and gradient-plasticity. *Comput. Mech.* 1995; **17**:115–129.

Maier G, Miccoli S, Novati G and Sirtori S. A Galerkin symmetric boundary-element method in plasticity: formulation and implementation. In *Advances in Boundary Element Techniques*, Kane JH, Maier G, Tosaka N and Atluri SN (eds). Springer-Verlag, 1993; 288–328.

Maier G and Polizzotto C. A Galerkin approach to boundary element elastoplastic analysis. *Comput. Methods Appl. Mech. Eng.* 1987; **60**:175–194.

Margonari M and Bonnet M. Fast multipole method applied to the coupling of elastostatic BEM with FEM. *Comput. Str.* 2005; **83**:700–717.

Martin PA and Rizzo FJ. Hypersingular integrals: how smooth must the density be? *Int. J. Numer. Methods Eng.* 1996; **39**:687–704.

Martin PA, Rizzo FJ and Cruse TA. Smoothness relaxation strategies for singular and hypersingular integral equations. *Int. J. Numer. Methods Eng.* 1998; **42**:885–906.

Matsumoto T, Tanaka M, Miyagawa M and Ishii N. Optimum design of cooling lines in injection moulds by using boundary element design sensitivity analysis. *Finite Elem. Anal. Des.* 1993; **14**:177–185.

Mellings SC and Aliabadi MH. Flaw identification using the boundary element method. *Int. J. Numer. Methods Eng.* 1995; **38**:399–419.

Mi Y and Aliabadi MH. Dual boundary element method for three-dimensional fracture mechanics analysis. *Eng. Anal. Bound. Elem.* 1992; **10**:161–171.

Mindlin RD. Force at a point in the interior of a semi-infinite solid. *Physics* 1936; **7**:195–201.

Mouhoubi S, Bonnet M and Ulmet L. Une formulation symétrique pour le couplage éléments finis – éléments de frontière en mécanique. *Rev. Eur. Elem. Finis* 2002; **11**:277–289.

Mukherjee S and Chandra A. Nonlinear solid mechanics. In *Boundary Element Methods in Mechanics*, Beskos DE (ed.). North Holland, 1987; 285–332.

Mukherjee S and Chandra A. A boundary element formulation for design sensitivities in problems involving both geometric and material nonlinearities. *Math. Comput. Modell.* 1991; **15**:245–255.

Mura T. *Micromechanics of Defects in Solids*. Martinus Nijhoff: The Hague, 1982.

Nedelec JC. Integral equations with non integrable kernels. *Integr. Equ. Oper. Theory* 1982; **5**:562–572.

Nguyen QS. On the elastic-plastic initial-boundary value problem and its numerical integration. *Int. J. Numer. Methods Eng.* 1977; **11**:817–832.

Nishimura N. Application of boundary integral equation method to various crack determination problems. In *Dynamic Fracture Mechanics*, Aliabadi M (ed.). Computational Mechanics Publications: Southampton, 1995.

Nishimura N. Fast multipole accelerated boundary integral equation methods. *Appl. Mech. Rev.* 2002; **55**:299–324.

Nishimura N, Furukawa A and Kobayashi S. Regularized boundary integral equations for an inverse problem of crack determination in time domain. In *Boundary Element Methods*, Kobayashi S and Nishimura N (eds). Springer-Verlag, 1992; 252–261.

Nishimura N and Kobayashi S. Determination of cracks having arbitrary shape with boundary integral method. *Eng. Anal. Bound. Elem.* 1995; **15**:189–197.

Niu Z, Wendland WL, Wang X and Zhou H. A semi-analytical algorithm for the evaluation of the nearly singular integrals in three-dimensional boundary element methods. *Comput. Methods Appl. Mech. Eng.* 2005; **194**:1057–1074.

Of G, Steinbach O and Wendland WL. The fast multipole method for the symmetric boundary integral formulation. *IMA J. Numer. Anal.* 2006; **26**:272–296.

Pan YC and Chou TW. Point force solution for an infinite transversely isotropic solid. *ASME J. Appl. Mech.* 1976; **43**:608–612.

Parreira P and Guiggiani M. On the implementation of the Galerkin approach in the boundary element method. *Comput. Struct.* 1989; **33**:269–279.

Partheymuller P, Haas M and Kuhn G. Comparison of the basic and the discontinuity formulation of the 3D-Dual boundary element method. *Eng. Anal. Bound. Elem.* 2000; **24**:777–788.

Parton VZ and Perlin PI. *Integral Equations in Elasticity*. Mir Publishers: Moscow, 1982.

Patterson C and Sheikh MA. Interelement continuity in the boundary element method. In *Topics in Boundary Element Research*, vol. 1, Brebbia C (ed.). Springer-Verlag, 1984.

Paulino GH and Liu Y. Implicit consistent and continuum tangent operators in elastoplastic boundary element formulations. *Comput. Methods Appl. Mech. Eng.* 1999; **190**:2157–2179.

Petryk H and Mróz Z. Time derivatives of integrals and functionals defined on varying volume and surface domains. *Arch. Mech.* 1986; **38**:694–724.

Polch EZ, Cruse TA and Huang CJ. Traction BIE solutions for flat cracks. *Comput. Mech.* 1987; **2**:253–267.

Polizzotto C. An energy approach to the boundary element method; Part II: Elastic-plastic solids. *Comput. Methods Appl. Mech. Eng.* 1988; **69**:263–276.

Poon H, Mukherjee S and Bonnet M. Numerical implementation of a CTO-based implicit approach for the BEM solution of usual and sensitivity problems in elasto-plasticity. *Eng. Anal. Bound. Elem.* 1998a; **22**:257–269.

Poon H, Mukherjee S and Fouad Ahmad M. Use of 'simple solution' in regularizing hypersingular boundary integral equations in elastoplasticity. *ASME J. Appl. Mech.* 1998b; **65**:39–45.

Pozrikidis C. *A Practical Guide to Boundary Element Methods with the Software Library BEMLIB*. CRC Press. 2002.

Rezayat M, Shippy DJ and Rizzo FJ. On time-harmonic elastic wave analysis by the boundary element method for moderate to high frequencies. *Comput. Methods Appl. Mech. Eng.* 1986; **55**:349–367.

Rizzo FJ. An integral equation approach to boundary value problems of classical elastostatics. *Q. Appl. Math.* 1967; **25**:83–95.

Rizzo FJ and Shippy DJ. An advanced boundary integral equation method for three-dimensional elasticity. *Int. J. Numer. Methods Eng.* 1977; **11**:1753–1768.

Rjasanow S and Steinbach O. *The Fast Solution of Boundary Integral Equations*. Springer-Verlag. 2007.

Rokhlin V. Rapid solution of integral equations of classical potential theory. *J. Comput. Phys.* 1985; **60**:187–207.

Rongved L. Force interior to one of two joined semi-infinite solids. In *Proceedings of 2nd Midwestern Conference Solid Mechanics*, 1955; 1–13.

Rüberg T and Schanz M. Coupling finite and boundary element methods for static and dynamic elastic problems with non-conforming interfaces. *Comput. Methods Appl. Mech. Eng.* 2008; **198**:449–458.

Rungamornrat J and Mear ME. Weakly-singular, weak-form integral equations for cracks in three-dimensional anisotropic media. *Int. J. Solids Struct.* 2008; **45**:1283–1301.

Rus G and Gallego R. Hypersingular shape sensitivity boundary integral equation for crack identification under harmonic elastodynamic excitation. *Comput. Meth. Appl. Mech. Eng.* 2007; **196**:2596–2618.

Saad Y and Schultz MH. GMRES: a generalized minimal residual algorithm for solving nonsymmetric linear systems. *SIAM J. Sci. Stat. Comput.* 1986; **7**:856–869.

Salvadori A. Analytical integrations of hypersingular kernel in 3D BEM problems. *Comput. Methods Appl. Mech. Eng.* 2001; **190**:3957–3975.

Salvadori A. Analytical integrations in 2D BEM elasticity. *Int. J. Numer. Methods Eng.* 2002; **53**:1695–1719.

Salvadori A. A symmetric boundary integral formulation for cohesive interface problems. *Comput. Mech.* 2003; **32**:381–391.

Sauter SA and Schwab C. *Boundary Element Methods*. Springer-Verlag: Berlin Heidelberg, 2011.

Schwab C. Variable order composite quadrature of singular and nearly singular integrals. *Computing* 1994; **53**:173–194.

Schwab C and Wendland W. Kernel properties and representations of boundary integral operators. *Math. Nachr.* 1992; **156**:187–218.

Simo JC and Hugues TJR. *Computational Inelasticity*. Springer-Verlag: New York, 1998.

Simo JC and Taylor RL. Consistent tangent operators for rate-independent elastoplasticity. *Comput. Methods Appl. Mech. Eng.* 1985; **48**:101–118.

Sladek J and Sladek V. Three-dimensional curved crack in an elastic body. *Int. J. Solids Struct.* 1983; **19**:425–436.

Sladek V and Sladek J. Why use double nodes in BEM? *Eng. Anal. Bound. Elem.* 1991; **8**:109–112.

Snyder MD and Cruse TA. Boundary integral equation analysis of cracked anisotropic plates. *Int. J. Fract.* 1975; **11**:315–328.

Sokolowski J and Zolesio JP. Introduction to shape optimization. In *Shape Sensitivity Analysis*, Springer series in Computational Mathematics, vol. 16. Springer-Verlag, 1992.

Springhetti R, Novati G and Margonari M. Weak coupling of the symmetric Galerkin BEM with FEM for potential and elastostatic problems. *Comput. Model. Eng. Sci.* 2006; **13**:67–80.

Steinbach O. *Numerical Approximation Methods for Elliptic Boundary Value Problems*. Springer-Verlag: New York, 2008.

Stroud AH. *Approximate Calculation of Multiple Integrals*. Prentice Hall: Englewood Cliffs, NJ, 1971.

Stroud AH and Secrest D. *Gaussian Quadrature Formulas*. Prentice Hall: Englewood Cliffs, NJ, 1966.

Sutradhar A, Paulino G and Gray LJ. *Symmetric Galerkin Boundary Element Method*. Springer-Verlag: Berlin Heidelberg, 2008.

Swedlow JL and Cruse TA. Formulation of boundary integral equations for three-dimensional elasto-plastic flow. *Int. J. Solids Struct.* 1971; **7**:1673–1681.

Tanaka M, Sladek V and Sladek J. Regularization techniques applied to boundary element methods. *Appl. Mech. Rev.* 1994; **47**:457–499.

Telles JCF. A self-adaptive coordinate transformation for efficient numerical evaluation of general boundary element integrals. *Int. J. Numer. Methods Eng.* 1987; **24**:959–973.

Telles JCF and Brebbia CA. Boundary elements: new developments in elastoplastic analyses. *Appl. Math. Modell.* 1981; **5**:376–382.

Telles JCF and Carrer JAM. Implicit procedures for the solution of elastoplastic problems by the boundary element method. *Math. Comput. Modell.* 1991; **15**:303–311.

Telles JCF and Carrer JAM. Static and transient dynamic nonlinear stress analysis by the boundary element method with implicit techniques. *Eng. Anal. Bound. Elem.* 1994; **14**:65–74.

Telles JCF, Castor CS and Guimaraes S. A numerical Green's function approach for boundary elements applied to fracture mechanics. *Int. J. Numer. Methods Eng.* 1995; **38**:3259–3274.

Toh KC and Mukherjee S. Hypersingular and finite part integrals in the boundary element method. *Int. J. Solids Struct.* 1994; **31**:2289–2312.

Trinh QT, Mouhoubi S, Chazallon C and Bonnet M. Solving multizone and multicrack elastostatic problems: a fast multipole symmetric Galerkin boundary element method approach. *Eng. Anal. Bound. Elem.* 2015; **50**:486–495.

van Opstal TM and van Brummelen EH. A finite-element/boundary-element method for large-displacement fluid–structure interaction with potential flow. *Comput. Methods Appl. Mech. Eng.* 2013; **266**:57–69.

Vodička R. A quasi-static interface damage model with cohesive cracks: SQP-SGBEM implementation. *Eng. Anal. Bound. Elem.* 2016; **62**:123–140.

Vu M-N, Pouya A and Seyedi DM. Modelling of steady-state fluid flow in 3D fractured isotropic porous media: application to effective permeability calculation. *Int. J. Numer. Anal. Methods Geotech.* 2013; **37**:2257–2277.

Vu DK and Steinmann P. On 3D coupled BEM–FEM simulation of nonlinear electro-elastostatics. *Comput. Methods Appl. Mech. Eng.* 2012; **201**:82–90.

Watson JO. Boundary elements for cracks and notches in three dimensions. *Int. J. Numer. Methods Eng.* 2006; **65**:1419–1443.

Wendland W (ed.). *Boundary Element Topics*. Springer-Verlag: Berlin, Heidelberg, 1997.

Willis JR. The elastic interaction energy of dislocation loops in anisotropic media. *Q. J. Mech. Appl. Math.* 1965; **17**:157–174.

Xu G, Argon AS, Ortiz M and Bower A. Development of a variational boundary integral method for the analysis of fully three dimensional crack advance problems. In *Computational Mechanics '95*, vol. 2, Atluri SN, Yagawa G and Cruse TA (eds). Springer-Verlag, 1995; 2874–2889.

Ying L, Biros G and Zorin D. A kernel-independent adaptive fast multipole in two and three dimensions. *J. Comput. Phys.* 2004; **196**:591–626.

Yoshida K. *Applications of fast multipole method to boundary integral equation method*. PhD thesis. University of Kyoto, 2001.

Yoshida S, Nishimura N and Kobayashi S. Application of fast multipole Galerkin boundary integral equation method to elastostatic crack problems in 3D. *Int. J. Numer. Methods Eng.* 2001; **50**:525–547.

Zhang Q, Mukherjee S and Chandra A. Shape design sensitivity analysis for geometrically and materially nonlinear problems by the boundary element method. *Int. J. Solids Struct.* 1992; **29**:2503–2525.

Zienkiewicz OC, Kelly DW and Bettess P. The coupling of the finite element method and boundary solution procedures. *Int. J. Numer. Methods Eng.* 1977; **11**:355–375.